

The Application of Trimethylsilyl Diazomethane to the Synthesis of  
Optically Active Pyrazolines and Related Studies

A dissertation presented by  
Michael R. Mish

In Partial Fulfillment of the Requirements  
for the Degree of  
Doctor of Philosophy

California Institute of Technology  
Pasadena, California

2001  
(Submitted September 7, 2000)

© 2001  
Michael R. Mish  
All Rights Reserved

### Abstract

The 1,3-dipolar cycloadditions of trimethylsilyl diazomethane with camphorsultam-derived acrylates are reported as a means for the efficient synthesis of optically active pyrazolines. Trimethylsilyl diazomethane is a safe, commercially available diazoalkane which provides  $\Delta^1$ -pyrazolines in good yield and diastereoselectivity when camphorsultam-derived acrylates are used as the reaction dipolarophiles. These initial cycloadducts are subsequently converted to stable, characterizable  $\Delta^2$ -pyrazolines upon desilylation.

A manifold of reactions that can be applied to these  $\Delta^2$ -pyrazolines has been developed which includes pyrazoline reduction, N-N bond reduction, addition to the pyrazoline C=N by mild carbon nucleophiles, and both solvolytic and reductive chiral auxiliary removal. Additionally, it has been demonstrated that the pyrazoline reduction products can take part in peptide coupling reactions that allow for the pyrazolidines to serve as proline-like molecules. The development of this methodology is a general solution to the problem of highly substituted, functionalized pyrazoline synthesis. Importantly, the pyrazolines thus provided have been demonstrated to be amenable to reactions that add to their value as synthetic intermediates.

## Acknowledgments

First and foremost among those to whom I am grateful is my advisor, Professor Erick Carreira. His insight, advice, and encouragement with respect to my studies have been invaluable. His contribution to my development as a scientist cannot be overestimated.

I also thank Dr. Don Gauthier and Brian Ledford for the guidance they provided at the start of my graduate studies. I am indebted to Jeremy, Craig, Tehshik, and Jeff for helping to create an atmosphere of excitement for the process of chemical research that was instrumental to my early success in the laboratory. I am happy to have been able to collaborate with Dr. Francisco Guerra, an enthusiastic scientist who made important contributions to the research described in this thesis.

I feel very fortunate to have been able to work in the company of the other members of the Carreira group. At the beginning of my studies I was in awe of the knowledge and skill possessed by the group's senior members, and as I prepare to depart I now find myself inspired by the earnestness and intensity of my co-workers who are at the start of their own graduate careers.

I must express my gratitude to Professor Richard Glass of the University of Arizona, for taking me into his group during my time as an undergraduate there. It was in his labs that I began the transition from student to scientist, and much of my understanding of the purpose and meaning of my work can be traced back to the experience that I gained there.

The emotional support of my family, especially that of my grandparents, was indispensable to me during the course of my studies. I owe much that I have achieved to

them and the example which they provided to me. I also owe much gratitude to my father, who taught me to appreciate that nearly every situation can benefit from being approached with a sense of humor.

Above all, I thank my wife, Leane. The degree of patience and understanding she has displayed in response to the demands placed on us by the path we have followed is well beyond that for which I could have reasonably asked. Her unwavering faith in me has been a source of strength that I have drawn on throughout my career; I could not have done this without her.

*for Leane*

## Table of Contents

Abstract .....	iii
Acknowledgments .....	iv
Table of Contents.....	vii
List of Figures .....	ix
List of Schemes and Tables .....	x
List of Abbreviations .....	xi
Section 1. 1,3-Dipolar Cycloadditions to Give Optically Active Pyrazolines .....	1
Introduction .....	1
Background.....	2
$\Delta^1$ -Pyrazolines : A Role for Silicon-Directed Isomerization.....	7
Preliminary Investigations.....	12
Scope of the Cycloaddition Reaction - Results and Discussion .....	16
Section 2. Application of Optically Active Pyrazolines to Amino Acid Analogue Synthesis .....	23
Background.....	23
Pyrazolidines as Proline Analogue Systems.....	27
Transformations of Optically Active Pyrazolines .....	30
Application to Dipeptide Formation .....	32
Conclusion.....	38
Section 3. The Addition of Mild Carbon Nucleophiles to <i>N</i> -Acetyl Pyrazolines .....	39
Background.....	39
Development of a Nucleophilic Addition Process.....	41
Investigations with Allyl Tributylstannane and Various Lewis Acids .....	44
Scope of the Addition Reaction .....	45

Elaboration of the Nucleophilic Addition Product and Discussion .....	47
General Conclusion .....	50
Experimental Section .....	51
Appendix I: X-Ray Crystallographic Data for Pyrazoline <b>60</b> .....	149
Appendix II: X-Ray Crystallographic Data for Pyrazolidine <b>130</b> .....	157



## List of Figures

Figure 1.	Generalized cycloaddition of a propargyl-allenyl dipole to an alkene .....	1
Figure 2.	Transformations of the $\Delta^2$ -pyrazolines from the initial cycloadduct .....	2
Figure 3.	The high stereospecificity observed in Huisgen's experiments suggests a concerted mechanism .....	3
Figure 4.	Qualitative PMO diagram of diazomethane and ethyl acrylate.....	4
Figure 5.	MO considerations explain observed regioselectivity .....	5
Figure 6.	Isomerizations available to the initial cycloadduct .....	8
Figure 7.	Directed pyrazoline isomerization involving silicon .....	9
Figure 8.	Cation stabilization $\beta$ - to silicon.....	10
Figure 9.	Preliminary results suggested sulfonimide-derived acrylates .....	13
Figure 10.	The first application of the cycloaddition leads to Stelletamide A.....	15
Figure 11.	Conformations available to <i>N</i> -acryloyl sultams .....	17
Figure 12.	Pyrazoline substitution is modifiable at every position of the ring .....	23
Figure 13.	<i>Cis-trans</i> prolyl peptide isomerism.....	24
Figure 14.	Examples of conformationally constrained proline mimics.....	25
Figure 15.	Prolyl-dipeptide systems leading to turn motifs .....	27
Figure 16.	Conformational equilibria of piperazines and pyrazolines .....	27
Figure 17.	The MM2-minimized structures of prolyl-dipeptides and congeners.....	29
Figure 18.	The Molecumetics Ltd. synthesis of <i>N</i> -Boc pyrazolidine <b>107</b> .....	35
Figure 19.	Carreira and Sasaki's synthesis of $\alpha$ -methyl aspartic acid <b>108</b> .....	37
Figure 20.	Functionalization is possible via addition to the pyrazoline C=N.....	39
Figure 21.	Examples of previous organometallic additions to hydrazones .....	40
Figure 22.	Control of substituents can be extended to all pyrazoline carbons.....	41
Figure 23.	The HIV-protease inhibitor A-74704.....	43

Figure 24. <i>N</i> -acetyl pyrazolines provide a bidentate chelating motif .....	43
Figure 25. Observed nOe enhancements for pyrazolidines <b>127</b> and <b>131</b> .....	47
Figure 26. <i>N</i> -trichloroacetyl-derived pyrazolidines via the addition protocol.....	49

### List of Schemes and Tables

Scheme 1 .....	17
Scheme 2 .....	20
Scheme 3 .....	42
Scheme 4 .....	44
Scheme 5 .....	48
Table 1. The effect of reaction solvent on cycloaddition diastereoselectivity .....	19
Table 2. Diastereoselective cycloaddition applied to a range of acrylates .....	21
Table 3. Pyrazoline reduction with subsequent carbamate formation .....	30
Table 4. Peptide coupling through N <sub>α</sub> .....	33
Table 5. Peptide coupling between pyrazolidine and <i>N</i> -Cbz amino acids.....	34
Table 7. Optimization of addition of allyltributylstannane to pyrazoline <b>126</b> .....	45
Table 8. Addition of mild carbon nucleophiles to <i>N</i> -acetyl pyrazolines .....	46

**List of Abbreviations**

Å	Angstrom
Ac	acetyl
Bn	benzyl
Boc	<i>tert</i> -butyl Carbamate
Bu	butyl
Bz	benzoyl
°C	degrees Celcius
cat.	catalytic
cHx	cyclohexyl
Cbz	benzyl Carbamate
CI	chemical ionization
cm <sup>-1</sup>	reciprocal centimeters
δ	chemical shift
DCC	dicyclohexyl carbodiimide
4-DMAP	4-dimethylamino pyradine
DMSO	dimethyl sulfoxide
ε	dielectric constant
EDC	1-(3-dimethylaminopropyl)-3-ethylcarbodiimide hydrochloride
EI	electron impact
Eq	equation
equiv	equivalents
Et	ethyl
FAB	fast atom bombardment
Fmoc	9-fluorenylmethyl
g	gram
h	hour
HOMO	highest occupied molecular orbital

HMDS	hexamethyl disilazane
h $\nu$	light
HRMS	high resolution mass spectroscopy
Hz	Hertz
FTIR	Fourier transform infrared spectroscopy
L	liter
LDA	lithium diisopropyl amine
LUMO	lowest occupied molecular orbital
M	molar
M+	molecular ion
Me	methyl
MeOH	methanol
mg	milligram
MHz	megahertz
min	minutes
mL	milliliter
mM	millimolar
mol	mole
mp	melting point
$\mu$ L	microliter
nm	nanometer
NMR	nuclear magnetic resonance
nOe	nuclear Overhauser enhancement
Ph	phenyl
PMO	perturbation molecular orbital
ppm	parts per million
ppt	precipitate
Pr	propyl
R <sub>f</sub>	retention factor
TBS	<i>tert</i> -butyldimethylsilyl
THF	tetrahydrofuran

TFA	trifluoroacetic acid
TLC	thin layer chromatography
Ts	<i>para</i> -toluene sulfonyl
TMS	trimethylsilyl
UV	ultraviolet

## Section 1. 1,3-Dipolar Cycloadditions to Give Optically Active Pyrazolines

### Introduction

Cycloaddition reactions in which an alkene reacts with a 1,3-dipole provide for the efficient construction of diversely functionalized five-membered heterocycles (Figure 1).<sup>1</sup> These dipolar cycloadditions provide a means to accomplish diastereoselective and enantioselective transformations where the resulting products possess increased stereochemical and functional group complexity.

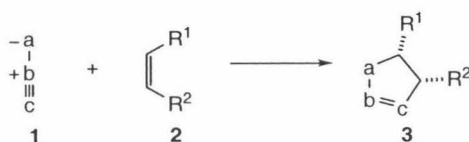


**Figure 1.** Generalized cycloaddition of a propargyl-allenyl type dipole to an alkene

Ring-opening reactions applied to the heterocyclic products provide access to highly functionalized acyclic fragments which serve as useful building blocks in complex molecule synthesis.<sup>2</sup> Substantial precedent exists for the use of 1,3-dipoles such as nitrile oxides,<sup>3a</sup> nitrones,<sup>3b</sup> nitronates,<sup>3c</sup> carbonyl ylides,<sup>3d</sup> and azomethine ylides<sup>3e</sup> in this context.

By contrast, the use of diazoalkanes for 1,3-dipolar cycloaddition reactions has not seen the same degree of application to complex molecule synthesis. We have developed a cycloaddition protocol using trimethylsilyl diazomethane as a stabilized dipole in the cycloaddition with chiral acrylates. Beyond the increased stability of trimethylsilyl diazomethane facilitating its manipulation in the lab, a novel feature of the

<sup>1</sup> (a) Huisgen, R. In *1,3-Dipolar Cycloaddition Chemistry*; Padwa, A. Ed. Wiley : New York, 1984; p.1. (b) Carruthers, W. *Cycloadditions in Organic Chemistry*, Pergamon: Oxford, 1990, p. 269. Jørgensen, K. A.; Gothelf K. V.; *Chem. Rev.*, **1998**, 98, 909.

<sup>2</sup> (a) Curran, D. P.; Yoon, M. H. *Tetrahedron*, **1993**, 49, 293 and references cited therein. (b) Denmark, S. E.; Thorarensen, A. *Chem. Rev.* 1996, 96, 223.

<sup>3</sup> (a) Zhang, J. C.; Curran, D. P. *J. Chem. Soc. Perkins Trans. I* **1991**, 11, 1991. (b) Baggolioni, E. G.; Lee, H. L.; Pizzolato, G.; Uskokovic, M. R. *J. Am. Chem. Soc.* **1982**, 104, 6460. (c) Denmark S. E.; Herbert B. J. *Org. Chem.* **2000**, 65, 2887. (d) Kinder F. R.; Bair, K. W. *J. Org. Chem.* **1994**, 59, 6965.

cycloaddition products employing this 1,3-dipole is the resulting presence of the trimethylsilyl group in the first-formed  $\Delta^1$ -pyrazolines (Figure 2). We have established that this allows for the regioselective generation of  $\Delta^2$ -pyrazolines in good yield. We have utilized these pyrazolines in a wide array of subsequent transformations to provide a range of diversely functionalized products including pyrazolidines, diamines, and amino

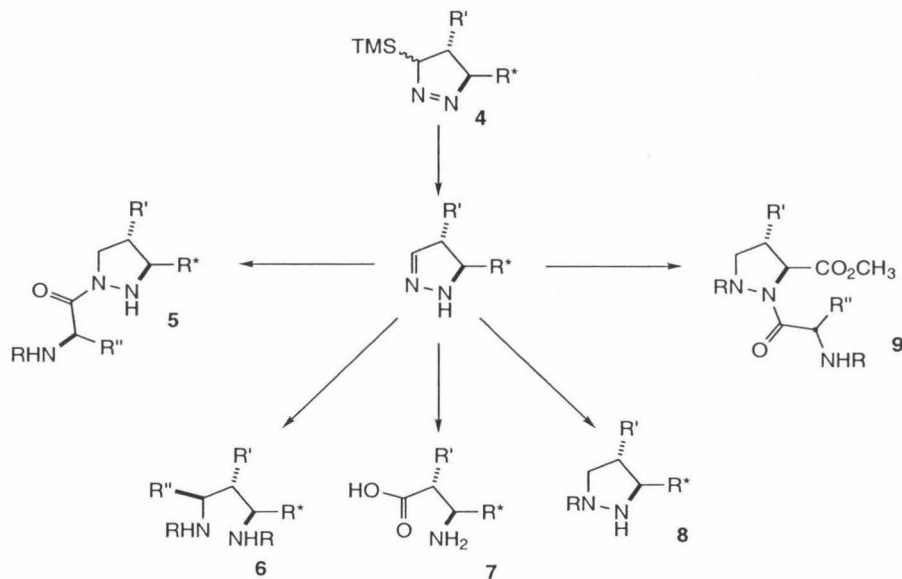


**Figure 2.** Transformations of the  $\Delta^2$ -pyrazolines from the initial cycloadduct acids. In addition to the diamine and amino acid products derived from heterocycle fragmentation, the pyrazolidine products may be employed as novel analogues of proline.

## Background

The earliest examples of reactions between diazoalkanes and unsaturated species were recorded by Buchner<sup>4</sup> and von Pechman<sup>5</sup> at the end of the 19<sup>th</sup> century, predating the concept of cycloaddition reactions. Subsequently, the high stereospecificity empirically

(e) Garner, P.; Dogan, O. *J. Org. Chem.* **1994**, *59*, 4.

<sup>4</sup> Buchner, E. *Ber. Dtsch. Chem. Ges.*, **1888**, *21*, 2637.

<sup>5</sup> von Pechman, H. *Ber. Dtsch. Chem. Ges.*, **1894**, *27*, 1888.

observed in dipolar cycloadditions led to careful work by Huisgen<sup>6</sup> and co-workers that involved the cycloaddition between diazomethane and the tiglic and angelic esters. They demonstrated that the cycloaddition was stereospecific to within 99.997% (the limit of GC detection), implying that if a stepwise mechanism were operating, that the rotational barrier about any pre-cyclization diradical intermediate would need to be in excess of 6.4 kcal/mol higher than the pathway giving collapse to product (Figure 3).

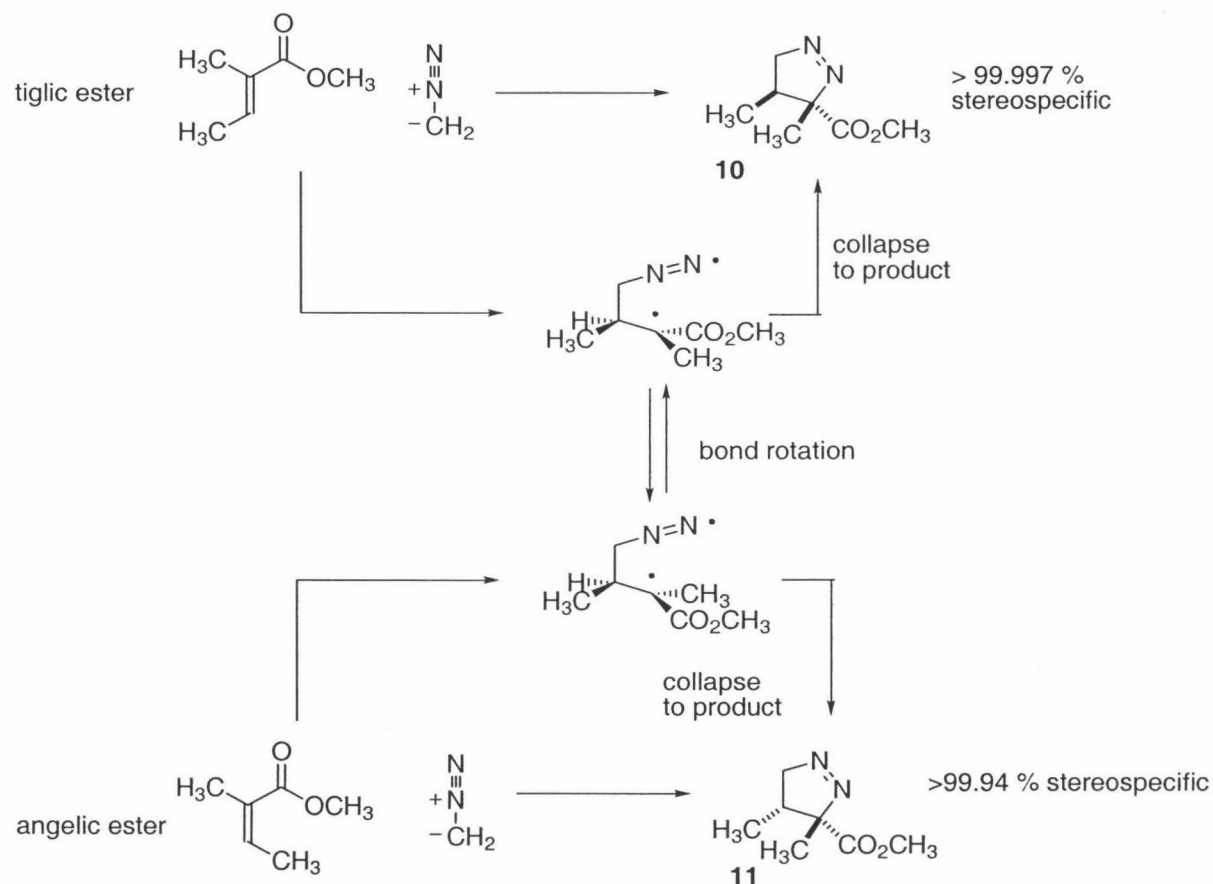


**Figure 3.** The high stereospecificity observed in Huisgen's experiments suggests a concerted mechanism

<sup>6</sup> Bihlmaier, W.; Geittner, J.; Huisgen, R.; Reissig, H. U. *Heterocycles* **1978**, *10*, 147.



A rotational barrier of this magnitude is excessively high.<sup>7</sup> A lower degree of stereospecificity would be expected if the stepwise diradical mechanism were at play. This evidence, coupled with the insensitivity of the reaction rate to the polarity of the solvent medium empirically observed by Houk<sup>8</sup> in the reaction between mesitronitrile oxide and tetracyanoethylene (wherein the rate of a stepwise mechanism should be accelerated upon increasing the solvent polarity) led to dipolar cycloaddition reactions being classified as concerted stereospecific reactions.

A theoretical treatment of the 1,3-dipolar cycloaddition between diazoalkanes and alkenes was performed by Houk.<sup>9</sup> The observed regioselectivity and reactivity of diazoalkanes is well explained by a MO picture where diazoalkanes react through the interaction of the dipole HOMO with the LUMO of the alkene dipolarophile (Figure 4).

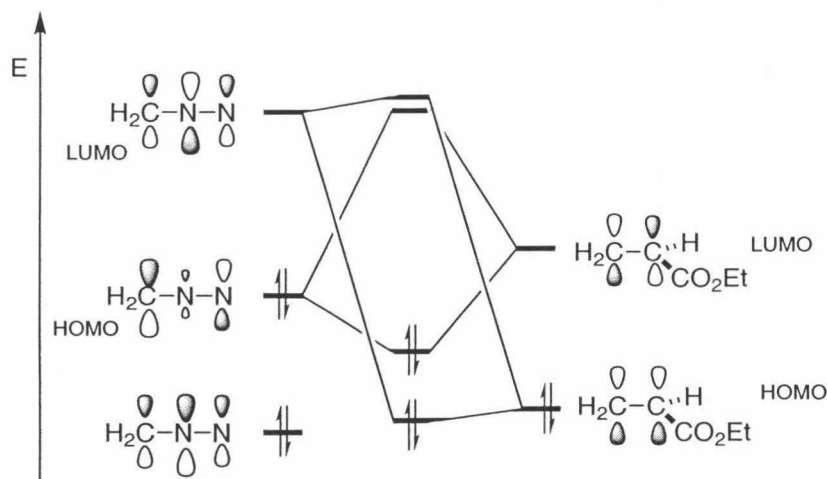


**Figure 4.** Qualitative PMO diagram of diazomethane and ethyl acrylate

In the case illustrated above, reactivity of the dipolarophile is enhanced relative to ethylene by the presence of electron withdrawing substituents which lower the dipole

<sup>7</sup> Krusic, P.; Meakin, P.; Jesson, J. P. *J. Phys. Chem.* **1971**, *75*, 3438.

<sup>8</sup> Chang, Y. -M.; Sims, J.; Houk, K. N. *Tetrahedron Lett.* **1975**, 4445.

<sup>9</sup> Houk, K. N. *J. Am. Chem. Soc.* **1972**, *94*, 8953.

HOMO–dipolarophile LUMO gap by lowering the dipolarophile LUMO. Because of this, it was expected that activated alkenes bearing electron withdrawing substituents would react in the most facile manner with trimethylsilyl diazomethane, itself bearing a higher lying HOMO than diazomethane due to the presence of the electron donating silyl substituent.

Additionally, a consideration of the molecular orbital coefficients of alkene dipolarophiles shows that the LUMO of the dipolarophile has the largest coefficient  $\alpha$  to the carbon bearing the electron withdrawing group. Because the diazoalkane cycloaddition proceeds through the diazoalkane HOMO, the predictions made by FMO theory along with consideration of the supporting empirical evidence indicate that cycloaddition between diazoalkanes and alkenes that are monosubstituted with an electron withdrawing group display a high level of regioselectivity for the 3-substituted  $\Delta^1$ -pyrazoline **12** in preference to the 4-substituted  $\Delta^1$ -pyrazoline **13** (Figure 5).<sup>10</sup>

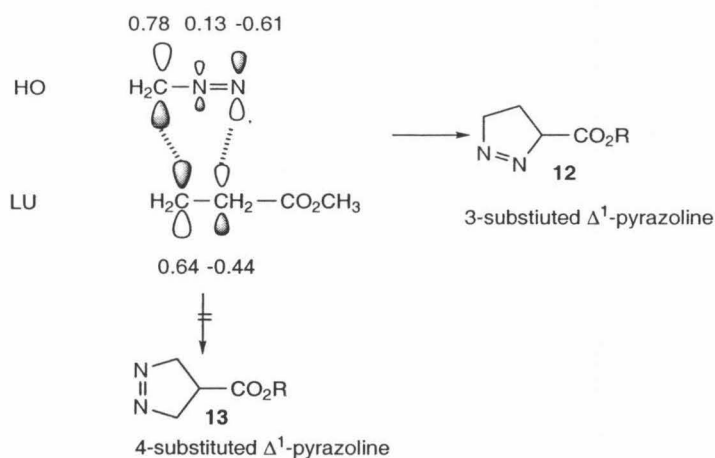
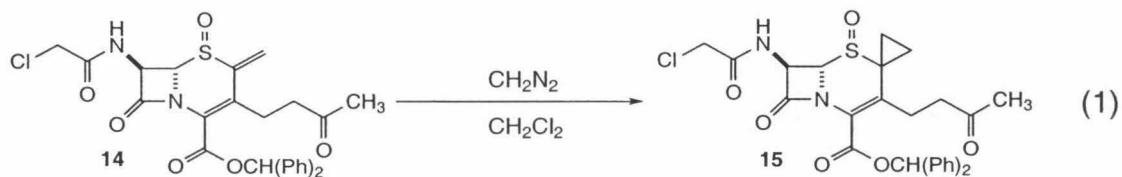


**Figure 5.** MO considerations explain observed regioselectivity

<sup>10</sup> For a detailed theoretical rationale of the observed regioselectivity in diazoalkane cycloadditions with both electron poor and electron rich alkenes, see Houk, K.N. in *1,3-Dipolar Cycloaddition Chemistry Vol. 2, Ch.13* Patai, A. Ed. Wiley, New York, 1984.

The results obtained in these experiments shaped our expectations regarding the likely course of dipolar cycloadditions between trimethylsilyl diazomethane and an activated acrylate. We expected that the cycloaddition reaction would be a stereospecific, highly regioselective process which would permit the development of a diastereoselective protocol which furnished optically active products when a chiral dipolarophile was used.

Previous applications of diazoalkane dipolar cycloadditions have been rather narrow in scope. The products from cycloadditions with alkenes are converted to cyclopropanes via nitrogen extrusion upon heating or upon irradiation with UV light.<sup>11</sup> Alternatively, the cycloadducts with alkynes are an intermediate preceding aromatization to the corresponding pyrazoles. Although the approach to cyclopropanes involving the decomposition of a pyrazoline has been largely supplanted by metal-carbenoid processes,<sup>12</sup> a recent example of a cyclopropane synthesis involving a diazoalkane was employed in the construction of carbacephem **15** (eq 1).<sup>13</sup> Examples of diazoalkane cycloadducts giving pyrazoles upon aromatization have been reported; a recent example wherein the initial diazoalkane cycloaddition with alkyne **16** leads to pyrazole **17** is shown in equation 2.<sup>14</sup>

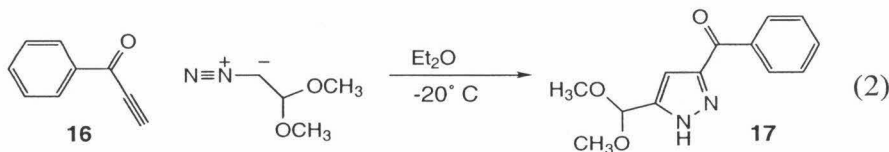


<sup>11</sup> Van Auken, T. V.; Rinehart, K. L. *J. Am. Chem. Soc.* **1962**, *84*, 3736.

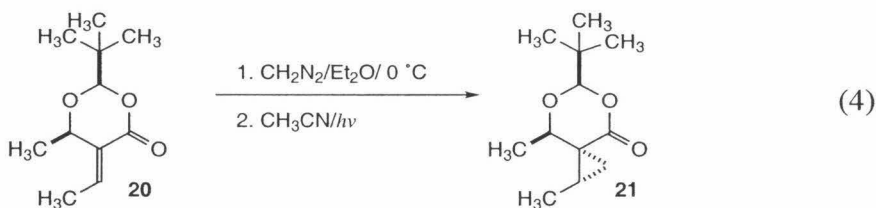
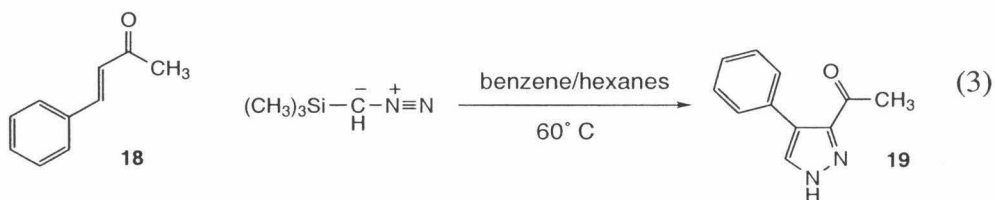
<sup>12</sup> Doyle, M. P.; Forbes, D. C. *Chem. Rev.* **1998**, *98*, 911 and references cited therein.

<sup>13</sup> Pitlik, J.; Jaszberenyi, J. C.; Komaromi, I. *Liebigs Ann. Chem.* **1991**, 699.

<sup>14</sup> Abdallah, H.; Gree, R.; Carrie, R. *Bull. Chim. Soc. Fr.* **1985**, 794.



In an early application of trimethylsilyl diazomethane, Shioiri and co-workers have reported the cycloaddition between trimethylsilyl diazomethane and an aromatic ketone, which gave pyrazole **19** upon loss of the silyl group (eq 3).<sup>15</sup> A diastereoselective cyclopropanation employing diazomethane was recently reported where nitrogen extrusion was effected by UV irradiation to furnish cyclopropane **21** (eq 4).<sup>16</sup>



### $\Delta^1$ -Pyrazolines : A Role for Silicon-Directed Isomerization

In addition to the possibility for the initial cycloaddition product to engage in pyrazole or cyclopropane formation, the first-formed  $\Delta^1$ -pyrazoline may also undergo isomerization under the cycloaddition reaction conditions to furnish the corresponding  $\Delta^2$ -pyrazolines **22** and **23** (Figure 6). Precedent for both types of  $\Delta^2$ -pyrazoline formation had been encountered in the literature. Where possible, the isomerization generally favors formation of a conjugated or more highly substituted pyrazoline product.

<sup>15</sup> Aoyama, T.; Iwamoto, Y.; Nishigaki, S.; Shioiri, T. *Chem.Pharm.Bull.* **1989**, *37*, 253.

<sup>16</sup> Bartels, A.; Liebscher, J. *Tetrahedron-Asymmetry* **1994**, *5*, 1451.

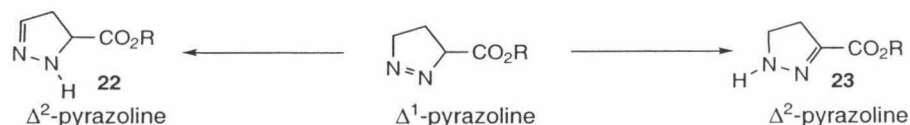
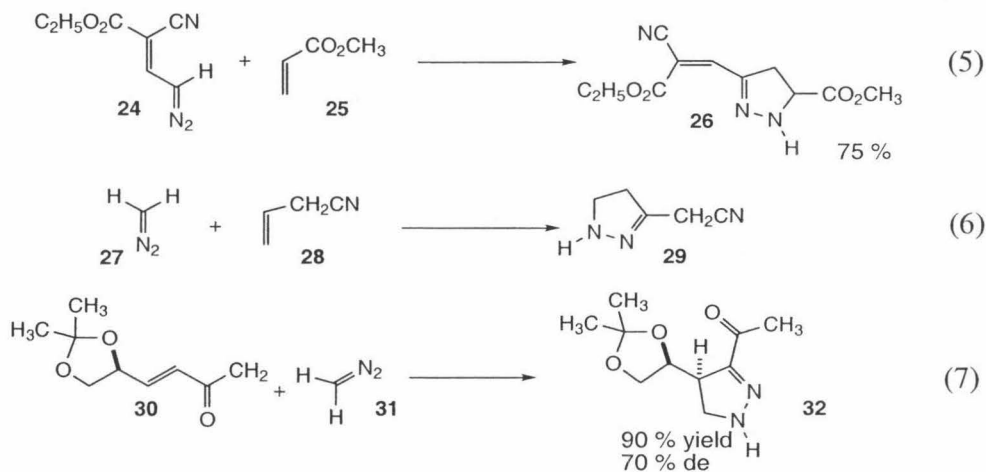


**Figure 6.** Isomerizations available to the initial cycloadduct

If this isomerization were to take place in a system such as that shown in Figure 6 to give the conjugated product **23**, it would do so with loss of chirality in the isomerization product. This behavior was documented in examples of isomerizations to give the  $\Delta^2$ -pyrazolines **26** (eq 5),<sup>17</sup> **29** (eq 6),<sup>18</sup> and **32** (eq 7).<sup>19</sup>



Because of this demonstrated preference for the formation of conjugated pyrazolines, we were mindful of the need to develop reaction conditions that would minimize or eliminate this mode of isomerization to obtain pyrazolines chirality  $\alpha$ -to the activating group. The past decade has seen the popularization of trimethylsilyl diazomethane as a commercially available diazomethane substitute for the *O*-methylation of acids,<sup>20a</sup> enols,<sup>20b</sup> and alcohols.<sup>20c</sup> We speculated that the use of trimethylsilyl

<sup>17</sup> Sasaki, T.; Shoji, E.; Kojima, A. *J. Heterocycl. Chem.* **1968**, *5*, 243.

<sup>18</sup> Mihalikova V. N.; Bulat, A. D. *Zh. Org. Chim.* **1971**, 2223.

<sup>19</sup> Galley, G.; Pätzelt, M.; Jones, P. G. *Tetrahedron* **1995**, *51*, 1631.

<sup>20</sup> a) Hashimoto, N.; Aoyama, T.; Shioiri, T. *Chem. Pharm. Bull.* **1981**, *29*, 1475. b) Aoyama, T.; Tenshwa, S.; Sudo, K.; Shioiri, T. *Chem. Pharm. Bull.* **1984**, *32*, 3759. c) Aoyama, T.; Shioiri, T. *Tetrahedron Lett.* **1990**, *31*, 5507.

diazomethane in the synthesis of pyrazolines would offer advantages beyond its enhanced safety that would make its application to 1,3-dipolar cycloadditions useful.

We anticipated that the presence of the trimethylsilyl group in the first-formed  $\Delta^1$ -

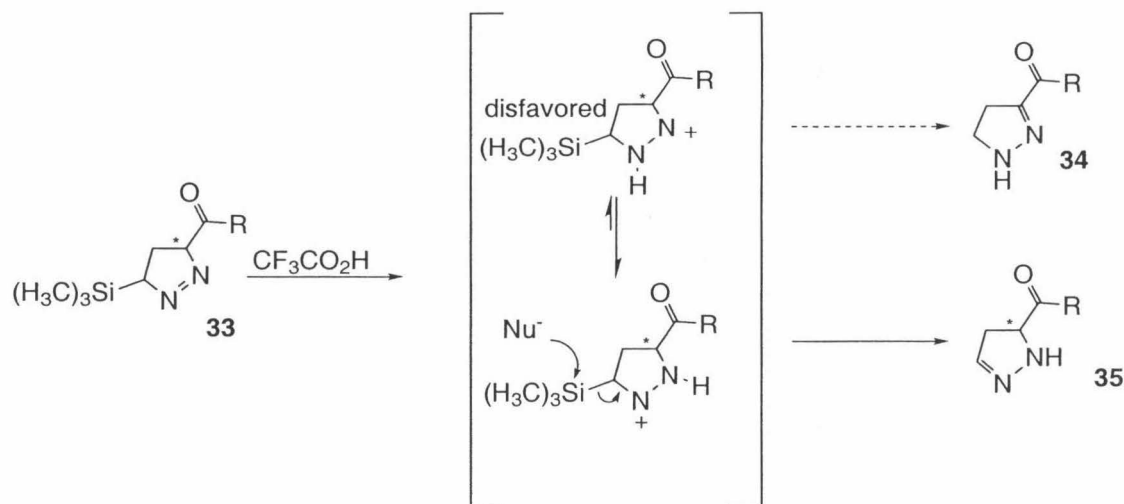


**Figure 7.** Directed pyrazoline isomerization involving silicon

pyrazoline would offer a handle which could be employed in the acid promoted isomerization to the desired  $\Delta^2$ -pyrazoline. This would avoid the mode of isomerization that results in the loss of the important  $\alpha$ -carbon stereocenter (Figure 7).

This expectation was guided by the precedent established by the groups of Fleming<sup>21</sup> and Denmark<sup>22</sup> in their work with silicon-modified cationic cyclizations. We saw the potential for selective isomerization of the first-formed cycloadduct in a way that would not be possible in the absence of the trimethylsilyl substituent. Based on the documented ability of silicon species to stabilize  $\beta$ -cationic character,<sup>23</sup> we hoped to use this feature as a handle that could be used for the regioselective formation of the

<sup>21</sup> Fleming, I.; Terret, N. K. *Pure and Appl. Chem.* **1983**, *55*, 1707.

<sup>22</sup> Denmark, S. E. *J. Am. Chem. Soc.* **1982**, *104*, 2642.

comparatively stable  $\Delta^2$ -pyrazolines which are known to be less prone to aromatization and nitrogen extrusion than the corresponding  $\Delta^1$ -pyrazolines.<sup>24</sup>

The electropositive character of silicon allows for polarization of the carbon-silicon bond. This polarization provides stabilization of the empty p-orbital of a carbocation  $\beta$  to the silicon atom.<sup>21</sup> The recognition of the  $\beta$ -carbocation stabilizing ability of silicon (Figure 8) has resulted in the development of modified reactions where the presence of a silicon atom directs the regiochemistry of double bond formation in

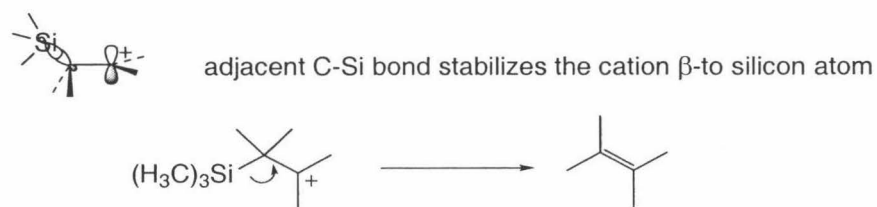


**Figure 8.** Cation stabilization at the  $\beta$ -position

processes which would otherwise generate alkene regioisomers.<sup>25</sup>

An early example of this is provided by Fleming and Pearce<sup>26</sup> where the cationic cyclization of a trimethylsilyl-containing-acetal took place with complete regioselectivity in double bond formation (eq 8), while previously the use of the same conditions with the unsubstituted acetal furnished the cyclization product giving a distribution of alkene regioisomers (eq 9).<sup>27</sup> Similar regioselectivity of alkene formation was observed in the

<sup>23</sup> C. Eaborn and R.W. Bott in *'Organometallic Compounds of Group IV Elements' Vol. 1, Part 1*, A. G. MacDiarmid, Ed. Dekker, New York, 1968.

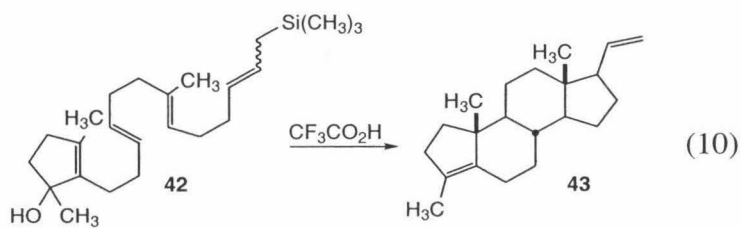
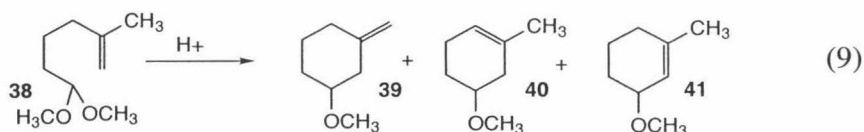
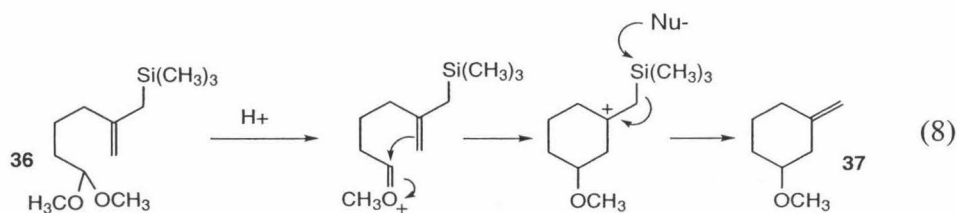
<sup>24</sup> Jones, W. M.; Sanderfer, P. O.; Baarda, D. G. *J. Org. Chem.* **1967**, *32*, 1367.

<sup>25</sup> Denmark, S. E.; Habermas, K. L.; Hite, G. A.; Jones, T. K. *Tetrahedron* **1986**, *11*, 2821.

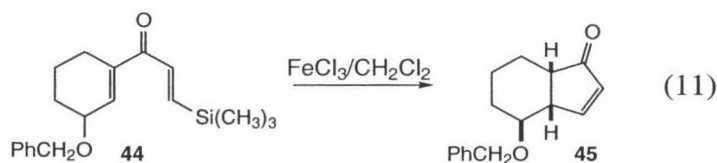
<sup>26</sup> Fleming, I.; Pearce, A.; Snowden, R. L. *J. Chem Soc. Chem. Comm.* **1976**, 182.

<sup>27</sup> van der Gen, A.; Wiedhaup, K.; Swoboda, J. J.; Dunathan, H. C.; Johnson, W. S. *J. Am Chem. Soc.* **1973**, *95*, 2656.

trimethylsilyl-modified cationic cyclization Johnson employed in his synthesis of ( $\pm$ ) progesterone (eq 10).<sup>28</sup>



Denmark's work with silicon-modified Nazarov cyclizations is similarly instructive. In contrast to conventional Nazarov cyclizations where the position of unsaturation in the product is capricious, the  $\beta$ -cation stabilizing ability of silicon is used to facilitate regioselective alkene formation (eq 11).



Based on these precedents, we believed that an isomerization protocol could be established which would preserve the stereocenter set at the carbon  $\alpha$ -to the acrylate carbonyl in the initial cycloaddition. This would then allow for the development of a

<sup>28</sup> Hughes, R. L.; Schmid, R.; Johnson, R. S. *Bioorg. Chem.* **1979**, *8*, 513.



diastereoselective cycloaddition process providing that the dipolarophile was a chiral molecule.

### **Preliminary Investigations**

A primary goal in the development of our diazoalkane cycloaddition methodology was to provide synthetically useful cycloadducts that were optically active. These products would serve as valuable building blocks in asymmetric complex-molecule synthesis. The application of these pyrazolines and pyrazolidines as proline surrogates and also as precursors for novel acyclic products necessitated a protocol that would furnish optically active  $\alpha$ -amino acid analogues.

At the outset of this research, diastereoselective trimethylsilyl diazomethane dipolar cycloadditions with optically active alkenes had not been reported. In preliminary experiments in the Carreira group by Dr. Wheesong Lee, cycloadditions between trimethylsilyl diazomethane and achiral ester, imide and sulfonimide dipolarophiles were performed. Consistent with the respective abilities of these groups to lower the dipolarophile LUMO, the cycloaddition reaction was found to proceed most rapidly (in a matter of hours) when the sulfonimide moiety was employed (Figure 9). This result suggested the use of a chiral sulfonimide as an auxiliary for the asymmetric version of this reaction due to its capacity to serve as both 1) an activating group which lowers the alkene LUMO; and 2) a chiral directing group which allows discrimination between the alkene stereofaces upon approach of the 1,3-dipole to the camphorsultam-bearing alkene.

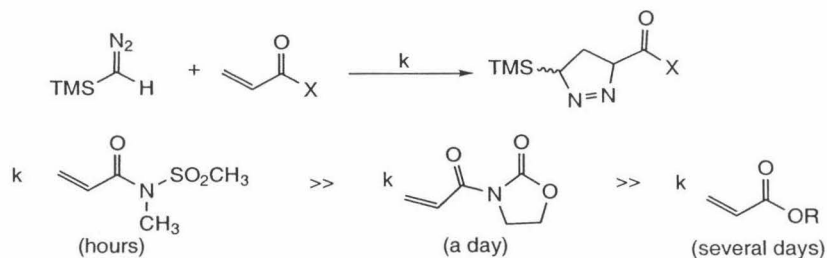
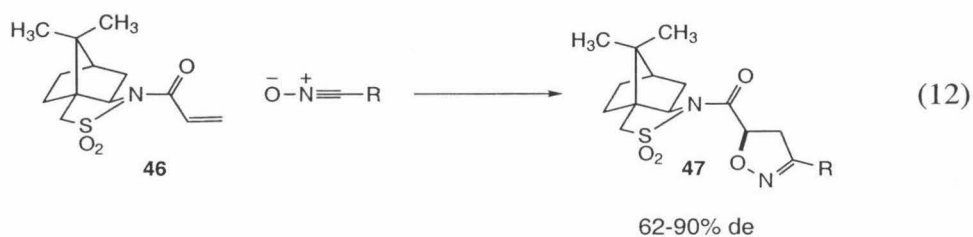
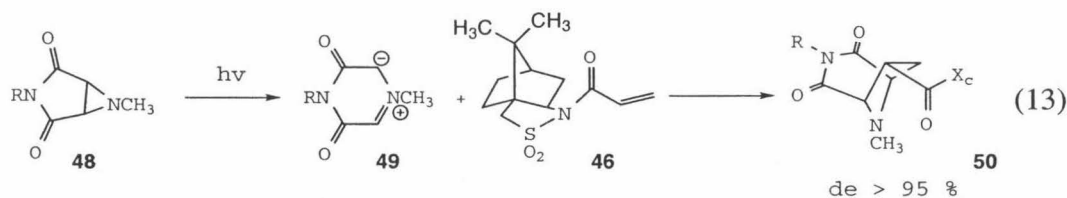


**Figure 9.** Preliminary results suggested sulfonimide-derived acrylates

While it was Oppolzer and co-workers who first developed the camphorsultam auxiliary and explored its application to asymmetric reactions including aldol additions,<sup>29</sup> enolate alkylations,<sup>30</sup> and Diels-Alder cycloadditions,<sup>31</sup> its initial successful application to 1,3-dipolar cycloadditions was reported by Curran for nitrile oxide cycloadditions to chiral acrylates (eq 12).<sup>32</sup>



Subsequent to this initial disclosure, camphorsultam derived acrylates have served as dipolarophiles in reactions with a variety of 1,3 dipoles including azomethine imines (eq 13),<sup>33</sup> silyl nitronates (eq 14),<sup>34</sup> and nitrones (eq 15).<sup>35</sup>



<sup>29</sup> Oppolzer, W.; Starkemann, C. *Tetrahedron Lett.* **1992**, *33*, 2439.

<sup>30</sup> Oppolzer, W.; Moretti, R.; Thomi, S. *Tetrahedron Lett.* **1989**, *30*, 6009.

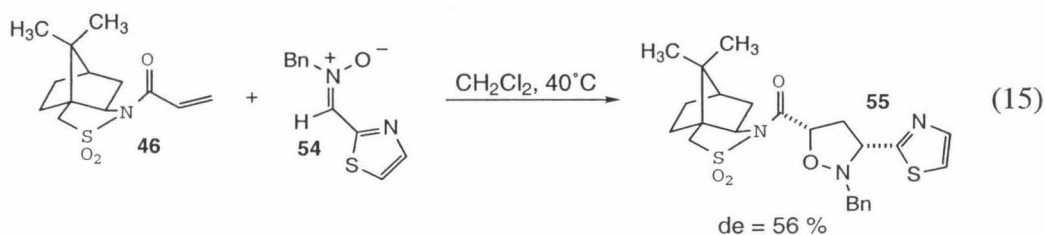
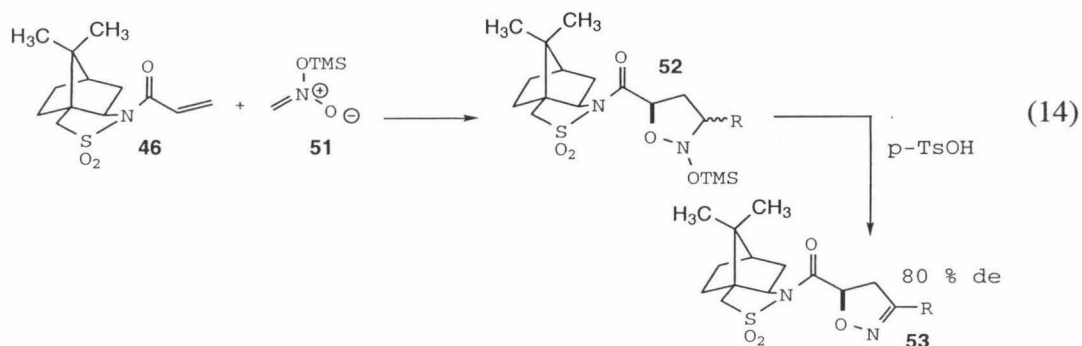
<sup>31</sup> Oppolzer, W.; Chapuis, C.; Bernardelli, G. *Helv. Chim. Acta* **1984**, *67*, 1397.

<sup>32</sup> Curran, D. P.; Kim, B. H.; Daugherty, J.; Heffner, T. A. *Tetrahedron Lett.* **1988**, *29*, 3555.

<sup>33</sup> Garner, P.; Ho, W.B. *J. Org. Chem.* **1990**, *55*, 3973.

<sup>34</sup> Kim, B. H.; Lee, J. Y.; Kim, K. M.; Whang, D. M. *Tetrahedron: Asymmetry* **1991**, *2*, 27.

<sup>35</sup> Tejero, T.; Dondoni, A.; Rojo, I.; Merchan, F. L.; Merino, P. *Tetrahedron* **1997**, *53*, 3301.



The first use of a camphorsultam-derived acrylate as a substrate for the dipolar cycloaddition reaction with trimethylsilyl diazomethane was performed by Dr. Gavin Whitlock in the context of the synthesis of Stelletamide A (**56**).<sup>36</sup> In this effort, the  $\beta$ -substituted dipolarophile **59** was found to undergo the desired cycloaddition reaction to give the pyrazoline product in a 93:7 ratio of diastereomers. Subsequent treatment with silver triflate and ethyl chloroformate gave the desilylated pyrazoline **58** in 76% yield. This pyrazoline was subsequently elaborated to the natural product in a short sequence of transformations via key intermediate **57**. It is noteworthy that both of the nitrogens and both of the stereocenters present in the advanced intermediate **57** are introduced in the cycloaddition step (Figure 10). Encouraged by the success of the cycloaddition route to provide the pyrazoline **58**, we turned to the task of establishing the generality of the

<sup>36</sup> Whitlock, G. A.; Carreira, E. M. *J. Org. Chem.* **1997**, *62*, 7916.

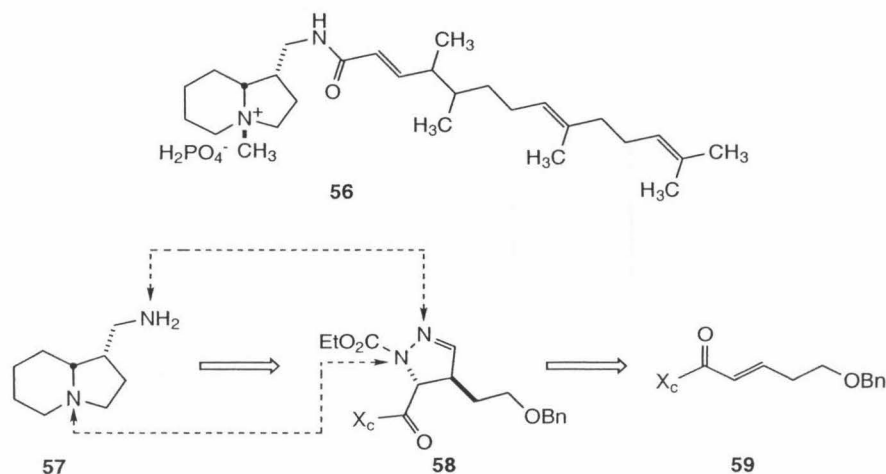


**Figure 10.** The first application of the cycloaddition leads to Stellettamide A

cycloaddition process and exploring the scope of the transformations which the resulting pyrazoline products could undergo.

Herein is reported the general protocol that we have developed for the diastereoselective synthesis of  $\Delta^2$ -pyrazolines via the cycloaddition of trimethylsilyl diazomethane with camphorsultam-derived acrylates. This procedure makes use of the camphorsultam auxiliary to effect  $\pi$ -facial selectivity in the cycloaddition reaction and subsequently exploits the presence of the trimethylsilyl group in the first-formed  $\Delta^1$ -pyrazoline to allow regioselective isomerization to the desired  $\Delta^2$ -pyrazoline. In keeping with our desire to discover the scope of transformations which these pyrazolines may undergo, this intermediate has been subjected to reduction, fragmentation, and nucleophilic addition reactions that deliver optically active pyrazolidines, diamines, and  $\alpha$ -amino acid products that are not accessible by means of previously investigated diazoalkane dipolar cycloadditions.

## Scope of the cycloaddition Reaction - Results and Discussion

Our initial efforts focused on the cycloaddition of camphorsultam-derived acrylic acid, prepared via treatment of the camphorsultam auxiliary with 1.1 equiv NaH in toluene, followed by addition of an equivalent of acryloyl chloride.<sup>37</sup> Treatment of a 0.1 M solution of acrylate **46** in CH<sub>2</sub>Cl<sub>2</sub> with 1.1 eq. TMSCHN<sub>2</sub> (utilized as the commercially supplied 2.0 M solution in hexanes) at room temperature resulted in the consumption of starting material and the concomitant generation of the cycloaddition product as identified by <sup>1</sup>H NMR (Scheme 1). This initial Δ<sup>1</sup>-pyrazoline, isolated as a glassy solid upon removal of solvent and excess diazoalkane via rotary evaporation, was found to be unstable to purification by column chromatography.

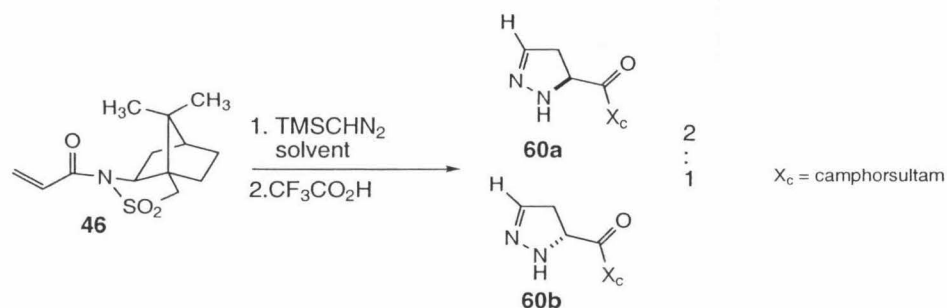
These difficulties were overcome by treatment of a CH<sub>2</sub>Cl<sub>2</sub> solution of the initial Δ<sup>1</sup>-pyrazoline cycloadduct with an equivalent of trifluoroacetic acid. This procedure led to the desilylation of the cycloadduct with concomitant isomerization to the Δ<sup>2</sup>-pyrazoline with an overall yield of 72%, as calculated from the starting acrylate. The Δ<sup>2</sup>-pyrazoline was found to be chromatographically stable. We were pleased to observe that none of the isomerization to furnish the regioisomeric conjugated Δ<sup>2</sup>-pyrazoline, with a loss of stereochemistry at C<sub>ω</sub> was detected. Under the initial conditions used for the cycloaddition, <sup>1</sup>H NMR evaluation showed a 2:1 mixture of diastereomeric products **60a** and **60b**, this ratio being determined by integration of the individual methine proton resonances of the diastereomeric pyrazolines which appeared at δ 6.72 and 6.86 ppm (Scheme 1) respectively.

---

<sup>37</sup> Oppolzer, W.; Starkemann, C. *Tetrahedron Lett.* **1992**, *33*, 2439.

A consideration of the model which Curran has proposed for the origin of diastereoselectivity in cycloadditions utilizing camphorsultam-derived acrylates<sup>38</sup> guided

### Scheme 1



our subsequent efforts to optimize the dipolar cycloaddition reaction with trimethylsilyl diazomethane. The four limiting conformations available to the camphorsultam-derived acrylate which may lead to cycloaddition are presented in Figure 11.

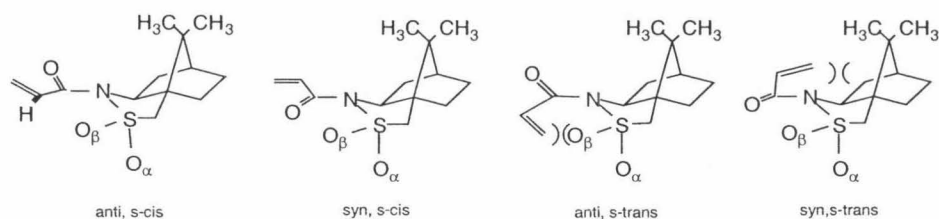


**Figure 11.** Conformations available to *N*-acryloyl sultams

The *anti, s-trans* and *syn, s-trans* rotamers of acrylate derived camphorsultam are discounted on the grounds of unfavorable steric interactions between the auxiliary and enoate portions of the molecule. Of the remaining *syn, s-cis* and *anti, s-cis* rotamers, the *anti, s-cis* rotamer is the ground state energy minimum, as the *syn, s-cis* rotamer is higher in energy due to unfavorable dipolar interactions. The approach of the reagent is assumed to occur from the face opposite to O<sub>α</sub> in any of the conformations. The typical direction of approach of trimethylsilyl diazomethane to the *anti, s-cis* conformer of the

<sup>38</sup> Kim, B. H.; Curran, D. P. *Tetrahedron* **1993**, *49*, 293.

2,10-(*R*)-camphorsultam bearing dipolarophile is seen to lead to the (*S*, *R*) diastereomer as the major product. The results of single crystal X-ray analysis of the pyrazoline products **60a**,<sup>39</sup> **64** and **65** (Table 2) support this analysis. This model for diastereoselectivity invokes an unfavorable dipole interaction as the source of the preference for the *anti-s-anti* conformer over the *syn-s-cis* conformer.

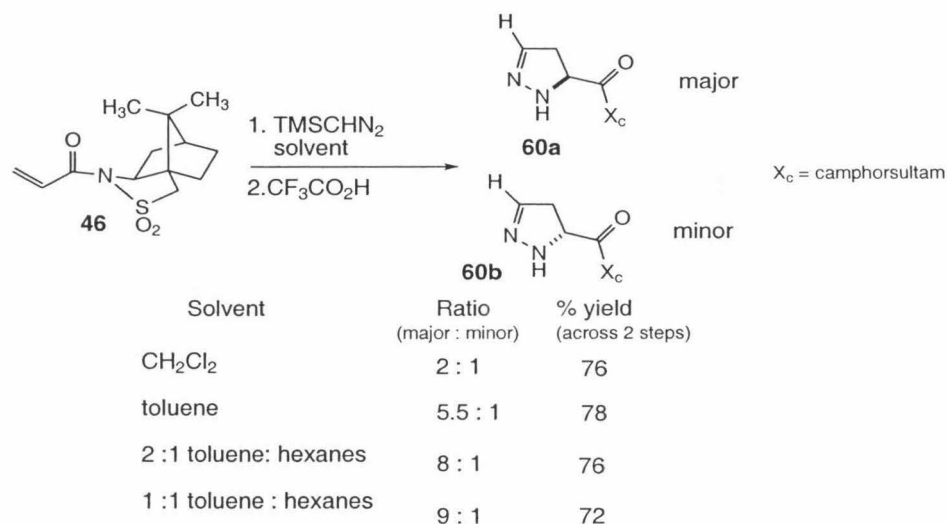
In an attempt to improve the cycloaddition diastereoselectivity, the reaction was performed in toluene ( $\epsilon=2.4$ ) instead of  $\text{CH}_2\text{Cl}_2$  ( $\epsilon=9.0$ ). After the first-formed cycloadduct was desilylated as described above,  $^1\text{H}$  NMR analysis showed that the cycloaddition had proceeded in a 5.5 :1 ratio in favor of the same diastereomer as in the case where  $\text{CH}_2\text{Cl}_2$  was used as reaction solvent.

Given the improvement in reaction diastereoselectivity upon changing the reaction solvent to toluene, we surveyed the effect of varying reaction solvent on the diastereoselectivity of the cycloaddition reaction. The results are presented in Table 1.

The solubility of the camphorsultam-derived acrylate ultimately proved to be the limiting factor in the extent to which exclusively non-polar solvent media could be employed. It was observed that while a solvent system comprised of a mixture of 1:1 toluene/hexanes provided the highest reaction diastereoselectivity (a 9:1 ratio), poor substrate solubility limited increasing the ratio of hexanes ( $\epsilon=1.9$ ) to toluene beyond this point. It should be noted that similar trends in cycloaddition diastereoselectivity were reported in Curran's study of nitrile oxide cycloadditions involving related camphorsultam-derived acrylate systems.<sup>30</sup>

---

<sup>39</sup> X-Ray crystal data for **60a** is reported in Appendix I

**Table 1.** The effect of reaction solvent on cycloaddition diastereoselectivity

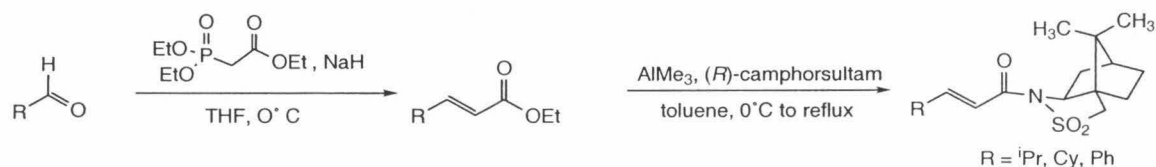
The results of the above study show that the ratio of diastereomeric products was influenced by the polarity of the solvent system. Because of the documented insensitivity of the rate of cycloaddition reactions to solvent polarity,<sup>8</sup> we judged it unlikely that the less polar solvent medium was accelerating the rate of cycloaddition for one diastereomeric transition state in preference to the other. An explanation for the observed trend in reaction diastereoselectivity as a function of solvent polarity may instead be provided by the model for stereoselectivity in the reactions of *N*-enyl camphorsultam derivatives that has been proposed by Curran. By this analysis, the relative population of the enyl sultam conformer leading to the minor diastereomer in the cycloaddition reaction is decreased in a non-polar solvent medium due to the reduced ability of the reaction solvent to mediate the unfavorable dipolar interaction present in this conformer. Because of the higher relative population of the *anti-s-cis* enyl sultam as the solvent medium polarity decreases, non-polar solvent systems lead to a diastereomer ratio that



reflects this shift in conformer population. With the optimization of reaction diastereoselectivity complete for the parent substrate, studies were then undertaken to evaluate which acrylates would participate in the cycloaddition reaction (Table 2).

Dipolarophiles **46**, and **61-63** were synthesized by treatment of Oppolzer's sultam with NaH, followed by addition of the appropriate acid chloride.<sup>29</sup> Substrates **65-67** were furnished by a two step sequence employing Horner-Wadsworth-Emmons olefination<sup>40</sup> of the corresponding aldehydes followed by amidation of the resulting enoates using trimethylaluminum<sup>41</sup> and camphorsultam auxiliary (Scheme 2).

### Scheme 2

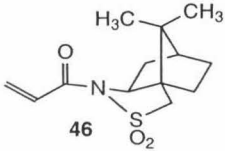
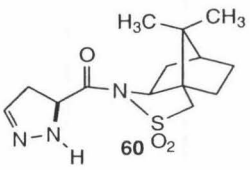
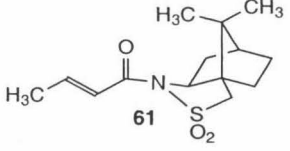
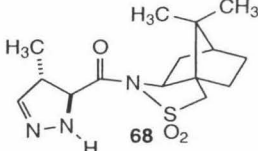
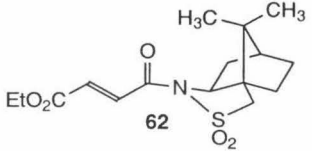
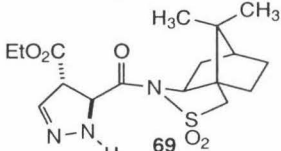
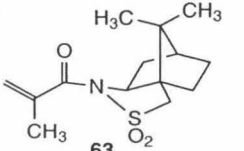
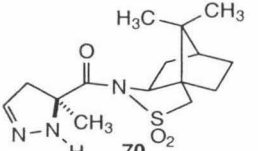
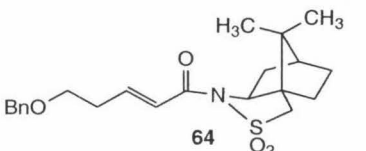
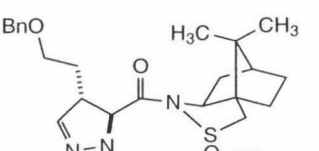
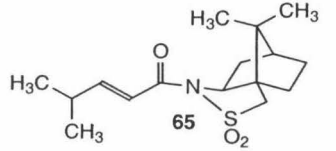
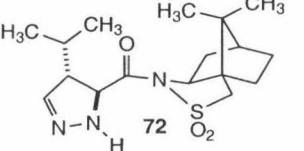
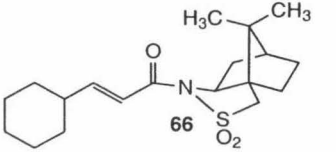
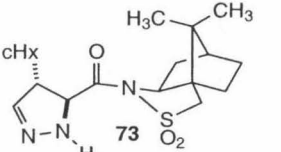
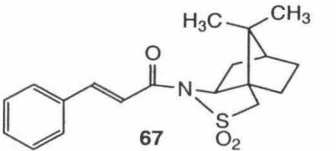
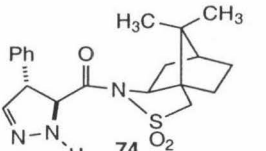


Each of the dipolarophiles examined led to pyrazoline products in good yield and diastereoselectivity. Chromatography proved effective in separating the diastereomeric products.

<sup>40</sup> Wadsworth, W. S.; Emmons, D. *Org. Synth.* **1965**, 45, 44.

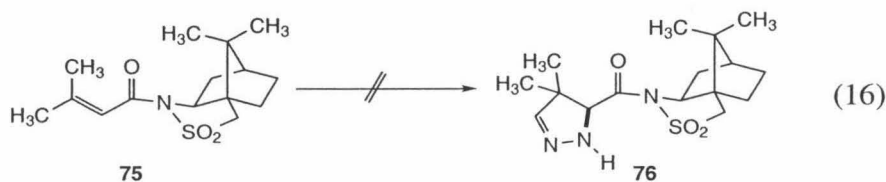
<sup>41</sup> Basha, A.; Lipton, M.; Weinreb, S. M. *Tetrahedron Lett.* **1977**, 4171.

**Table 2.** Diastereoselective cycloaddition applied to a range of acrylates

Dipolarophile	Product (major diastereomer)	yield	ds
 <p>46</p>	 <p>60</p>	72	9:1
 <p>61</p>	 <p>68</p>	67	9:1
 <p>62</p>	 <p>69</p>	78	91:9
 <p>63</p>	 <p>70</p>	65	94 : 6
 <p>64</p>	 <p>71</p>	91 <sup>a</sup>	10:1
 <p>65</p>	 <p>72</p>	67	95:5
 <p>66</p>	 <p>73</p>	67	95 : 5
 <p>67</p>	 <p>74</p>	58	8:1

Past precedent established by dipolar cycloadditions with related dipolarophiles led us to expect high cycloaddition regioselectivity in the cases of the non-conjugated, alkyl substituted dipolarophiles **46**, **61**, **63**, **65** and **66**. Single cycloaddition regioisomers were also obtained in the cases of dipolarophiles **62** and **67**, where the presence of a second electron withdrawing group in conjugation with the alkene increases the potential for regioisomeric cycloaddition mixtures.<sup>1</sup> The range of dipolarophiles examined shows a good tolerance for steric bulk at the position  $\beta$  to the acrylate carbonyl. Monosubstituted dipolarophiles with substituents ranging in size from methyl in the case of dipolarophile **61** to that possessing a substituent as bulky as in the cyclohexyl substituted dipolarophile **66** proceed in good yield and diastereoselectivity. The cycloaddition was found to proceed with good diastereoselectivity even in the case of the extremely hindered  $\alpha$ -substituted dipolarophile **63**, albeit requiring longer reaction times and a three-fold excess of TMSCHN<sub>2</sub> to effect cycloaddition in a period of one week.

The limit for steric bulk tolerated at the alkene terminus is apparently exceeded at camphorsultam-derived prenylate **75**, which showed no trace of product formation as judged by <sup>1</sup>H NMR, even after reaction times exceeding one week (eq 16).



Several of these pyrazolines have seen further use as intermediates in organic synthesis. The ability to effect cycloaddition on an  $\alpha$ -methyl substituted acrylate such as **57** offers new method for the synthesis of an important class of hindered  $\alpha$ -amino acid analogues. The cycloaddition product **71** provided the starting material for the naturally

occurring indolizidine alkaloid Stelletamide A (Figure 10), which demonstrates the ability for this cycloaddition methodology to provide highly functionalized, optically active products that may be used in complex molecule synthesis. The dipolarophiles that have taken part in the cycloaddition with trimethylsilyl diazomethane demonstrate that our methodology offers broad access to substituted, optically active pyrazolines.

## Section 2. Application of Optically Active Pyrazolines to Amino Acid Analogue Synthesis

The development of the 1,3-dipolar cycloaddition methodology to access pyrazolines was, in part, driven by our recognition that the resulting products may serve as novel analogues of proline. In the system which we planned to explore, a wide array of both steric and electronic modifications could be introduced at every position of the pyrazoline ring (Figure 12). We reasoned that such an analogue system would be a valuable addition to those which are available for the study of the behavior of peptides that include a proline residue.

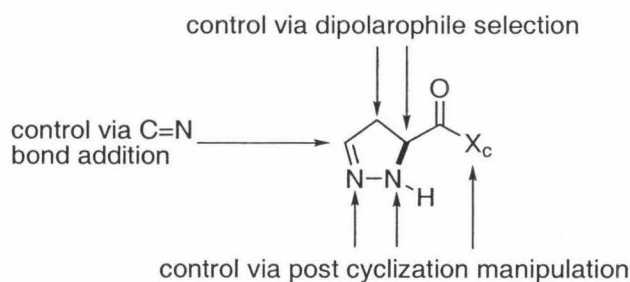


**Figure 12.** Pyrazoline substitution is modifiable at every position of the ring

### Background

Proline is unique among the proteinogenic  $\alpha$ -amino acids in that it is the sole example of a secondary amine. While other amino acids preferentially adopt the *trans*-

amide geometry to avoid steric interaction between the side chain of one residue and the amide moiety of the next that would be encountered in the *cis* conformation, the alkyl side chain cyclized back onto the amine in proline results in a competitive steric interaction in the *trans* amide geometry as well (Figure 13).

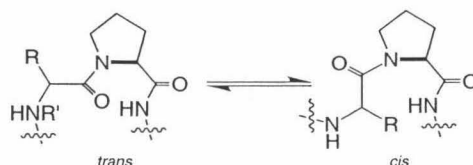


**Figure 13.** *Cis-trans* prolyl peptide isomerism

These factors result in the *cis* and *trans* amide forms of prolyl dipeptides being approximately equal in energy, but possessing a barrier of interconversion of approximately 20 kcal/mol,<sup>42</sup> essentially the barrier of rotation about the amide bond. The capacity for prolyl-peptides to engage in *cis*-amide bonds is thought to be related to the turns and other structural anomalies which often occur in peptides as structure-breakers in the vicinity of proline residues. Interconversion between the *cis*- and *trans*-amide geometries of prolyl peptides is a process which can be facilitated in proteins by proline isomerases.<sup>43</sup> The biological recognition of certain proline-containing peptide sequences has been found in some cases, such as those of the prolyl peptidases, to require the *trans* geometry about the N-terminal prolyl-amide bond.<sup>44</sup> It has been suggested that peptidyl inhibitors of prolyl peptide hydrolysis may operate through the inhibition of proline isomerases.<sup>45</sup>

<sup>42</sup> Schmid, F. X. *Annu. Rev. Biophys. Biomol. Struct.* **1993**, 22, 123.

<sup>43</sup> Merker, M. P.; Dawson, C. A.; Bongard, R. D.; Roerig, D. L.; Haworth, S. T.; Linehan, J. H. *J. Appl. Physiology*, **1993**, 75, 1519.

<sup>44</sup> Andres, C. J.; Macdonald, T. L.; Ocain, T. D.; Longhi, D. *J. Org. Chem.* **1993**, 58, 6609.

<sup>45</sup> Galat, A. *Eur. J. Biochem.* **1993**, 216, 689.

The extensive work reported regarding the development of proline analogues reflects the importance of the capacity for proline to engage in *cis*-amide bonds. Many analogues have been designed which lock the amide geometry into the *cis*-like conformation (Figure 14). This constraint has been effected in a number of ways. The first involves the use of monocyclic or bicyclic analogues such as **A**, **B**, and **C**, which mimic a prolyl dipeptide, and whose ring geometry mimics the structural orientation of a dipeptide with a *cis*-amide bond. The second method employs  $\delta$ -carbon substituted pyrrolidine rings such as **D**. By increasing the steric bulk at this location, the corresponding amide bond is effectively locked into a *cis*-amide orientation, or at least is driven out of the *trans*-amide geometry.

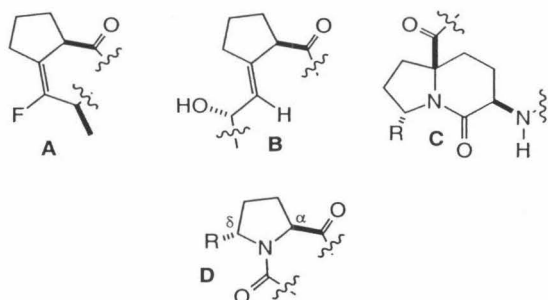


**Figure 14.** Examples of conformationally constrained proline mimics

Reliable, general methods for the asymmetric synthesis of novel  $\alpha$ -amino acids are plentiful,<sup>46</sup> however only a few of these strategies can be applied to the synthesis of proline surrogates.<sup>47</sup> Additionally, methodologies which specifically target proline-

<sup>46</sup>(a) Williams, R. M. In *Organic Chemistry Series Volume 7; Synthesis of optically active  $\alpha$ -amino acids*; Baldwin, J.E., Magnus, P.D., Eds.; Pergamon : Oxford, 1989. b) Duthaler, R. O. *Tetrahedron* **1994**, *50*, 1539. (c) Myers, A. G.; Gleason, J. L.; Yoon, T. Y. *J. Am. Chem. Soc.* **1995**, *117*, 8488 and references cited therein. (d) Trost, B.M.; Ariza, X. *J. Am. Chem. Soc.* **1999**, *121*, 10727 and references cited therein.

<sup>47</sup> (a) Delaney, N. G.; Madison, V. G. *J. Am. Chem. Soc.* **1982**, *104*, 6635. (b) Seebach, D., Boes, M.; Naef, R.; Bernd-Schweizer, W. *J. Am. Chem. Soc.* **1983**, *105*, 5390. (c) Beausoleil, E.; Lubell, W. D. *J. Am. Chem. Soc.* **1996**, *51*, 12902.

analogue synthesis typically do so by offering a means of incorporating novel alkyl-substitution elsewhere on the pyrrolidine ring.

A notable example of this type of proline analogue is that of Lubell, where it was demonstrated through the synthesis of a series of 5-alkyl prolines that increasing steric bulk at this position encourages polypeptides containing this analogue to adopt a *cis*-amide geometry (Figure 4).<sup>48</sup> This propensity also allowed for the construction of a type VI  $\beta$ -turn mimic.<sup>49</sup> Our own system, while electronically and structurally very different, would nevertheless allow for the capacity to build up steric bulk at the equivalent position of the pyrazolidine ring.

In a report pertinent to the construction of aza-analogues of  $\alpha$ -amino acids, Ciufolini has synthesized the six-membered aza-analogue<sup>50</sup> of the naturally occurring pipercolic acid. It was postulated that the interaction between the piperazic acid hydrazone-*N* and the neighboring amide C=O oxygen causes them to be oriented in such a way as to minimize unfavorable electrostatic interaction, leading to the increased conformational rigidity of piperazic-acid-containing dipeptides. Ciufolini further demonstrated that this conformational rigidity leads to a dipeptide conformation that was conducive to a turn motif (Figure 15).<sup>51</sup>

---

<sup>48</sup> Lomabart, H.-G.; Lubell, W. D.; Beausoleil, E. *J. Org. Chem.* **1994**, *59*, 6147.

<sup>49</sup> Halab, L.; Lubell, W. D.; *J. Org. Chem.* **1999**, *64*, 3312.

<sup>50</sup> Xi, N.; Alemany, L. B.; Ciufolini, M. A.; *J. Am. Chem. Soc.* **1998**, *120*, 80.

<sup>51</sup> Ciufolini, M. A.; Xi, N. *Chem. Soc. Rev.* **1998**, *27*, 437.

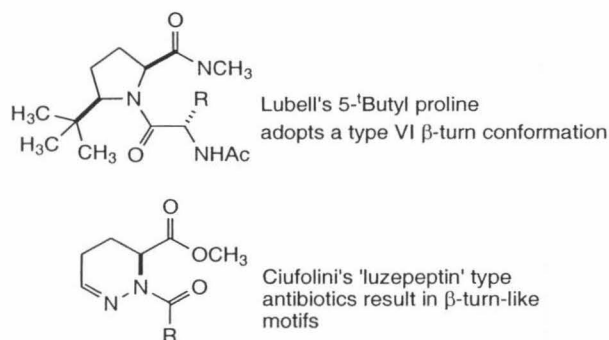


**Figure 15.** Prolyl-dipeptide systems leading to turn motifs

In a related report, molecular modeling was used to explore the likely conformational preferences of the analogous pyrazoline system. While ready access to the six-membered ring systems permitted the laboratory evaluation of these molecules, prior to the disclosure of the methodology reported here, the five-member-ring congeners were not so easily obtained.

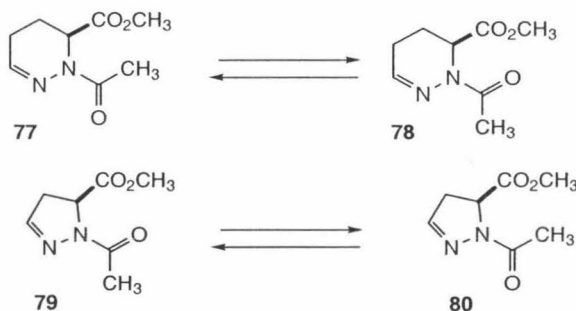


**Figure 16.** Conformational equilibria of piperazines and pyrazolines

### Pyrazolidines as Proline Analogue Systems

The application of our methodology to the synthesis of molecules which could serve as five-membered aza-analogues of proline would allow for the empirical study of these systems. We reasoned that the resulting substrates could then be submitted to the appropriate coupling reactions to provide a direct and convenient route to systems that



would permit further investigation of their behavior in the context of proline-like molecules.

An important feature our analogue system offers is the ability to control both the steric and electronic properties of substituents at every position of the pyrazolidine ring. Because of this control, a great deal of customization could be applied to the pyrazolidine that would allow for the fine tuning of its steric and electronic properties as desired.

By effecting peptide coupling through  $N_{\alpha}$ , a dipeptide could be produced that is similar to that which contains proline itself. Substituents incorporated in the initial dipolarophile at the carbon  $\alpha$ - or  $\beta$ - to the sulfonimide carbonyl could be varied as desired, while alkylation or acylation chemistry could be effected upon the remaining  $N_{\beta}$  nitrogen after the cyclization event to provide a range of electronic and steric environments which might influence the geometry about the peptide bond.

Alternatively, peptide coupling through  $N_{\beta}$  would provide a novel dipeptide which is conceptually related to the  $\beta$ -peptide amino acids which have been the subject of much recent interest.<sup>52</sup> Again, steric and electronic properties of the dipolarophile and the resulting pyrazoline  $N_{\alpha}$  nitrogen could be tailored through a combination of pre-cyclization and post-cyclization synthetic manipulations.

Finally, coupling through the C-terminal end of the pyrazoline is a process which required development in order for the pyrazoline or pyrazolidine to be incorporated into polypeptide systems. Figure 17 illustrates how each of these dipeptides incorporating the aza-proline would differ from a proline-containing dipeptide with respect to key dihedral

---

<sup>52</sup> Seebach, D.; Abele, S.; Schreiber, J. V.; Martinoni, B.; Nussbaum A. K.; Schild, H.; Schulz, H. Hennecke, H.; Woessner, R.; Bitsch, F. *Chimia* **1998**, 52, 734 and references cited therein.

angles and the distance between the two amide bonds of dipeptides.<sup>53</sup> As can be seen, the dipeptides formed at the  $N_\alpha$  present in the azaproline-derived dipeptide may allow for subtle tuning of a polypeptide structure at this location, while the  $N_\beta$ -coupled peptide allows for a more extreme modification of the amide-amide bond distance in comparison to the more proline-like dipeptides.

We had established a practical procedure for the cycloaddition of camphorsultam-derived acrylates with trimethylsilyl diazomethane and subsequently developed the needed chemistry to arrive at chromatographically stable, characterizable pyrazoline intermediates. We turned our attention to the development of a series of protocols that would render these products suitable reaction partners for construction of dipeptides. In order to explore the use of these compounds as proline-like amino acids, the pyrazoline must be reduced to the corresponding pyrazolidine prior to peptide coupling.

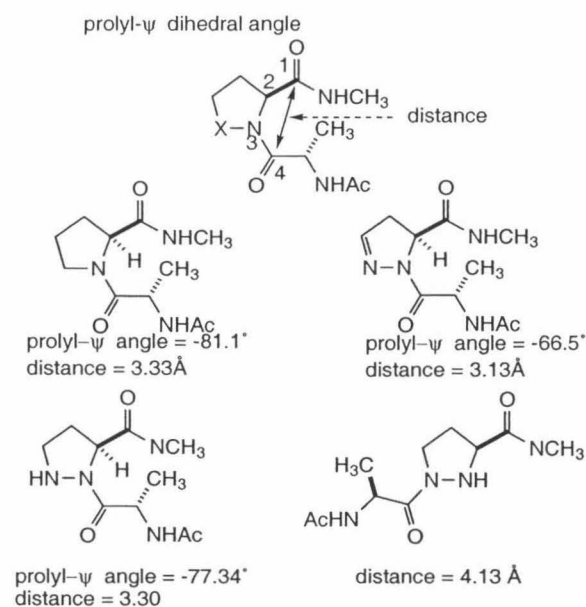


**Figure 17.** The MM2-minimized structures of prolyl-dipeptides and congeners

<sup>53</sup> The dihedral angles and amide-amide bond distances shown were calculated on structures that were MM2-minimized using the Chem3D software package.

## Transformations of Optically Active Pyrazolines

It was with these goals in mind that an efficient C=N reduction method was sought. Treatment of pyrazoline **60** with NaBH<sub>4</sub> in THF/MeOH was found to effect reductive auxiliary cleavage. The use of a milder reductant, namely NaCNBH<sub>3</sub> in AcOH, resulted in pyrazoline reduction to afford the pyrazolidine without competing auxiliary removal. While <sup>1</sup>H NMR spectroscopy confirmed the identity of the unpurified reaction product, the pyrazolidine was found to decompose upon attempted purification via column chromatography. The propensity for related dialkylhyrazine systems to decompose via oxidation is well documented in the literature.<sup>54</sup> To prevent decomposition, the pyrazolidines were protected using Boc-anhydride or Cbz-chloride (Table 3) to give the respective *N*-Boc or *N*-Cbz carbamates **81-84**.

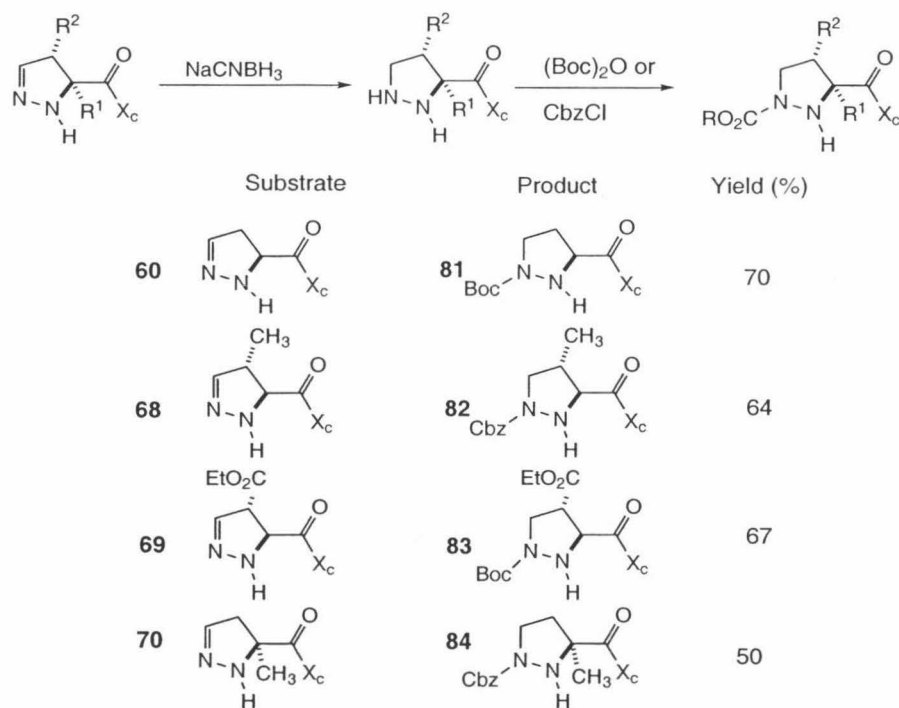


**Table 3.** Pyrazoline reduction with subsequent carbamate formation

<sup>54</sup> Denmark, S. E.; Weber, T.; Pitlowski, D. W. *J. Am. Chem. Soc.* **1987**, *109*, 224.

No trace of the regioisomeric carbamates resulting from the addition through the other pyrazolidine nitrogen was observed. In contrast to the unprotected reduction product, these compounds were found to be stable to chromatographic purification and amenable to characterization.

Attempted DCC coupling of these species with a number of N-terminal protected amino-acids failed to provide dipeptide product. We speculated that this lack of reactivity was attributable to the presence of the camphorsultam auxiliary in relative proximity to the N<sub>α</sub> nitrogen. It seemed likely that the steric bulk of the auxiliary which influenced the high regioselectivity seen in carbamate protection of the free pyrazolidine was in this case shielding the remaining nucleophilic nitrogen from being able to attack the activated ester electrophile. To remedy this problem, it was at this point that a trans-esterification protocol was sought to remove the chiral auxiliary from the pyrazolidines and exchange it for a less bulky group at this position.

Oppolzer and co-workers have reported a variety of methods for the removal of the camphor sultam auxiliary, with reductive removal via LiAlH<sub>4</sub>, trans-esterification in alcohol catalyzed by Ti(IV) species, and trans-esterification by NaOCH<sub>3</sub> among them.<sup>55</sup> Additionally, methods which are applicable to the removal of the oxazolidinone auxiliary of Evans, such as hydrolysis employing lithium hydroperoxide,<sup>56</sup> are also applicable to the removal of the sulfonimide moiety found in camphor sultam derived acrylates. Based on these reports, a number of these methods were attempted. Upon moving from the use of sodium methoxide to magnesium methoxide to a trans-esterification protocol involving the generation of the aluminum methoxide, the corresponding yield of the trans-esterified

---

<sup>55</sup> Oppolzer, W. *Tetrahedron* **1987**, *43*, 1969.

pyrazolidine was seen to significantly increase, from 50 to 71%. Having established a reliable procedure for this trans-esterification reaction using aluminum methoxide, an ester moiety that could be more easily converted to the free acid as needed was sought.

The generation of the aluminum alkoxide of allyl alcohol by treatment of the alcohol with lithium aluminum hydride, followed by the introduction of the camphor sultam bearing pyrazolidine, was found to deliver the desired allyl ester **85** in 77% yield. In addition to being the highest-yielding auxiliary removal method yet developed for our system, treatment of the allyl ester at a later stage of polypeptide synthesis with tetrakis (triphenylphosphine) palladium (0)<sup>57</sup> was expected to provide the free acid, which would be needed for the eventual incorporation of this class of pyrazolidines into polypeptide systems. A noteworthy feature of the allyl ester group is its orthogonality to the deprotection conditions used in classic amino acid protection/deprotection schemes employing Boc, Cbz, and Fmoc carbamates.

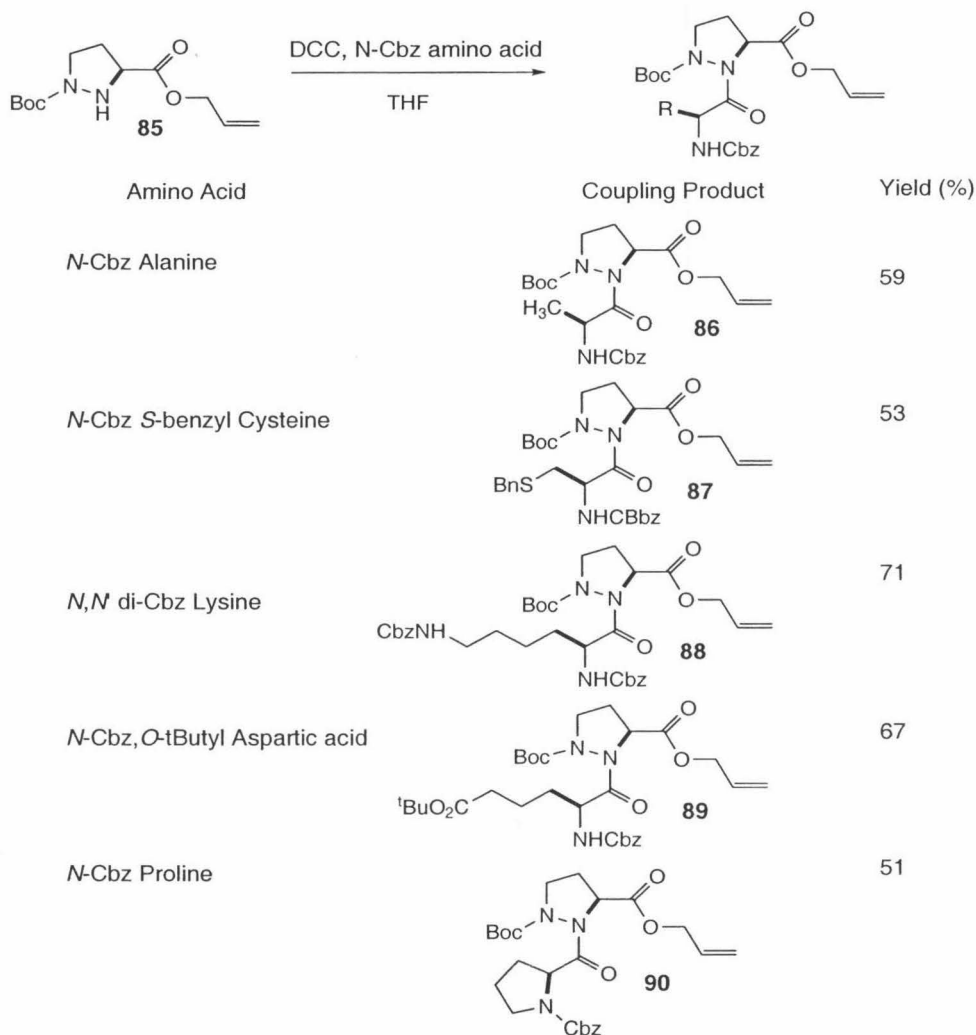
### Application to Dipeptide Formation

Having thus reduced the steric bulk present nearest to the N<sub>α</sub> nitrogen, it was observed that the N<sub>β</sub> –Boc protected pyrazolidines served as competent nucleophiles in the DCC promoted coupling between a range of *N*-protected amino acids (Table 4). The results of these coupling experiments demonstrate that a variety of functionality and steric bulk is tolerated in the side chain of the *N*-protected amino acids employed. These coupling products have the potential for further elaboration via either the removal of the allyl ester group to permit coupling through the free acid of the pyrazolidine residue, or

---

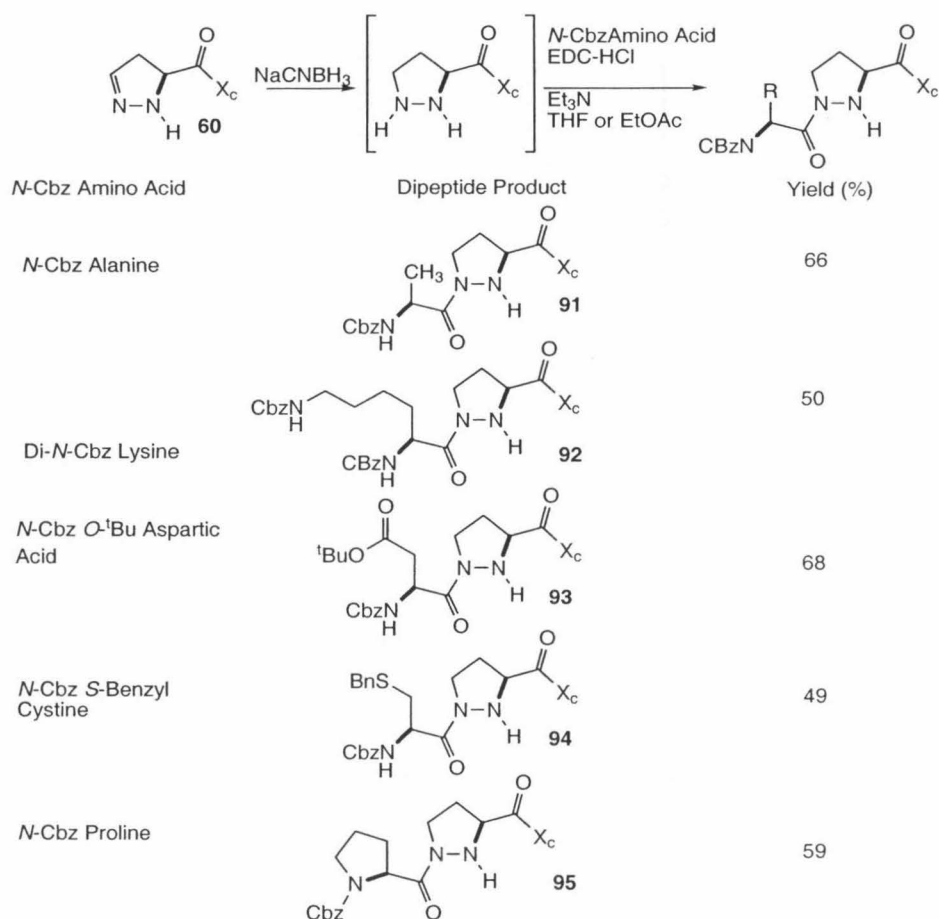
<sup>56</sup> Evans, D. A.; Britton, T. C.; Ellman, J. A. *Tetrahedron Lett.* **1987**, 28, 6141.

<sup>57</sup> Kunz, H.; Waldman, H. *Helv. Chim. Acta.* **1985**, 68, 618.

**Table 4.** Peptide coupling through  $N_\alpha$ 

alternatively via removal of the pyrazolidine  $N_\beta$  Boc protecting group followed by selective alkylation or acylation. The mode of peptide coupling between the pyrazolidine  $N_\beta$ -nitrogen and *N*-protected amino acids was next explored (Table 5).

Based on the observed regioselectivity of acylation displayed by intermediates bearing the camphorsultam auxiliary in the carbamate formation by intermediates bearing the camphorsultam auxiliary in the carbamate formation by intermediates bearing

**Table 5.** Peptide coupling between pyrazolidine and *N*-Cbz amino acids

the camphorsultam auxiliary in the carbamate formation conditions employed for peptide coupling. In this manner, the series of peptides linked through the  $N_{\beta}$  nitrogen were formed.

It should be noted that the reported yield of dipeptide obtained is calculated based on the amount of pyrazolidine initially used in the  $\text{NaCNBH}_3$  reduction step, and is therefore representative of the yield across these two synthetic steps. As in the cases reported above that involved coupling through the alternative pyrazolidine nitrogen, a range of side-chain functionality is tolerated in the reacting partner during the dipeptide

coupling step, suggesting that our proline analogues should be generally applicable in polypeptide systems.

Subsequent to dipeptide formation, the camphorsultam auxiliary could then be removed in good yield upon treatment by the aluminum alkoxide of allyl alcohol in THF. The relatively electrophilic nature of the sulfonimide permits its selective removal in this trans-esterification protocol without affecting the amide bonds and carbamate linkages present (Table 6).

Contemporaneous with our studies in this area, workers at Molecumetics Ltd. reported the synthesis of the pyrazolidine **107**, in connection with their work on the design and synthesis of  $\beta$ -turn mimetic templates.<sup>58</sup> Their synthetic route to this compound begins from malic acid **101** as a source of chirality. Acetonide formation, reduction of the free acid, bromination and acetonide removal furnish an intermediate **103**, which upon tosylation and displacement by *N*-Boc-derived hydrazine furnishes a hydrazide which cyclizes to give the pyrazolidine upon treatment with NaHMDS. After a

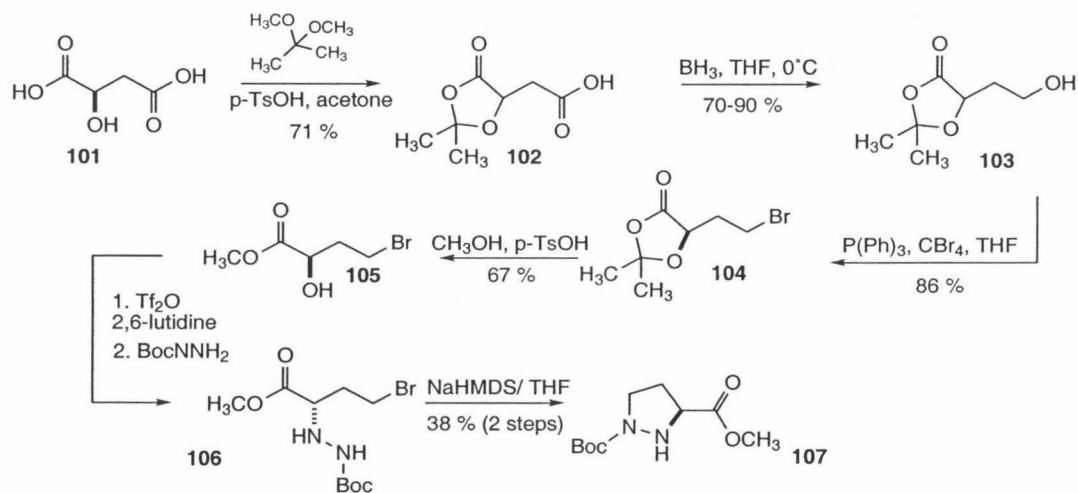


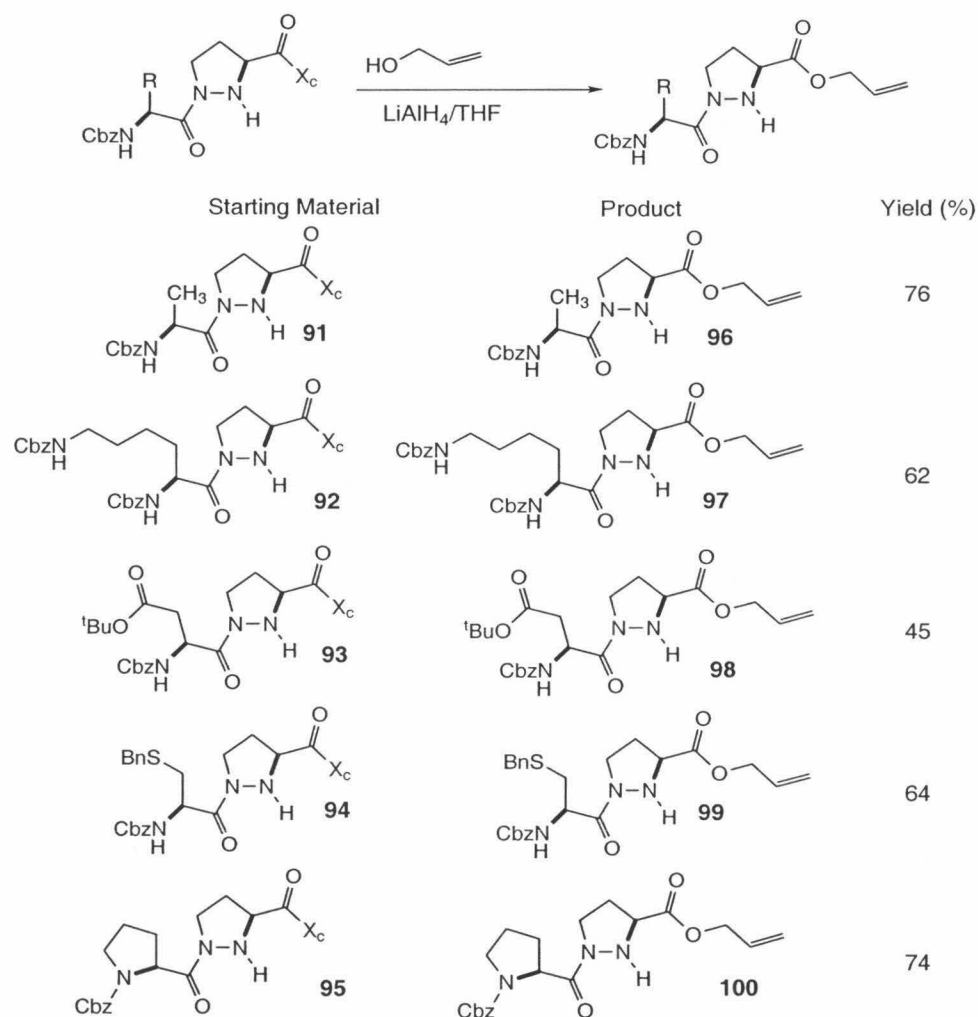
**Figure 18.** The Molecumetics Ltd. Synthesis of *N*-Boc Pyrazolidine **107**

<sup>58</sup> Kim, H.- O.; Lum, C.; Lee, M. S. *Tetrahedron Letters* **1997**, 38, 4935.



seven step synthetic sequence starting from material from the malic acid, the desired pyrazolidine is accessed (Figure 18).

**Table 6.** Trans-esterification of the dipeptides with aluminum allyl alkoxide



The approach that we had developed to access the identical pyrazolidine species possesses a number of benefits. The main advantage to our approach is that a family of related pyrazolidines can be produced via the selection of the initial cycloaddition dipolarophile, while the use of malic acid as the source of the carbons present in the

pyrazolidine ring imposes a clear limit on the type of substitution which is accessible. The flexibility our methodology provides with respect to the substituents that can be incorporated into peptide secondary structure mimetic templates may prove useful to the extent that it allows access to pyrazolidines that were not readily available prior to our disclosures in this area.

In addition to the ability for the pyrazoline products to serve as proline surrogates, related studies in our group by Hiroshi Sasaki have demonstrated that this cycloaddition reaction can provide novel surrogates of aspartic acid.<sup>59</sup> Here, the pyrazoline derived from dipolarophile **63** is subjected to a fragmentation reaction to provide  $\alpha$ -methyl aspartic acid **108** (Figure 19). It was found that treatment of this pyrazoline with 5 M NaOH at 150 °C led to the amino-diacid, presumably through the generation of the intermediate amino-nitrile followed by nitrile hydrolysis to give **108** in 68% yield. Acid promoted esterification of the acids with benzyl alcohol followed by N-acetylation with acetic anhydride gave the *N*-acetyl bis-benzyl ester **109** in 63% yield across these two steps.

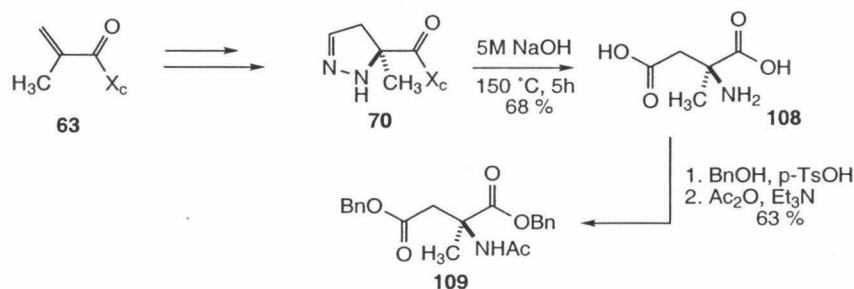


**Figure 19.** Carreira and Sasaki's synthesis of  $\alpha$ -methyl aspartic acid **108**

<sup>59</sup> Syntheses of this amino acid have been previously reported, see Cativela, C.; Diaz-de-Villegas, M. D.; Galves, J. A.; Lapena, Y. *Tetrahedron* **1997**, 53, 5891 and references cited therein.

The ability to differentiate the two carboxylic acids present in **108**, which would stem from the fact that one is more sterically hindered than the other, may provide the ability to construct a variety of  $\alpha$ -methyl amino acids from this fragmentation product. The synthesis of compound **108** is a very direct approach to a highly hindered amino acid analogue. Importantly, the use of the readily available antipodal chiral auxiliary would deliver the enantiomeric amino acid, providing access to both the D and L forms of the final product.

## Conclusion

The results of the studies presented above demonstrate that the pyrazoline products of the dipolar cycloaddition between trimethylsilyl diazomethane and camphorsultam-derived acrylates are well suited for use in studies requiring amino acid analogues. This was demonstrated to the extent that dipeptide systems in which either  $N_\alpha$  or  $N_\beta$  of the first-formed pyrazolidine formed an amide bond with a *N*-protected  $\alpha$ -amino acid, depending on the sequence of reduction, protection, and coupling reactions employed. These dipeptides were obtained in good yield utilizing standard peptide coupling chemistry. Finally, optimized conditions were developed that led to good yields of pyrazolidines in which the chiral auxiliary had been replaced with the allyl ester moiety.

### Section 3. The Addition of Mild Carbon Nucleophiles to N-Acetyl Pyrazolines

In our initial work on the dipolar cycloaddition between trimethylsilyl diazomethane and camphorsultam-derived acrylates, we established that the substituents on the resulting pyrazoline cycloadducts could be determined by the choice of substituents present on the dipolarophile. This feature permitted flexibility regarding the substitution of the pyrazoline at the positions both  $\alpha$  and  $\beta$  to the dipolarophile carbonyl. However, this method is limited with regard to the substituents present on the pyrazoline carbon originating from the trimethylsilyl diazoalkane species. We speculated that these pyrazolines could be further functionalized in a stereoselective fashion via a nucleophilic addition to the pyrazoline C=N bond (Figure 20).

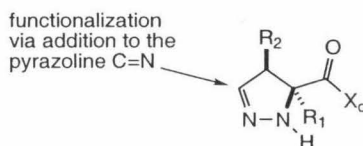


**Figure 20.** Functionalization is possible via addition to the pyrazoline C=N

#### Background

The addition of organometallic species to hydrazones is an area of synthesis that has received slight attention in comparison to the analogous nucleophilic additions to imines. Nevertheless, organometallic additions to chiral hydrazones derived from the condensation of aldehydes and chiral hydrazines have been developed as diastereoselective processes that render optically active amines upon hydrogenolysis of the hydrazine N-N bond.

Additions to proline-derived hydrazones such as **112** typify this approach to optically active amine synthesis.<sup>60</sup> Similar diastereoselectivity and yields have been obtained with hydrazones such as **110** where the chiral directing group is provided by an acetonide (Figure 21).<sup>61</sup>

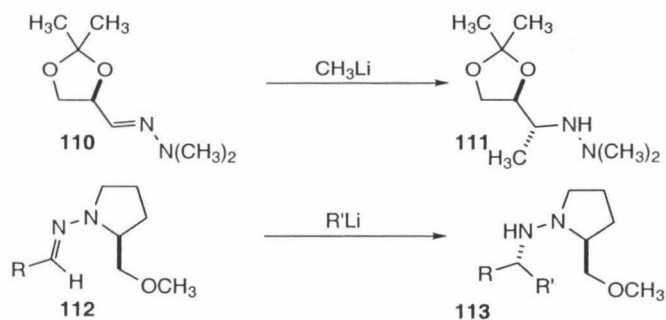
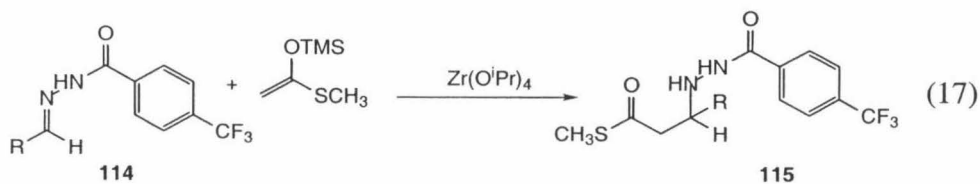


**Figure 21.** Examples of previous organometallic additions to hydrazones

More recently, protocols for the addition of silyl ketene thioacetals to acyclic hydrazones were reported by Kobayashi (eq 17).<sup>62</sup> In the context of cyclic cases, diastereoselective addition of carbon nucleophiles such as methyl lithium and methyl cesium to pyrazoline systems had been reported by Denmark (eq 18).<sup>63</sup> In a study on a related system, Mangeney showed that phenyl Grignard reagent would add to the pyrazoline **118** in good yield and diastereoselectivity in toluene at 70 °C (eq 19).<sup>64</sup>



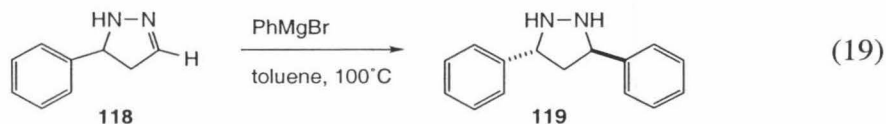
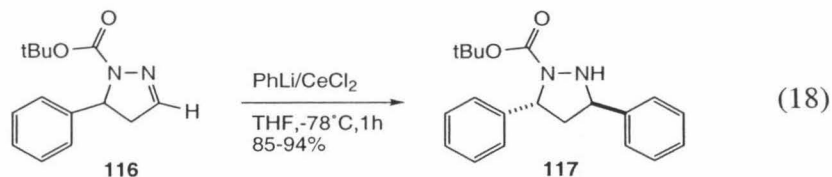
<sup>60</sup> Enders, D.; Schubert, H.; Nübling, C. *Angew. Chem., Int. Ed. Engl.* **1986**, 25, 1109.

<sup>61</sup> Claremon, D. A.; Lumma, P. K.; Phillips, B. T. *J. Am. Chem. Soc.* **1986**, 108, 8265.

<sup>62</sup> (a) Kobayashi, S.; Hirabayashi, R. *J. Am. Chem. Soc.* **1999**, 121, 6942. (b) Kobayashi, S.; Hasegawa, Y.; Ishitani, H. *Chem. Lett.* **1998**, 1131.

<sup>63</sup> Denmark, S. E.; Kim, J.-H. *Synthesis* **1992**, 229.

<sup>64</sup> Alexakis, A.; Lensen, N.; Tranchier, J.-P.; Mangeney, P. *J. Org. Chem.* **1992**, 57, 4563.



### Development of a Nucleophilic Addition Process

After developing the methodology needed to provide optically active pyrazolines via the 1,3-dipolar cycloaddition of trimethylsilyl diazomethane with camphorsultam-derived acrylates, we speculated that a diastereoselective process that allowed the addition of a carbon nucleophile to the pyrazoline carbon that originates from trimethylsilyl diazomethane would have a number of notable advantages. The most important advantage of this strategy is that it would allow for full control over the substitution on all three of the carbons present in the resulting pyrazolidine ring, by extending this control to substituents present at the 5-position of the pyrazolidine (Figure 22).

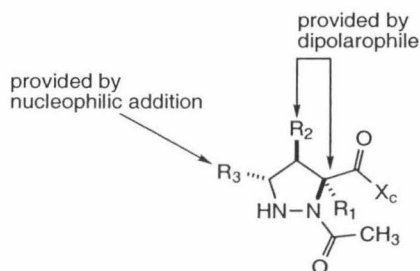


**Figure 22.** Control of substituents can be extended to all pyrazoline carbons

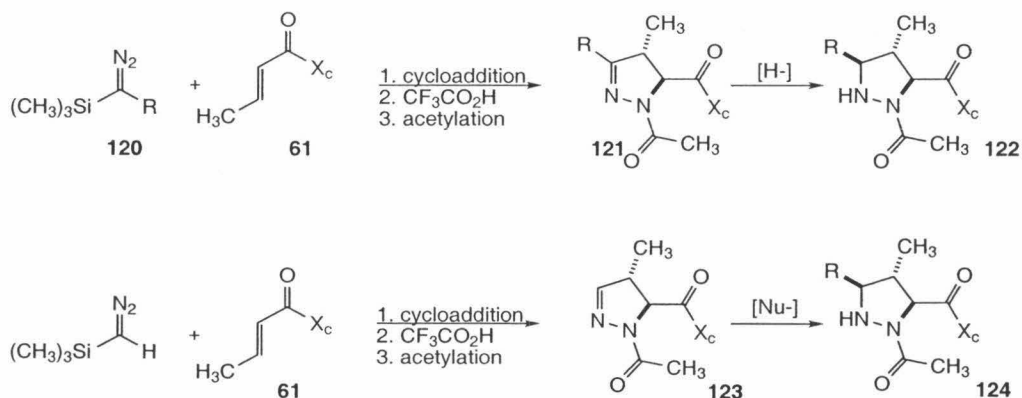
By the choice of dipolarophile, the substituents at the carbons  $\alpha$ - and  $\beta$ - to the sulfonimide carbonyl group are introduced in a stereospecific fashion in the initial cycloaddition. Acid treatment to give the pyrazoline followed by addition of a suitable

carbon nucleophile would then give the pyrazolidine which bears functionality at each of the three carbon atoms in the heterocycle.

The flexibility to add to the carbon skeleton after the cycloaddition event provides for a more powerful methodology. It is the synthetic equivalent of performing the initial dipolar cycloaddition with a substituted diazoalkane compound with complete stereospecificity, followed by pyrazoline reduction (Scheme 3).

Although less convergent than the hypothetical direct cycloaddition approach, the proposed protocol would offer the advantage of employing the readily available trimethylsilyl diazomethane to effect the initial cycloaddition, and also permit a variety of commercially available carbon nucleophiles to be incorporated into the pyrazolidine molecule that would otherwise require custom diazoalkane synthesis.

**Scheme 3**



The subsequent N-N bond reduction of these pyrazolidine systems offers direct access to optically active 1,3-diamines. Because of the flexibility provided by the choice of substitution on the dipolarophile as well as the range of nucleophiles which have been found to add into the pyrazoline C=N, this methodology may provide a general approach

to 1,3-diamine systems. Examples of previous 1,3-diamine syntheses have made use of more circuitous routes, such as the displacement of tosylate leaving groups in a 1,3-diol-derived substrate by an azide nucleophile. This displacement followed by reduction to furnish the diamine products was demonstrated by Enders in his synthesis of the HIV-protease inhibitor A-74704 (**125**) (Figure 23).<sup>65</sup> The cycloaddition/N-N fragmentation reported here provides the potential to reach 1,3-diamine systems of considerable diversity in a fairly short number of synthetic steps.

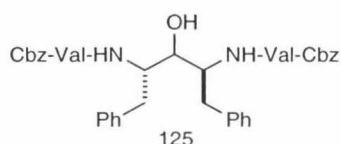


**Figure 23.** The HIV-Protease inhibitor A-74704

We reasoned that protection of the pyrazoline as the *N*-acetamide would be advantageous in several regards. In a nucleophilic addition process promoted by a Lewis acid, the presence of the *N*-acetamide would provide a motif for bidentate Lewis acid coordination to the substrate (Figure 24). Another benefit that we anticipated would result from the use of *N*-acetyl substrates in this addition protocol involved the enhanced stability of acyl hydrazides in comparison to alkyl hydrazine species.

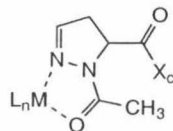


**Figure 24.** *N*-acetyl pyrazolines provide a bidentate chelating motif

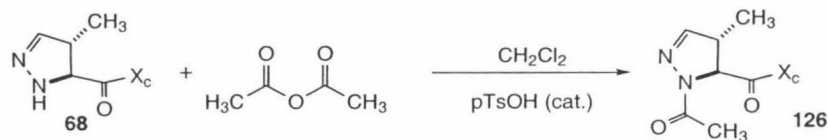
Acylation of the pyrazoline N-H was pursued in accord with these considerations. We discovered that while treatment of the pyrazoline with acetyl chloride and triethylamine failed to deliver protected product (possibly because of the presence of the

<sup>65</sup> Enders, D.; Jegelka, U.; Ducker, B. *Angew. Chemie Int. Ed. Engl.* **1993**, *32*, 423.



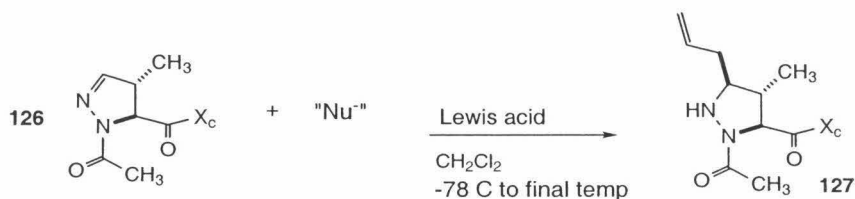
bulky camphorsultam auxiliary shielding the pyrazoline nitrogen), the toluenesulfonic acid catalyzed acetylation of our pyrazoline intermediates proceeded in high yield for the range of pyrazoline substrates examined (Scheme 4).

#### Scheme 4



#### Investigations with Allyl Tributylstannane and Various Lewis Acids

As a prototypical nucleophile for the addition to our *N*-acetamide protected pyrazolines, we chose the addition of allyl tributylstannane. This organometallic species had been shown to add to imines and hydrazones, albeit only in the presence of a Lewis acid promoter.<sup>66</sup> In order to effect addition, a solution of the *N*-acetamide protected pyrazoline in  $\text{CH}_2\text{Cl}_2$  was cooled to  $-78^\circ\text{C}$ , at which time the Lewis acid was added (0.5-2.0 eq, see Table 1) and the reaction removed from the cold bath with stirring for a period of ten minutes. At this time, the reaction was re-cooled to  $-78^\circ\text{C}$  and the allyl tributylstannane was added. The reaction was then removed from the cold bath and allowed to warm to room temperature. During his tenure as a postdoctoral scholar in the Prof. Carreira group, Dr. F.M. Guerra applied this protocol to a range of Lewis acids; the results are summarized in Table 7. This study established that the  $\text{TiCl}_4$  promoted reaction produced the best results in the prototype reaction.

**Table 7.** Optimization of addition of allyltributylstannane to pyrazoline **126**

LA	LA equiv	SnBu <sub>3</sub>	equiv	Time	Temp	Yield
BF <sub>3</sub> Et <sub>2</sub> O	1.1	2.1		14 h	reflux	41%
SnCl <sub>4</sub>	1.1	2.1		24 h	rt	49%
TiCl <sub>4</sub>	1.1	2.1		3 h	rt	67%
TiCl <sub>4</sub>	2.0	2.1		5h +14h	rt + reflux	no reaction
TiCl <sub>4</sub>	0.5	2.0		24 h	rt	26 %
TiCl <sub>4</sub>	0.5	4.0		24 h	reflux	29%
TiCl <sub>4</sub> <sup>a</sup>	1.1	2.1		24 h	rt	no reaction
Et <sub>2</sub> AlCl	1.1	2.1		48 h	rt	no reaction
TiCl <sub>2</sub> (OiPr) <sub>2</sub>	1.1	2.1		24 h	reflux	no reaction

<sup>a</sup> inverse addition

### Scope of the Addition Reaction

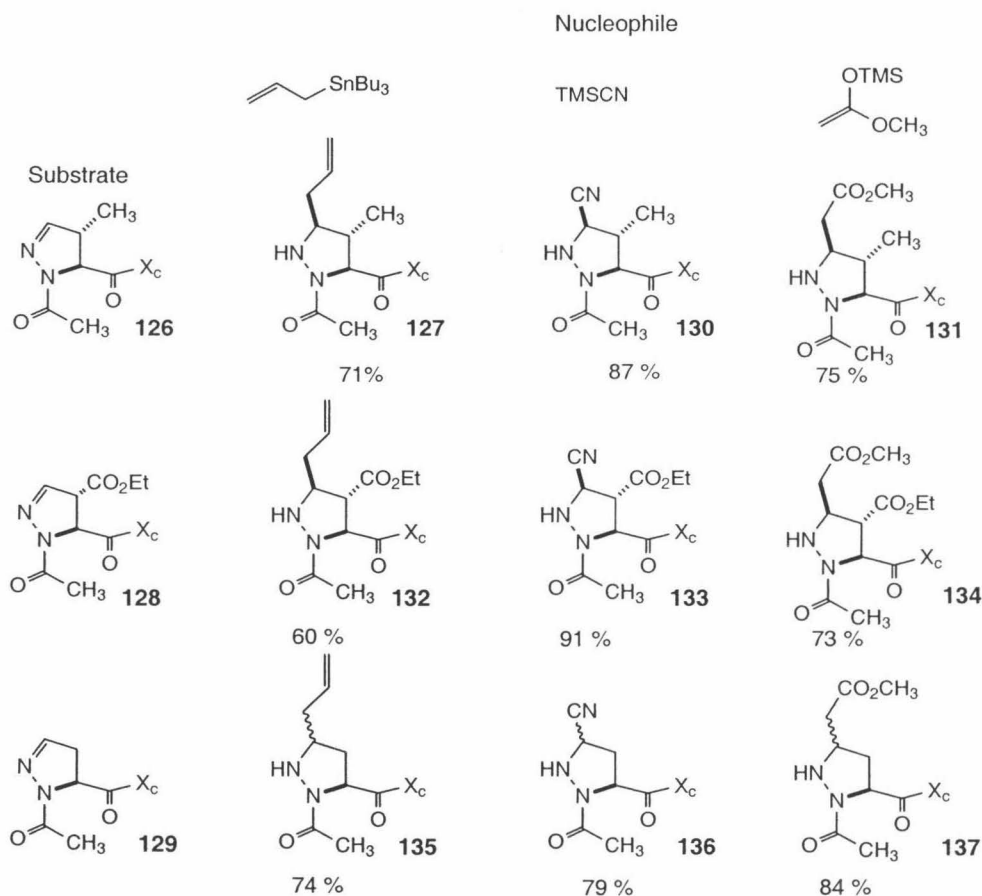
Encouraged by these results, we went on to test the generality of this addition process. It was further discovered that *N*-acetamide derived pyrazolines **128** and **129** were also amenable to the addition of allyltributyl stannane under these same conditions. We next attempted to expand the scope of this addition by testing the facility with which other carbon nucleophiles participated in this addition process. It was discovered that while allyl trimethylsilane proved unreactive under these conditions, conversely trimethylsilyl cyanide and the silyl ketene acetal derived from methyl acetate<sup>67</sup> both served as competent nucleophiles in this addition process, smoothly affording the respective pyrazolines **127** and **130-137** (Table 8).

<sup>66</sup> Bloch, R. *Chem. Rev.* **1998**, 98, 1407 and references cited therein.

<sup>67</sup> Carreira, E. M.; Singer, R. A.; Lee, W. S. *J. Am. Chem. Soc.* **1994**, 116, 8837.

In the cases where a substituent was present on the carbon adjacent to the pyrazoline C=N, the addition products were observed to be produced as single diastereomers as determined by  $^1\text{H}$  NMR. Alternatively, in the case of the pyrazoline **129**, the addition products were furnished with poor diastereoselectivity (1.5 :1 at best for pyrazolidine **36**).

**Table 8.** Addition of mild carbon nucleophiles to *N*-acetyl pyrazolines



These results suggest that the presence of a directing substituent is crucial for the addition process to proceed in a diastereoselective manner. In accordance with this observation, we expected that the sense of addition in the observed selective cases would

be such that the nucleophile would attack the pyrazoline C=N from the  $\pi$ -face opposite to that of the directing substituent at the  $\beta$ -position of the pyrazoline.

To confirm this prediction, the pyrazolidine **130** was submitted to single crystal X-ray analysis, and the resulting structure confirmed that the addition had occurred to the C=N bond face opposite to that of the vicinal directing substituent.<sup>68</sup> For two of the substrates where the pyrazolidine product was not crystalline, nOe enhancement experiments were conducted to confirm the sense of the reaction diastereoselectivity. In the cases of pyrazolines **127** and **131**, the relative stereochemistry was established via this means (Figure 25).

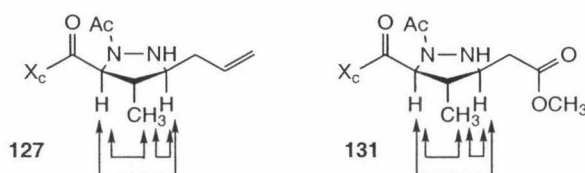


**Figure 25.** Observed nOe enhancements for pyrazolidines **127** and **131**

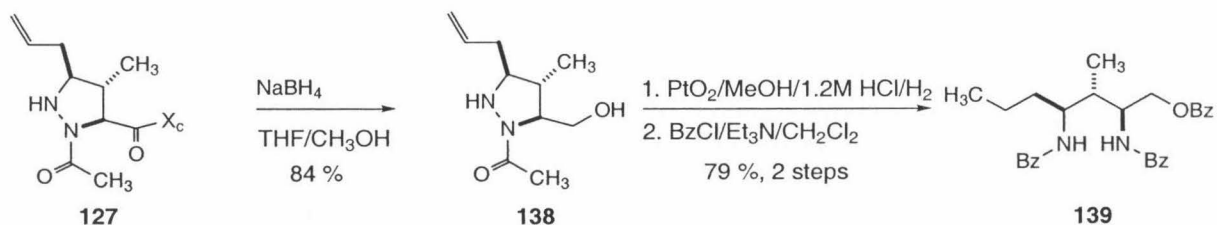
Although nucleophilic addition to hydrazone systems has been reported by several groups, our results are novel in that the system reported here has been demonstrated to work in conjunction with a broad class of carbon nucleophiles. With the ability to add either silyl ketene acetal, allyl tributyltin or trimethylsilyl cyanide, the diversity at this addition step permits the subsequent generation of a large variety of functional arrays in the addition products.

### Elaboration of the Nucleophilic Addition Products

These 5-substituted pyrazolidines may be applied to a number of uses. For example, they could be employed as more highly substituted proline surrogates wherein substituents at each of the pyrazolidine carbon atoms are fully modifiable via a selection

of a suitable dipolarophile for the initial cycloaddition followed by subsequent choice of nucleophile in the  $\text{TiCl}_4$ -promoted addition to the *N*-acylated pyrazoline. Alternatively, reductive N-N bond cleavage would allow the use of the highly substituted pyrazolidine addition products as optically active building blocks which may be employed in complex molecule synthesis. As proof of this concept, treatment of pyrazolidine **127** with  $\text{NaBH}_4$  furnished the free alcohol **138**.<sup>69</sup> This intermediate was then subjected to hydrogenation at 5 atm in acidic methanol a catalytic amount of  $\text{PtO}_2$  to give the ring cleavage product.<sup>70</sup> This very polar diamino-alcohol was isolated, purified and characterized as its tris-*N*-benzoyl protected derivative **139** in an overall yield of 79% (Scheme 5). The addition of mild carbon nucleophiles to a variety of *N*-acyl pyrazolines was extended to include the use of *N*-acyl groups other than those employing the *N*-acetyl protecting group.

### Scheme 5



Depending on the ultimate application of the reaction product, a more easily removed *N*-acyl group may be desired. Dr. F. M. Guerra found that the optimized nucleophilic addition procedures were compatible with *N*-trichloroacetyl pyrazolines as well, leading to a series of pyrazolidine addition products bearing this protecting group (Figure 26).

<sup>68</sup> X-Ray crystal data for pyrazolidine **130** is presented in Appendix II.

<sup>69</sup> Katayiri, N.; Takebayashi, M.; Kokufuda, H.; Kaneko, C.; Kanehira, K.; Torihara, M. *J. Org. Chem.* **1997**, *62*, 1580.

<sup>70</sup> Dolle, R.M.; Branden, M.C.; Brennan, P.E.; Ahmed, G.; Tran, V; Ho, D.M. *Tetrahedron. Lett.* **1999**, *40*, 2907.

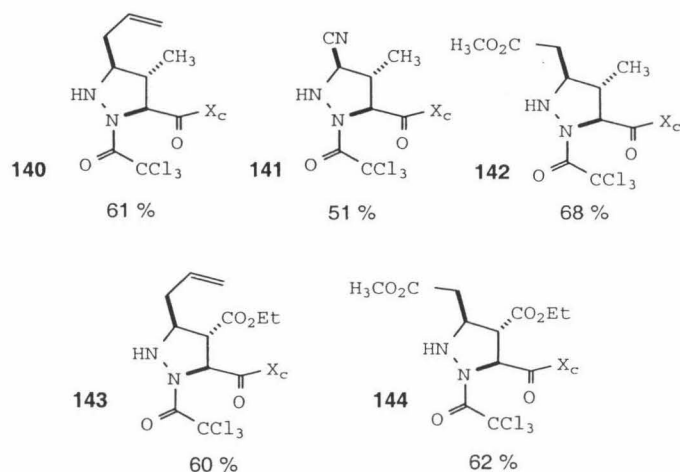


**Figure 26.** *N*-trichloroacetyl-derived pyrazolidines via the addition protocol

These substrates may prove useful in that the *N*-trichloroacetyl group can be removed under milder conditions than the corresponding *N*-acetyl group.<sup>71</sup> Depending on their intended application, pyrazolidines with relatively robust or relatively labile *N*-acyl groups could be produced.

The nucleophilic reagents trimethylsilyl cyanide, the silyl ketene acetal of methyl acetate and allyltributyl stannane have been shown to add to *N*-acetyl and *N*-trichloroacetyl derived pyrazolines in a process that is promoted by TiCl<sub>4</sub>. This process is highly diastereoselective when a substituent at the β-position is present. The reported additions are a meaningful advancement of the nucleophilic addition methodologies that have been previously reported for pyrazolines, especially in terms of the mildness of the nucleophiles used and the functionality added to the pyrazolidine products at the addition step. This methodology may find further application as a direct method for the synthesis of optically active, densely functionalized 1,3-diamine molecules, which result from reductive N-N bond cleavage.

<sup>71</sup> Weygand, F.; Frauendorfer, E. *Chem. Ber.* **1970**, *103*, 2437.

## General Conclusion

The 1,3-dipolar cycloaddition between trimethylsilyl diazomethane and camphorsultam-derived acrylates provides for the efficient, general synthesis of optically active pyrazolines with good levels of diastereoselectivity. The first formed  $\Delta^1$ -pyrazolines can be desilylated to give stable, characterizable  $\Delta^2$ -pyrazolines in a regioselective fashion. These  $\Delta^2$ -pyrazolines are stable, characterizable compounds which serve as the platform for additional transformations.

It has been shown that these pyrazolidines can serve as substrates for fragmentation reactions that provide ring-opened products as 1,3-diamines or 1,3-amino acids, further enhancing their usefulness in organic synthesis. Additionally, the  $\Delta^2$ -pyrazolines have served as pyrazolidine precursors that can form dipeptides which are linked alternatively through either of the nitrogens present in the pyrazolidine ring. Related systems have been targeted as templates for  $\beta$ -turn mimics.

The  $\text{TiCl}_4$ -promoted addition of mild carbon nucleophiles to *N*-Acetyl pyrazolines has been developed as an efficient process for the synthesis of highly substituted, densely functionalized pyrazolidines. The process developed has extended the range of nucleophiles that are known to be capable of addition to pyrazoline systems, and has been found to be amenable to the production of highly substituted 1,3-diamines upon reductive N-N bond cleavage.

The application of trimethylsilyl diazomethane to optically active pyrazoline synthesis reported here permits access to useful, functionally rich products in a process that uses stable, readily available starting materials. Because of the convenient access to pyrazolines that this method provides, as well as the manifold of subsequent

transformations which have been developed for these intermediates, the cycloaddition methodology we have developed should find further application as an efficient and direct means for the synthesis of highly substituted pyrazolines, pyrazolidines, and 1,3-diamine compounds that are rich in functionality.



## Experimental Section

### General Procedures

Where appropriate, reagents were purified prior to use by standard procedures. Trimethylsilyl diazomethane was purchased from Aldrich as a 2M solution in hexanes and used without purification. All non-aqueous reactions were performed using oven-dried glassware under an atmosphere of dry nitrogen. Air- and moisture-sensitive liquids and solutions were transferred *via* syringe or stainless steel cannula. Organic solutions were concentrated by rotary evaporation below 45 °C at  $\approx$ 25 mmHg (water aspirator). Tetrahydrofuran was distilled from sodium benzophenone ketyl prior to use. Triethylamine and dichloromethane were distilled from calcium hydride prior to use. Toluene was distilled from calcium hydride or sodium prior to use. Chromatographic purification was carried out using forced-flow chromatography on Baker 7024-R silica gel. Thin layer chromatography was performed on EM Reagents 0.25 mm silica gel 60F plates (230 - 400 mesh). Visualization of the developed plate was performed by fluorescence quenching, aqueous ceric ammonium molybdate (CAM), ethanolic *p*-anisaldehyde or aqueous potassium permanganate stains.

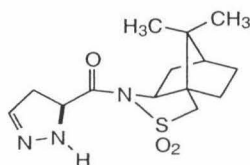
NMR spectra were recorded on General Electric 300 and Varian Gemini and Mercury spectrometers operating at 300 and 75 MHz for  $^1\text{H}$  and  $^{13}\text{C}$  respectively, and a Bruker AM-500 spectrometer operating at 500 MHz for  $^1\text{H}$  and 125 MHz for  $^{13}\text{C}$ . Spectra were referenced internally to residual protio solvent signals. Data for  $^1\text{H}$  are reported as follows: chemical shift ( $\delta$ , ppm), integration, multiplicity, and coupling constant ( $J$ , Hz).

Data for  $^{13}\text{C}$  are reported in terms of chemical shift ( $\delta$ , ppm). IR spectra were recorded on a Perkin-Elmer Paragon 1000 spectrometer using NaCl plates or solution cell, and are reported in terms of frequency of absorption ( $\nu$ ,  $\text{cm}^{-1}$ ). Melting points were determined on a Mel-Temp apparatus and are uncorrected. High-resolution mass spectrum were obtained from the UC Irvine and Caltech mass spectral facilities. Optical rotations were measured on a JASCO DIP-1000 digital polarimeter operating at 589 nm, and are reported as follows:  $[\alpha]_{\text{D}}^{\text{temp}}$ , concentration (g/100 mL) and solvent. HPLC analysis were conducted with a Hewlett Packard 1050 system equipped with a Chiralcel OJ column (25 cm x 0.46 cm i.d.).

### General Procedure for Synthesis of $\Delta^2$ -Pyrazolines

To a 0.05 M solution of  $\alpha,\beta$ -unsaturated sulfonamide in a 1:1 mixture of toluene/hexanes was added  $\text{Me}_3\text{SiCHN}_2$  (1.0 - 3.0 equiv, 2 M solution in hexanes). The reaction was stirred at 23 °C until TLC showed that the reaction had gone completely to product (4 h - 7 days). Reaction solvent and excess  $\text{Me}_3\text{SiCHN}_2$  were removed by rotary evaporation to yield the cycloadduct as a glassy solid.  $\text{CH}_2\text{Cl}_2$  was added to the residue to make a 0.1 M solution, at which time trifluoroacetic acid (1.1 equiv) was added to the reaction solution. After reaction had gone to completion (15 min – 2 h), the reaction was quenched with aqueous sodium bicarbonate solution, the aqueous layer separated and back extracted with  $\text{CH}_2\text{Cl}_2$ , and the combined organics washed with brine and dried over anhydrous  $\text{Na}_2\text{SO}_4$ . Removal of solvent by rotary evaporation provided the unpurified reaction product. Purification by chromatography on silica gel (2:1

hexanes/EtOAc) afforded the desired  $\Delta^2$ -pyrazoline as a crystalline solid.



**60**

Product obtained (72%) as a crystalline solid.

**mp** 154-156 °C;

$[\alpha]_D^{23.5}$  200.0° (c = 0.12, CHCl<sub>3</sub>);

**<sup>1</sup>H NMR** (300 MHz, CDCl<sub>3</sub>):  $\delta$  6.74 (1H, bs), 4.71 (1H, dd,  $J$  = 11.3, 9.6 Hz), 3.86 (1H, dd,  $J$  = 7.7, 4.9), 3.53 (1H, d,  $J$  = 13.9 Hz), 3.45 (1H, d,  $J$  = 13.9 Hz), 3.29 (1H, ddd,  $J$  = 17.6, 9.4, 1.5 Hz), 3.08 (1H, d,  $J$  = 2.6 Hz), 2.86 (1H, ddd,  $J$  = 17.6, 11.5, 1.5 Hz), 1.13 (3H, s), 0.94 (3H, s);

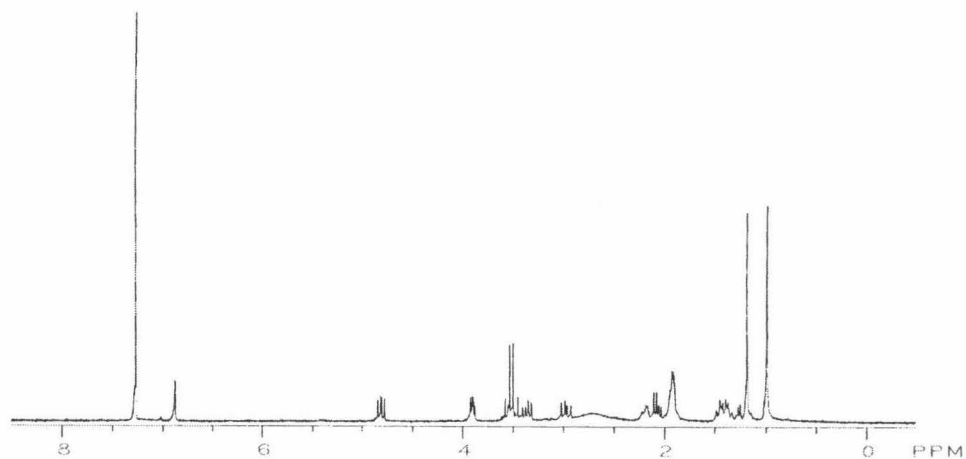
**IR** (thin film)  $\nu$  3352, 2958, 2885, 1701, 1327, 1275, 1239, 1218, 1130;

**<sup>13</sup>C NMR** (75MHz, CDCl<sub>3</sub>):  $\delta$  168.7, 143.6, 65.2, 60.0, 52.8, 49.0, 47.8, 44.3, 37.8, 35.8, 32.6, 26.4, 20.7, 19.8;

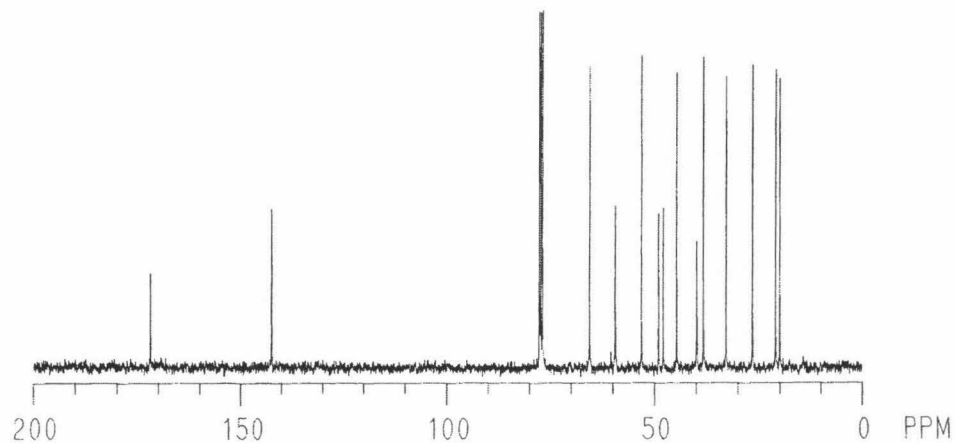
**HRMS** (FAB<sup>+</sup>) calculated for C<sub>14</sub>H<sub>22</sub>N<sub>3</sub>O<sub>3</sub>S (MH<sup>+</sup>) 312.1382 found 312.1385.

$^1\text{H}$  NMR

300 MHz

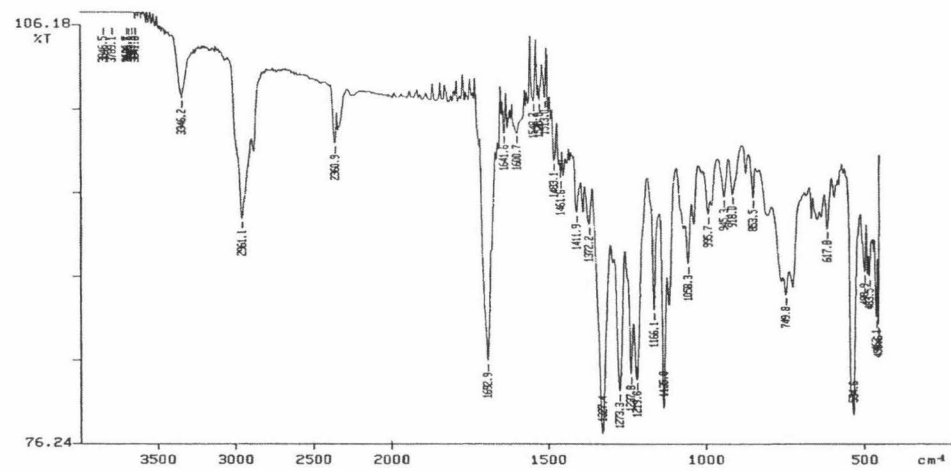
 $\text{CDCl}_3$  $^{13}\text{C}$  NMR

75 MHz

 $\text{CDCl}_3$ 

IR

thin film



Minor diastereomer: Isolated as a colorless oil.

$[\alpha]_D^{27.8}$  69.34° (c=1.76, CHCl<sub>3</sub>);

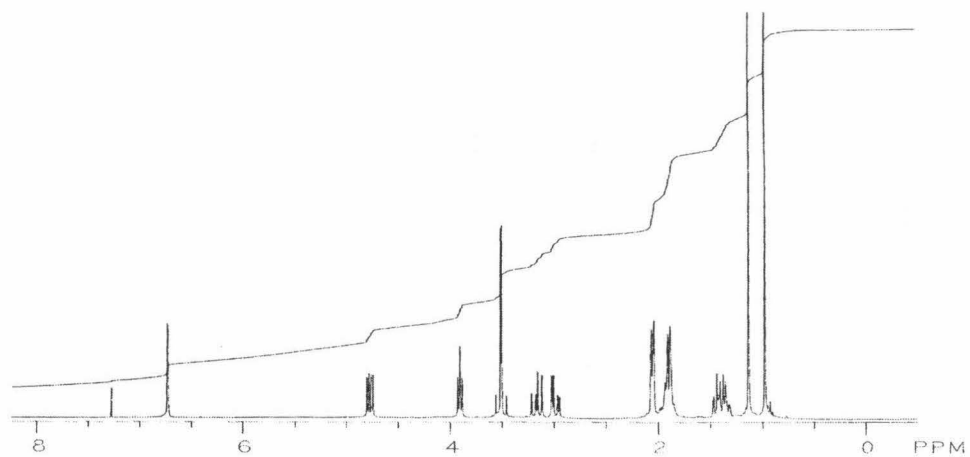
**IR** (thin film)  $\nu$  3346, 2961, 1692, 1600, 1327, 1273, 1238, 1220, 1135;

**<sup>1</sup>H NMR** (CDCl<sub>3</sub>, 300MHz):  $\delta$  6.72 (1H, m), 4.76 (1H, m), 3.90 (1H, m) 3.53 (1H, d,  $J$  = 13.8 Hz), 3.47 (1H, d,  $J$  = 13.8 Hz), 3.18 (1H, ddd,  $J$  = 18.0, 12.0, 1.5 Hz), 2.98 (1H, ddd,  $J$  = 18.0, 5.7, 1.8 Hz), 2.04 (2H, m), 1.90 (3H, m), 1.35 (2H, m), 1.16 (3H, s), 1.13 (3H,s);

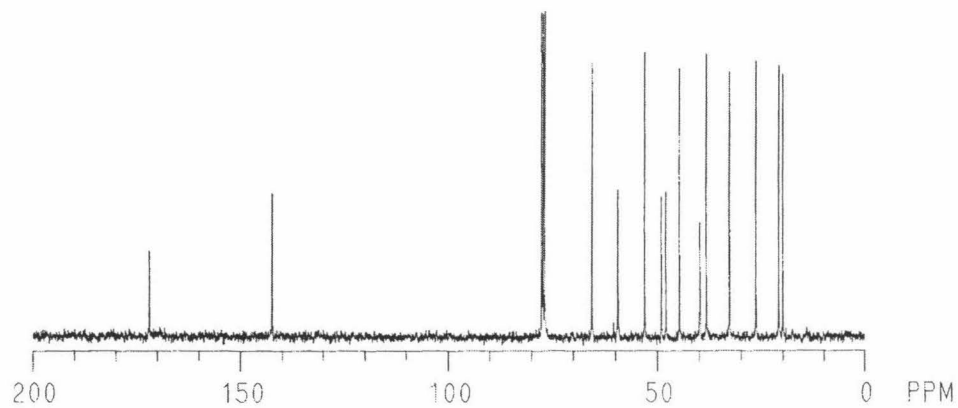
**<sup>13</sup>C NMR** (75 MHz,CDCl<sub>3</sub>):  $\delta$  171.8, 142.3, 65.4, 59.2, 52.9, 48.9, 47.7, 44.5, 39.6, 38.1, 32.7, 26.3, 20.8, 19.8;

**HRMS** (CI<sup>+</sup>) calculated for C<sub>14</sub>H<sub>22</sub>N<sub>3</sub>O<sub>3</sub>S (MH<sup>+</sup>) 312.1382 found 312.1384.

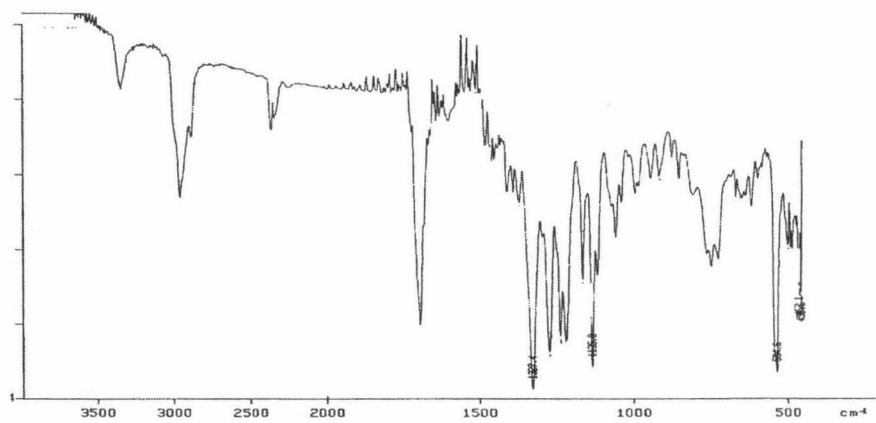
$^1\text{H}$  NMR  
300 MHz  
 $\text{CDCl}_3$

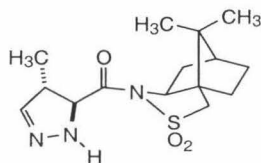


$^{13}\text{C}$  NMR  
75 MHz  
 $\text{CDCl}_3$



IR  
thin film



**68**

Product obtained (65%, two steps) as white crystals.

**mp** 144-146 °C (EtOAc/Hexanes),

$[\alpha]_D^{23.5}$  291.7 ° (c=0.16, CHCl<sub>3</sub>);

**IR** (thin film)  $\nu$  3358, 2963, 2883, 1704, 1596, 1457, 1386, 1319, 1275, 1134, 545;

**<sup>1</sup>H NMR** (CDCl<sub>3</sub>, 300 MHz):  $\delta$  6.66 (1H, d,  $J$  = 1.3 Hz), 4.31 (1H, d,  $J$  = 9.5 Hz), 3.90 (1H, dd,  $J$  = 7.7, 4.9 Hz), 3.67 (1H, dqd,  $J$  = 9.5, 7.1, 1.3 Hz), 3.54 (d, 1H,  $J$  = 13.9 Hz), 3.47 (1H, d,  $J$  = 13.9 Hz), 2.25-1.80 (6H, m), 1.5-1.3 (2H, m), 1.21 (3H, d,  $J$  = 7.1 Hz), 1.15 (3H, s), 0.96 (3H, s);

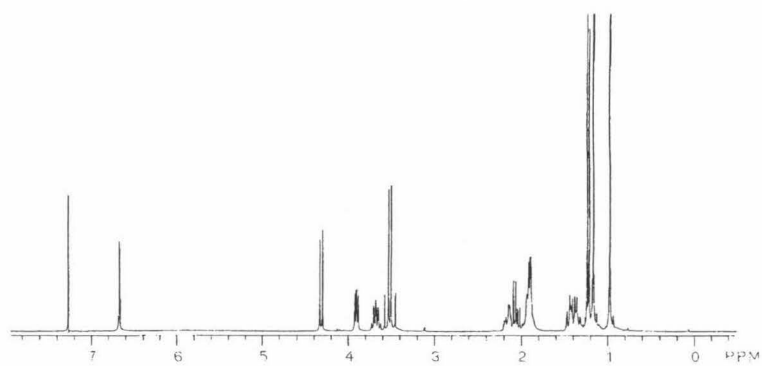
**<sup>13</sup>C NMR** (CDCl<sub>3</sub>, 75 MHz):  $\delta$  168.3, 148.7, 68.1, 65.2, 52.9, 48.9, 47.8, 44.3, 43.3, 37.8, 32.6, 26.4, 20.7, 19.8, 16.0;

**HRMS** (FAB+) calculated for C<sub>15</sub>H<sub>24</sub>N<sub>3</sub>O<sub>3</sub>S (MH<sup>+</sup>) 326.1543, found 326.1543.

$^1\text{H}$  NMR

300 MHz

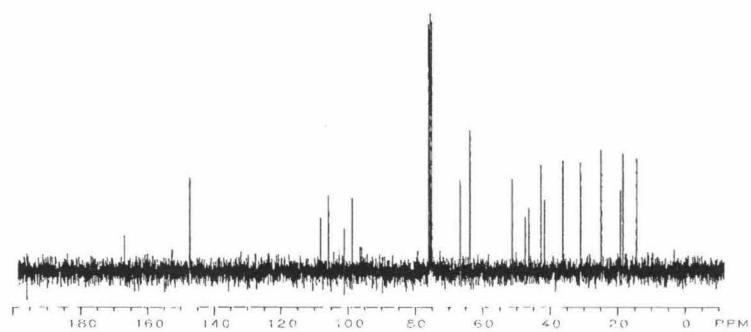
$\text{CDCl}_3$



$^{13}\text{C}$  NMR

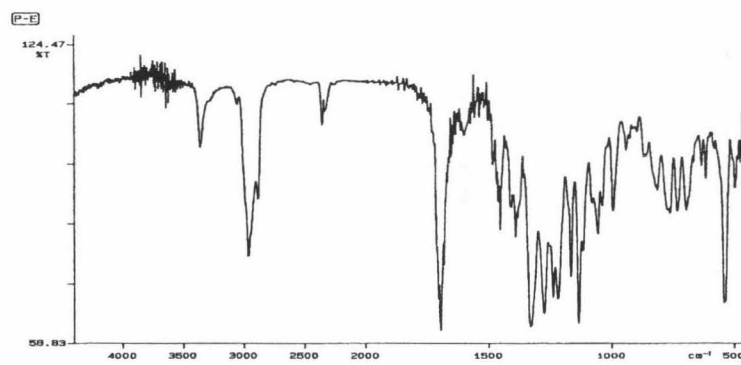
75 MHz

$\text{CDCl}_3$



IR

thin film





Minor diastereomer: Isolated as a colorless oil.

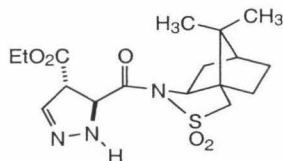
$[\alpha]_D^{28.0} -7.2^\circ$  ( $c=0.16$ ,  $\text{CHCl}_3$ );

**IR** (thin film)  $\nu$  3350, 2963, 1694, 1329, 1220, 1135, 1068, 755, 541;

**$^1\text{H}$  NMR** ( $\text{CDCl}_3$ , 300 MHz):  $\delta$  6.65 (1H, br s), 4.38 (1H, d,  $J = 4.3$  Hz), 3.89 (1H, dd,  $J = 7.0, 5.6$  Hz), 3.52 (1H, d,  $J = 13.9$  Hz), 3.47 (1H, d,  $J = 13.9$  Hz), 3.25 (1H, ddd,  $J = 7.0, 4.3, 1.5$  Hz), 1.26 (3H, d,  $J = 7.0$  Hz), 1.13 (3H, s), 0.97 (3H, s);

**$^{13}\text{C}$  NMR** ( $\text{CDCl}_3$ , 75 MHz):  $\delta$  171.9, 147.0, 66.9, 65.5, 52.9, 48.8, 47.7, 47.4, 44.5, 38.2, 32.8, 26.3, 20.9, 19.8, 16.0;

**HRMS** ( $\text{CI}^+$ ) calculated for  $\text{C}_{15}\text{H}_{24}\text{N}_3\text{O}_3\text{S}$  ( $\text{MH}^+$ ) 326.1538, found 326.1541.

**69**

Product obtained (78%) was a clear, colorless oil.

$[\alpha]_D^{25.8}$  355.20 ° ( $c = 0.475$ ,  $\text{CHCl}_3$ );

**IR** (thin film)  $\nu$  3662, 2962, 2257, 1738, 1698, 1596, 1458, 1393, 1370  $\text{cm}^{-1}$ ;

**$^1\text{H}$  NMR** (300 MHz,  $\text{CDCl}_3$ )  $\delta$  6.78 (1H, d,  $J = 2.3$ ), 5.11 (1H, d,  $J = 10.7$ ), 4.64 (1H, dd,  $J = 10.7, 2.3$  Hz), 4.20 (2H, q,  $J = 5.4$  Hz), 3.95 (1H, dd,  $J = 4.9, 2.8$  Hz), 3.56, (1H, d,  $J = 13.8$  Hz), 3.48 (1H, d,  $J = 13.8$  Hz), 2.13 - 2.00 (2H, m), 1.90 (2H, m), 1.46 - 1.34 (2H, m), 1.27 (3H, t,  $J = 5.4$  Hz), 1.16 (3H, s), 0.97 (3H, s);

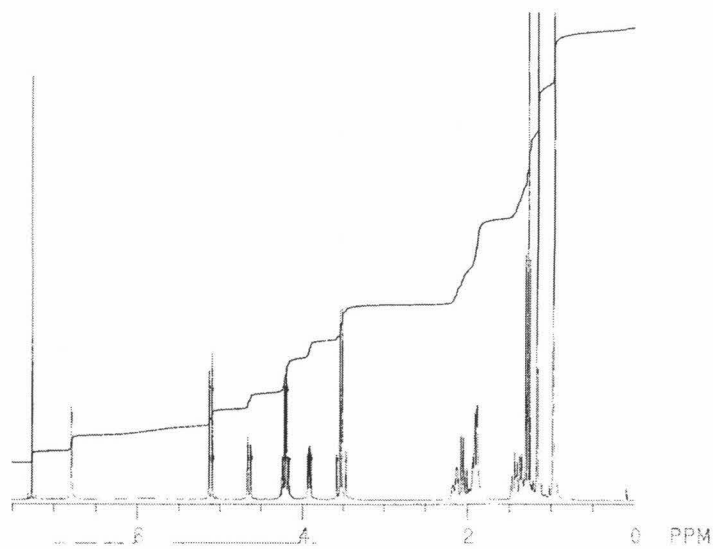
**$^{13}\text{C}$  NMR** (75 MHz,  $\text{CDCl}_3$ )  $\delta$  168.1, 166.8, 139.5, 65.1, 63.3, 61.7, 53.7, 49.0, 47.8, 44.4, 37.6, 32.5, 26.3, 20.6, 19.7, 14.0;

**HRMS** ( $\text{CI}^+$ ) calculated for  $\text{C}_{17}\text{H}_{26}\text{N}_3\text{O}_5\text{S}$  ( $\text{MH}^+$ ) 384.1595, found 384.1593.

$^1\text{H}$  NMR

300 MHz

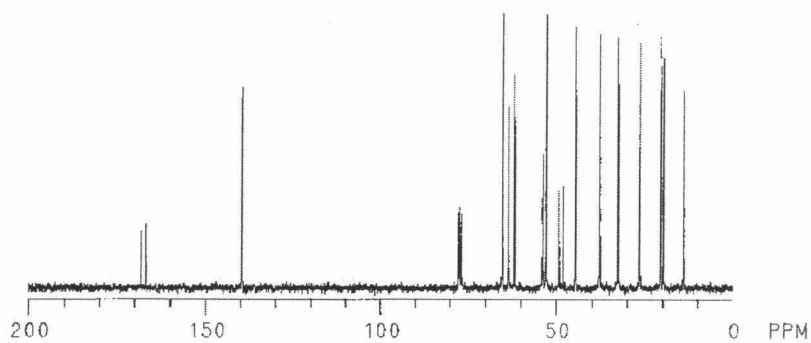
$\text{CDCl}_3$



$^{13}\text{C}$  NMR

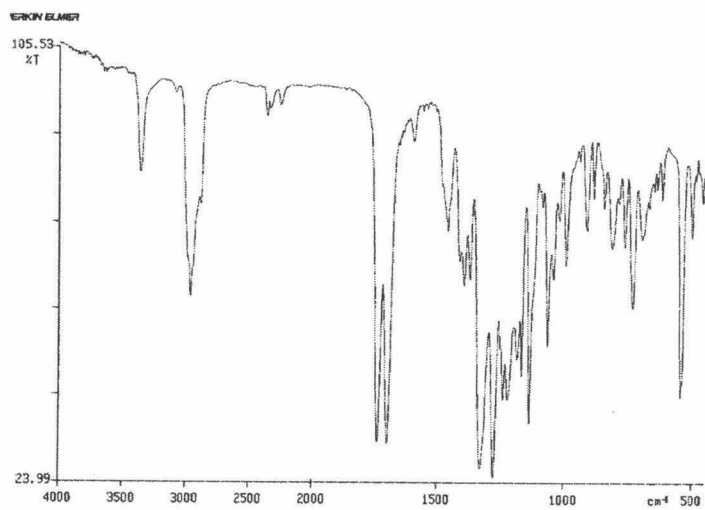
75 MHz

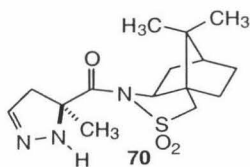
$\text{CDCl}_3$



IR

thin film



**70**

Product obtained (50%, two steps) as white crystals.

**mp** 127-129 °C (EtOAc/Hexanes),

$[\alpha]_D^{25.0}$  98.5 ° (c=0.20, CHCl<sub>3</sub>);

**IR** (thin film)  $\nu$  3373, 2958, 2885, 1680, 1327, 1192, 1130, 1056, 972, 536;

**<sup>1</sup>H NMR** (CDCl<sub>3</sub>, 300 MHz):  $\delta$  6.68 (1H, br s), 3.93 (1H, dd,  $J = 7.9, 4.6$  Hz), 3.49 (1H, d,  $J = 13.7$  Hz), 3.44 (1H, d,  $J = 13.7$  Hz), 3.40 (1H, dd,  $J = 17.4, 1.5$  Hz), 2.63 (1H, dd,  $J = 17.4, 1.5$  Hz), 2.10-1.75 (6H, m), 1.54 (3H, s), 1.54-1.10 (3H, m), 1.10 (3, s), 0.926 (3H, s);

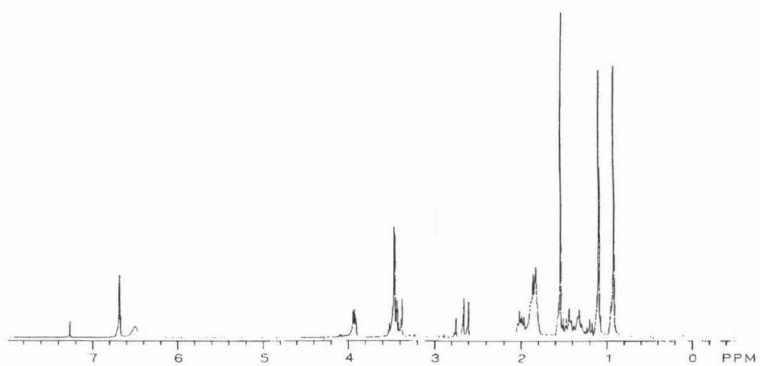
**<sup>13</sup>C NMR** (CDCl<sub>3</sub>, 75 MHz):  $\delta$  175.5, 142.4, 70.0, 66.5, 53.2, 48.5, 47.8, 45.3, 44.0, 38.4, 32.5, 26.4, 22.9, 20.4, 19.8;

**HRMS** (FAB<sup>+</sup>) calculated for C<sub>15</sub>H<sub>24</sub>N<sub>3</sub>O<sub>3</sub>S (MH<sup>+</sup>) 326.1538, found 326.1539.

$^1\text{H}$  NMR

300 MHz

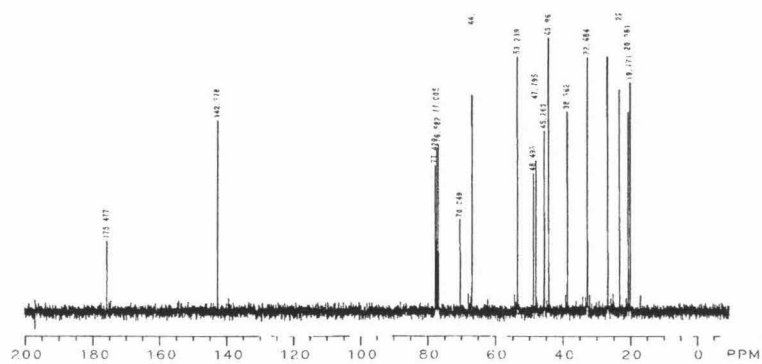
$\text{CDCl}_3$



$^{13}\text{C}$  NMR

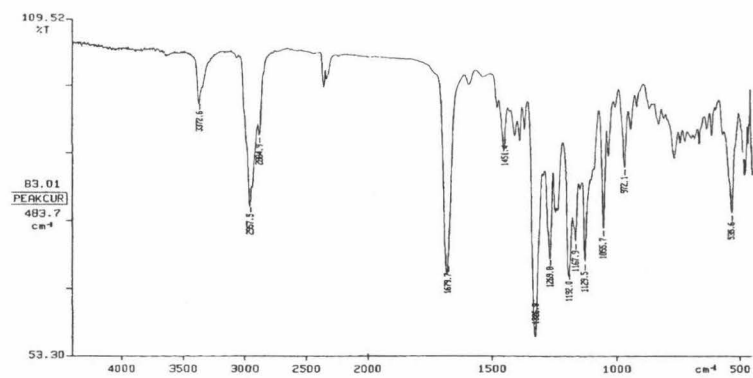
75 MHz

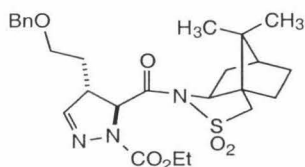
$\text{CDCl}_3$



IR

thin film





71

To a solution of the  $\alpha,\beta$ -unsaturated sulfonamide (9.2 g, 23 mmol) in  $\text{CH}_2\text{Cl}_2$  (60 mL)/hexanes (250 mL) was added powdered 4Å molecular sieves (4.5 g), followed by trimethylsilyl diazomethane (25.0 mL of 2M solution in hexanes, 50.0 mmol), and the reaction was stirred at 23 °C for 90 h. The reaction mixture was filtered and the filtrate was concentrated to afford the intermediate cycloadduct. Integration of signals at  $\delta$  5.58 and 5.43 in the  $^1\text{H}$  NMR ( $\text{CDCl}_3$ , 300 MHz) showed the adduct was formed as a mixture of diastereomers in a 93:7 ratio. This material was dissolved in  $\text{CH}_2\text{Cl}_2$  (150 mL), cooled to 0 °C and then ethyl chloroformate (21.7 mL, 227 mmol) was added followed by silver trifluoromethanesulfonate (8.8 g, 34 mmol), and the reaction was stirred at 0 °C for 1.5 h. Saturated aqueous  $\text{NaHCO}_3$  solution (100 mL) was added, the mixture was warmed to 23 °C and stirred vigorously for 15 min. The mixture was filtered through celite and the filter cake was washed thoroughly with  $\text{CH}_2\text{Cl}_2$  ( $3 \times 100$  mL). Water (100 mL) was added to the combined filtrates, the layers were separated and the aqueous layer was extracted with  $\text{CH}_2\text{Cl}_2$  ( $2 \times 100$  mL). The combined organic layers were dried over  $\text{Na}_2\text{SO}_4$  and concentrated under reduced pressure to a yellow oil. Purification by flash chromatography on silica gel (2:1 hexanes/EtOAc) afforded the major diastereoisomer (8.4 g, 71%) as a pale yellow solid; mp 49 - 52 °C; TLC  $R_f$  = 0.40 (1:1 hexanes/EtOAc);

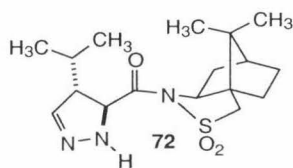
$[\alpha]_{\text{D}}^{26} = -128.9$  ( $c = 0.86$ ,  $\text{CHCl}_3$ );

$^1\text{H NMR}$  ( $\text{CDCl}_3$ , 300 MHz)  $\delta$  7.38 - 7.28 (m, 5H), 6.92 (s, 1H), 5.05 (d, 1H,  $J = 4.0$  Hz), 4.52 (d, 1H,  $J = 11.9$  Hz), 4.47 (d, 1H,  $J = 12.0$  Hz), 4.30 - 4.24 (m, 2H), 3.92 (dd, 1H,  $J = 7.5, 5.0$  Hz), 3.60 - 3.42 (m, 5H), 2.32 - 2.17 (m, 2H), 2.08 - 1.87 (m, 4H), 1.47 - 1.30 (m, 6H), 1.28 (s, 3H), 1.00 (s, 3H);

$^{13}\text{C NMR}$  ( $\text{CDCl}_3$ , 75 MHz)  $\delta$  168.7, 153.1, 148.7, 138.1, 128.5, 127.7, 127.7, 73.0, 67.5, 65.5, 63.0, 62.7, 53.1, 54.4, 44.5, 38.0, 32.7, 32.4, 26.6, 20.6, 20.0, 14.7;

**IR** ( $\text{CHCl}_3$ )  $\nu$  3012, 2965, 1697, 1435, 1384, 1337, 1272, 1240, 1131, 1067, 877, 699;

**HRMS** 517.2247, found 518.237 ( $\text{M}+\text{H}$ ) $^+$ .



72

Product obtained in 67 % yield as a white powder. **m.p.** 150°-152° C (dec.)

$[\alpha]_D^{23.8} + 323.1^\circ$  (CHCl<sub>3</sub>, c = 0.37);

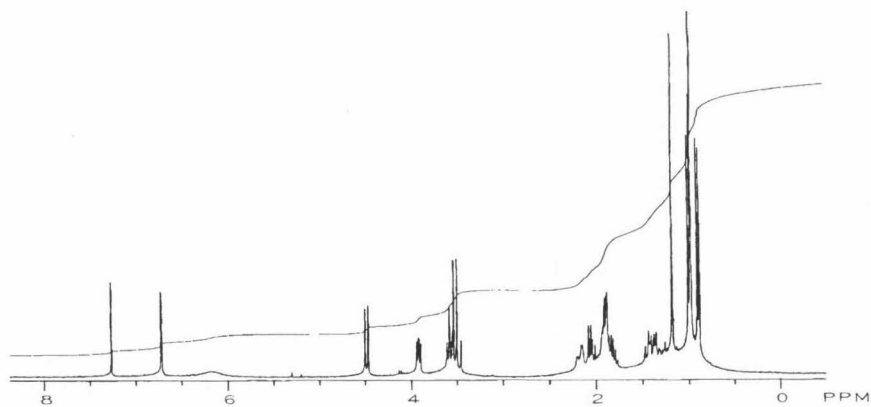
**<sup>1</sup>H NMR** (300 MHz, CDCl<sub>3</sub>)  $\delta$  : 6.71 (1H,d,  $J$  = 1.2 Hz), 6.20(1H, bs), 4.48 (1H, d,  $J$  = 10.2 Hz), 3.91 (1H, m), 3.59 (3H, m), 2.35-1.80 (8H,cm), 1.52-1.21 (4H,m), 1.17 (3H,s), 0.98 (6H,m), 0.88, (3H, d,  $J$  = 6.9 Hz);

**<sup>13</sup>C NMR** (75 MHz, CDCl<sub>3</sub>)  $\delta$  : 168.0, 146.3, 76.665.1, 64.1, 55.0, 52.8, 48.9, 47.8, 44.3, 37.7, 32.5, 29.6, 26.4, 20.6, 20.4, 20.3, 19.8.

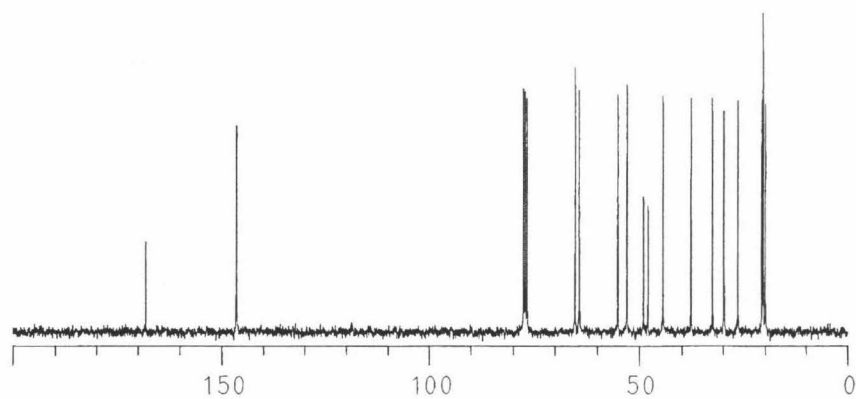
**IR** (thin film, cm-1) 3357, 2959, 2880, 1700, 1463, 1391, 1326, 1273, 1237, 1165, 1134, 1060, 992.



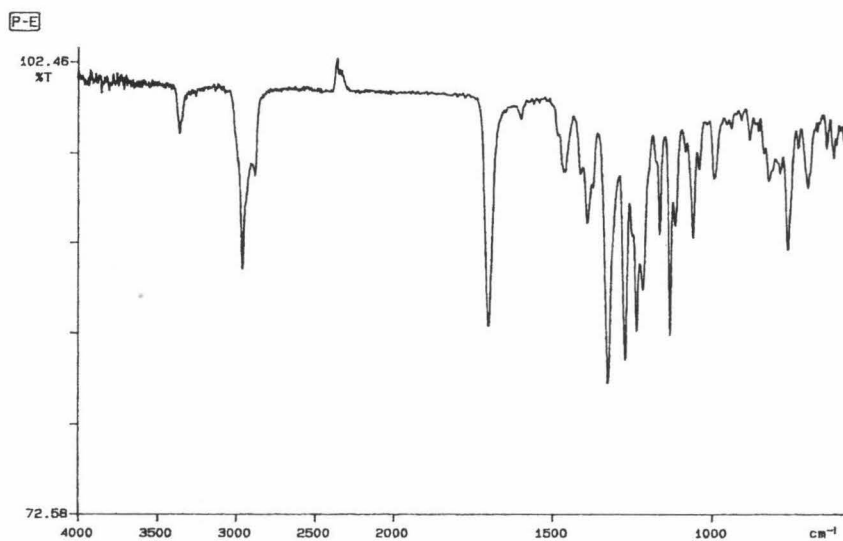
$^1\text{H}$  NMR  
300 MHz  
 $\text{CDCl}_3$

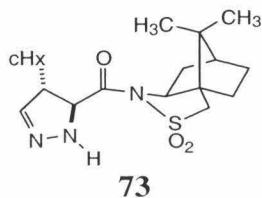


$^{13}\text{C}$  NMR  
75 MHz  
 $\text{CDCl}_3$



IR  
thin film





Product obtained in 67% yield as a colorless oil.

$[\alpha]_D^{25.2} + 253.1^\circ$  (CHCl<sub>3</sub>, c = 0.39);

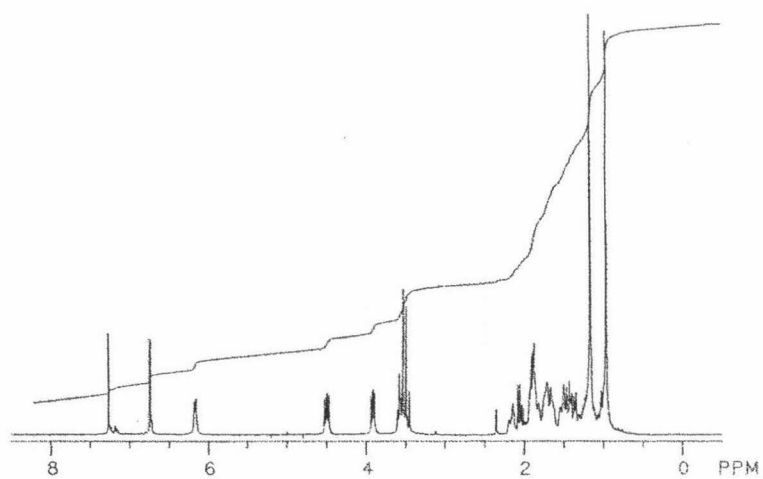
<sup>1</sup>H NMR (300 MHz, CDCl<sub>3</sub>)  $\delta$  : 6.74 (1H, d,  $J$  = 1.3 Hz), 4.49 (1H, d,  $J$  = 10.6 Hz), 3.91 (1H, m), 3.54 (2H, m), 3.47 (1H, d,  $J$  = 13.8 Hz), 2.14-2.07 (1H,m), 2.00-1.93 (1H,m), 1.90-1.62 (8H,cm), 1.54-1.31 (4H, m), 1.17 (3H,s), 0.97 (3H,s);

<sup>13</sup>C NMR (75MHz, CDCl<sub>3</sub>)  $\delta$  : 168.1, 146.3, 65.2, 64.3, 54.1, 52.9, 48.9, 47.8, 44.4, 39.3, 37.8, 32.6, 31.2, 30.9, 26.4, 26.1, 26.0, 20.7, 19.8;

IR (thin film)  $\nu$  3358, 2923, 2851, 1702, 1449, 1326, 1273, 1237, 1221, 1166, 1134, 1062, 992 cm<sup>-1</sup>.

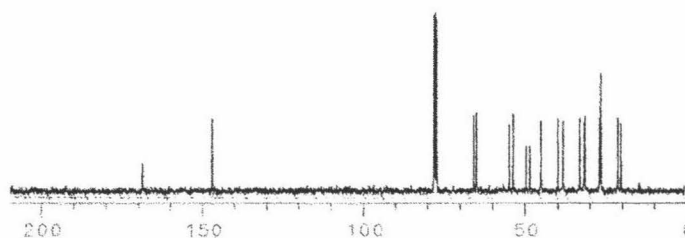
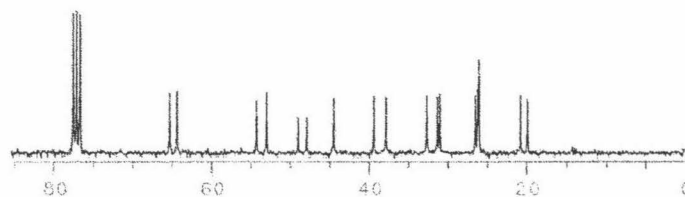
$^1\text{H}$  NMR

300 MHz  
 $\text{CDCl}_3$

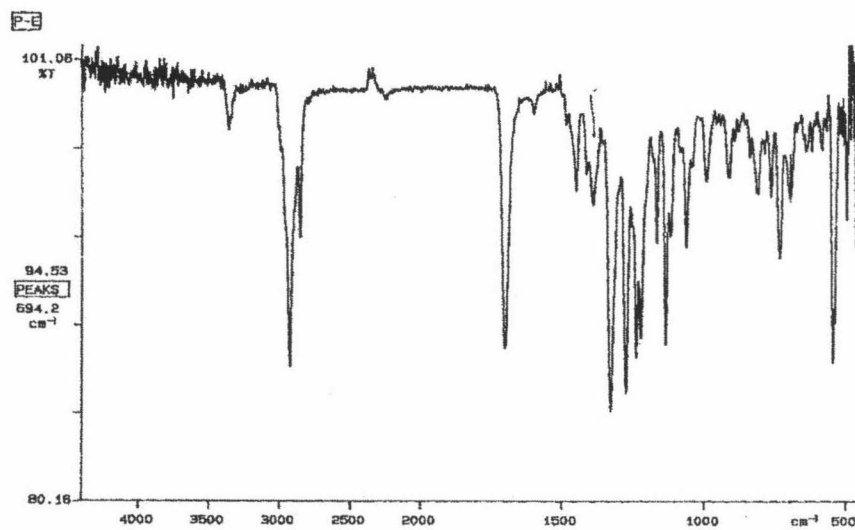


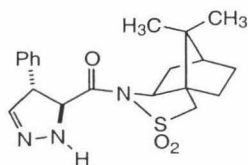
$^{13}\text{C}$  NMR

75 MHz  
 $\text{CDCl}_3$



IR  
thin film





74

Product obtained in 58% yield as a colorless oil.

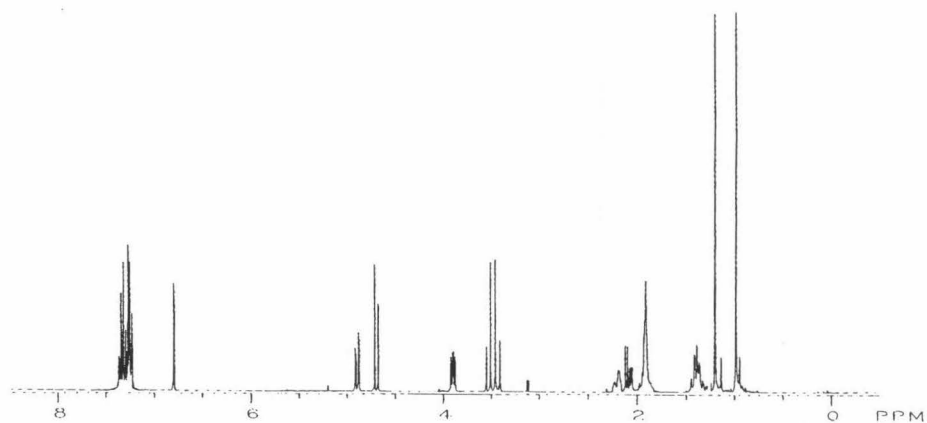
$[\alpha]_D^{27.0} +353.^\circ$  (CHCl<sub>3</sub>, c = 0.70);

<sup>1</sup>H NMR (300 MHz, CDCl<sub>3</sub>)  $\delta$  : 7.37-7.28 (5H, m), 6.79 (1H, d,  $J = 1.3$ Hz), 4.90 (1H, dd,  $J = 10.2, 1.3$  Hz), 4.69 (1H, d,  $J = 10.2$  Hz), 3.90 (1H, m), 3.52 (1H,  $J = 13.6$  Hz), 3.43 (1H,  $J = 13.6$  Hz), 2.27-2.20 (1H, m), 2.15(1H,  $J = 10.2$  Hz), 1.98-1.85 (6H, m), 1.48-1.35 (4H, m), 1.13 (3H,s), 0.98(3H,s);

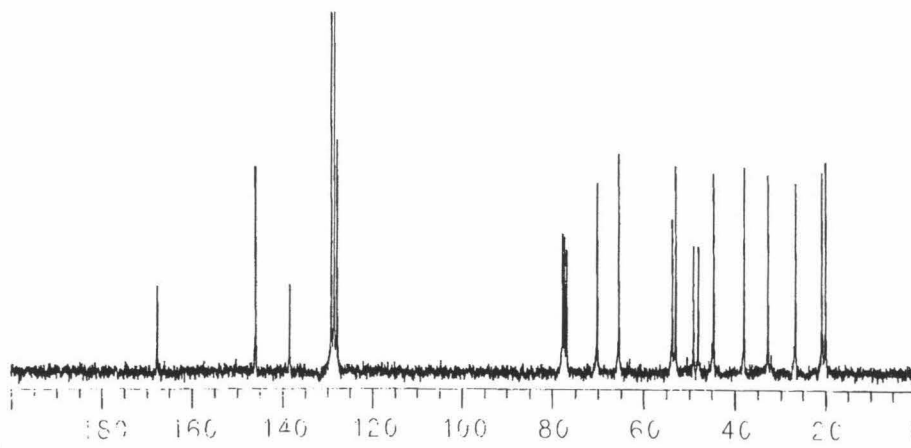
<sup>13</sup>C NMR (75 MHz, CDCl<sub>3</sub>)  $\delta$  : 167.5, 145.7, 138.2, 128.9, 128.1, 127.5, 69.9, 65.2, 53.5, 52.7, 48.9, 47.8, 44.3, 37.7, 32.5, 26.4, 20.6, 19.8;

IR (thin film, cm<sup>-1</sup>) 3360, 2960, 1697.6, 1601, 1494, 1455, 1392, 1327, 1272, 1236, 1222, 1166, 1134, 1063, 997.

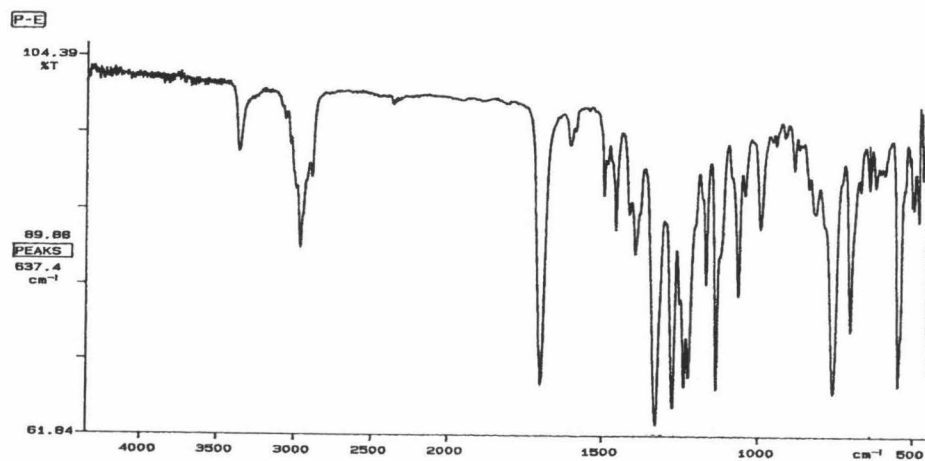
$^1\text{H}$  NMR  
300 MHz  
 $\text{CDCl}_3$



$^{13}\text{C}$  NMR  
75 MHz  
 $\text{CDCl}_3$



IR  
thin film



### **General Procedure for Reduction / *N*-Boc Protection of $\Delta^2$ -Pyrazolines to Carbamates**

To a 0.3 M solution of the  $\Delta^2$ -pyrazoline in glacial acetic acid was added NaCNBH<sub>3</sub> (2.5 equiv). The reaction was stirred at 23 °C for 1 h, at which time the reaction mixture was diluted with EtOAc and quenched by addition of a saturated aqueous solution of potassium carbonate. The organic layer was washed with brine and dried over anhydrous Na<sub>2</sub>SO<sub>4</sub>. Solvent was removed by rotary evaporation and the resulting product dissolved in sufficient THF to make a 0.25 M solution. To this solution was added (Boc)<sub>2</sub>O (1.2- 1.5 equiv), triethylamine (2 equiv), and 4-dimethylamino pyridine (0.1 equiv). The reaction was stirred for 4 h, at which time solvent was removed by rotary evaporation. The resulting residue was submitted to purification by flash chromatography on silica gel (2:1 hexanes/EtOAc), which afforded the pure carbamate as a clear, colorless oil.

### **General Procedure for *N*-Cbz Protection of $\Delta^2$ -Pyrazolines to Carbamates**

To a 0.3 M solution of the pyrazolidine (resulting from reduction of the  $\Delta^2$ -Pyrazoline with NaCNBH<sub>3</sub> as above) in dichloromethane was added CbzCl (1.2 equiv) and triethylamine (1 equiv). The reaction was stirred at 23 °C for 40 min, at which time the reaction mixture was quenched by addition of water. The aqueous layer was extracted with dichloromethane and the combined organic layers were washed with brine and dried over anhydrous Na<sub>2</sub>SO<sub>4</sub>. Solvent was removed by rotary evaporation and the residue

submitted to purification by flash chromatography on silica gel (3:1 hexanes/EtOAc), which afforded the pure carbamate.

### **General Procedure for the synthesis of dipeptide compounds 86-90**

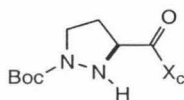
To a 0.1 to 1 M solution of **85** in THF was added 1.1 equiv of the respective *N*-Cbz protected amino acid. Then, 1.1 equiv dicyclohexyl carbodiimide(DCC) was added, along with 2 to 4 equiv triethylamine. Within minutes of addition of DCC, the clear solution became cloudy with a white ppt. After TLC indicated no additional generation of the spot taken to be product, the reaction was diluted with ethyl acetate and partitioned between ethyl acetate and 1 N HCl. The collected organic layer was washed with NaHCO<sub>3</sub> and then with brine. Drying over Na<sub>2</sub>SO<sub>4</sub> followed by rotary evaporation to remove solvent furnished the crude product as a glassy solid. Purification by filtration of a concentrated ethyl acetate solution of the product through celite to remove dicyclohexylurea followed by flash chromatography on silica gel (between 1:1 hexanes/EtOAc and 2:1 EtOAc/hexanes) afforded the pure dipeptide as a colorless oil.

### **General Procedure for synthesis of dipeptide compounds 91-95**

To a 0.1 to 1 M solution of the crude reduction product from the reduction of **60** in THF was added 1.1 equiv of the respective *N*-Cbz protected amino acid. Then, 1.1 equiv 1-(3-dimethylaminopropyl)-3-ethylcarbodiimide hydrochloride(EDC) was added, followed by 1.1 equiv 1-Benzoxotriazole hydrate and 2 to 4 equiv triethylamine. Within minutes of addition of DCC, the clear solution became cloudy with a white ppt. After TLC indicated no additional generation of the spot taken to be product, the reaction was

diluted with ethyl acetate and partitioned between ethyl acetate and 1 N HCl. The collected organic layer was washed with  $\text{NaHCO}_3$  and then with brine. Drying over  $\text{Na}_2\text{SO}_4$  followed by rotary evaporation to remove solvent furnished the crude product as a glassy solid. Purification by flash chromatography on silica gel (between 1:1 hexanes/EtOAc and 2:1 EtOAc/hexanes) afforded the pure dipeptide as a colorless oil.



**Physical Data****81**

Product obtained (60%) as a clear, colorless oil.

$[\alpha]_D^{28.7} + 67.8^\circ$  ( $c = 0.255$ ,  $\text{CHCl}_3$ );

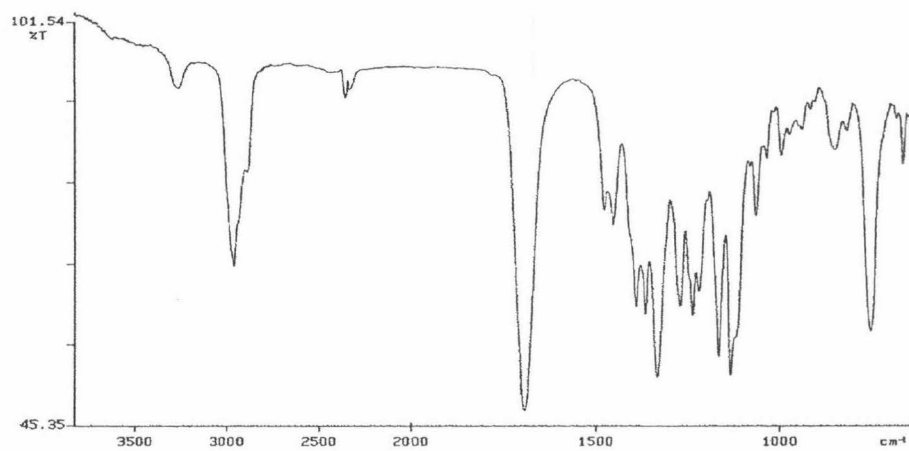
**IR** (thin film)  $\nu$  3261, 2964, 1693, 1480, 1456, 1392, 1336, 1334, 1273, 1239, 1221, 1166, 1134, 1067  $\text{cm}^{-1}$ ;

**$^1\text{H}$  NMR** (300 MHz,  $\text{CDCl}_3$ ):  $\delta$  4.35 (1H, m), 3.86 (1H, dd,  $J = 5.1, 2.7$  Hz), 3.60 - 3.55 (2H, m), 3.48 (2H, ab,  $J = 13.8$  Hz), 2.55 (1H, m), 2.1 (3H, m), 1.9 (3H, m), 1.47 (9H, s), 1.38 (2H, m), 0.98 (3H, s), 0.96 (3H, s);

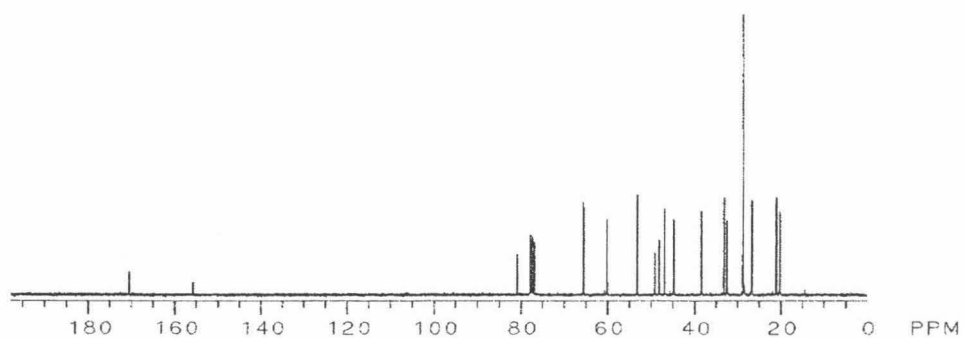
**$^{13}\text{C}$  NMR** (75 MHz,  $\text{CDCl}_3$ ):  $\delta$  170.3, 155.5, 80.66, 65.5, 60.0, 53.1, 49.0, 48.0, 46.8, 44.7, 38.3, 33.0, 32.4, 28.5, 28.4, 26.6, 20.9, 20.1;

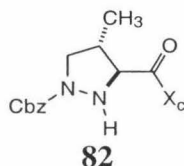
**HRMS** ( $\text{CI}^+$ ) calculated for  $\text{C}_{19}\text{H}_{31}\text{N}_2\text{O}_5\text{S}$  414.1984, found 413.1988.

IR  
thin film



<sup>13</sup>C NMR  
75 MHz  
CDCl<sub>3</sub>





Product obtained (42%, two steps) as a colorless oil.

$[\alpha]_D^{27.8}$  76.6 ° (c=0.17, CHCl<sub>3</sub>);

**IR** (thin film)  $\nu$  3279, 2961, 2885, 1698, 1456, 1411, 1331, 1284, 1284, 1239,

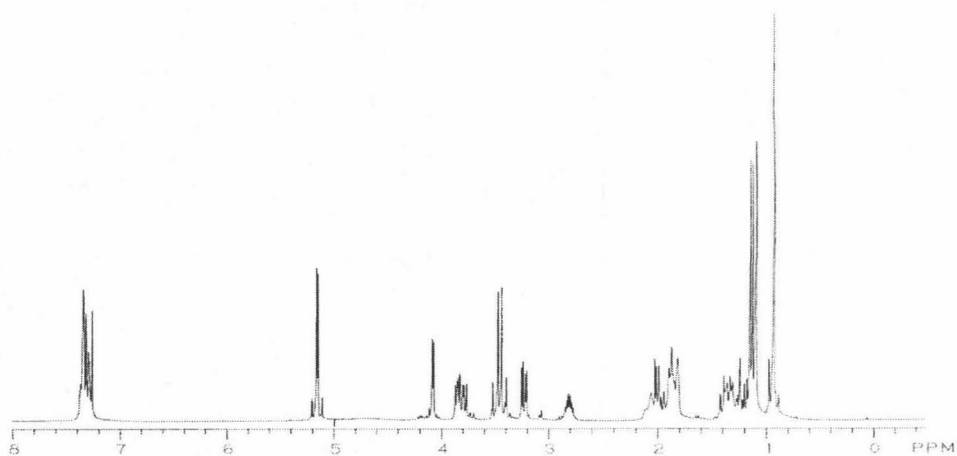
1222, 1167, 1136, 735, 699 cm<sup>-1</sup>;

**<sup>1</sup>H NMR** (CDCl<sub>3</sub>, 300 MHz):  $\delta$  7.32 (5H,m), 5.18 (1H, d,  $J$  =12.5 Hz), 5.13 (1H, d, 12.5 Hz), 4.07 (1H, d,  $J$  =3.5 Hz), 3.85 (1H, dd,  $J$  =7.6, 5.1 Hz), 3.79 (1H, dd,  $J$  = 11.8, 8.7 Hz), 3.50 (1H, d,  $J$  =13.8 Hz), 3.41 (1H, d,  $J$  =13.8 Hz), 3.23 (1H, dd,  $J$  =10.7, 4.2 Hz), 2.81 (1H, m), 1.14 (3H, d,  $J$  =6.9 Hz), 1.09 (3H, s), 0.93 (3H, s);

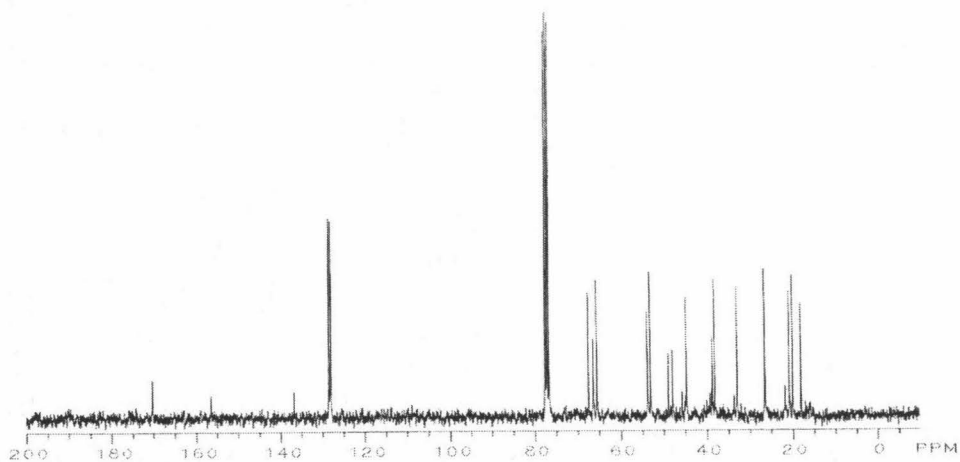
**<sup>13</sup>C NMR** (CDCl<sub>3</sub>, 75 MHz):  $\delta$  170.2, 156.4, 136.7, 128.4, 128.0, 127.9, 67.4, 66.3, 65.4, 53.7, 53.0, 48.8, 47.8, 44.6, 38.7, 38.1, 32.8, 24.5, 20.7, 19.9, 18.0;

**HRMS** (CI<sup>+</sup>) calculated for C<sub>23</sub>H<sub>31</sub>N<sub>3</sub>O<sub>5</sub>S 461.1984 , found 461.1986.

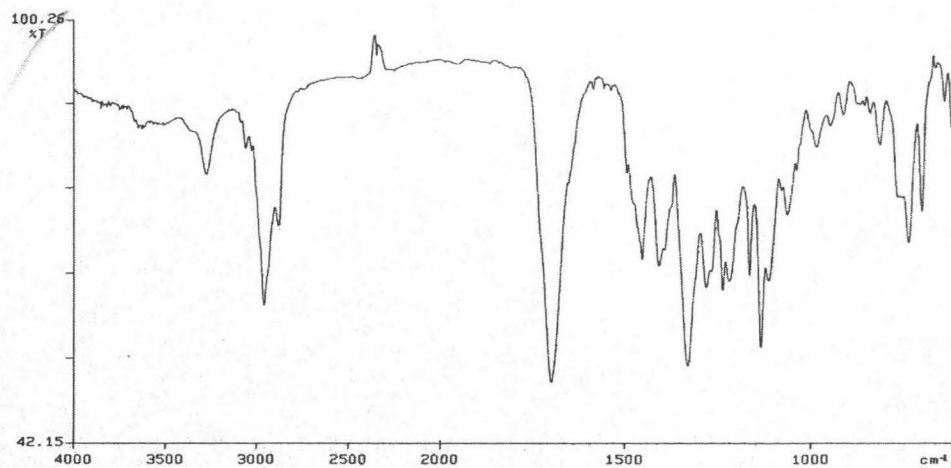
$^1\text{H}$  NMR  
300 MHz  
 $\text{CDCl}_3$

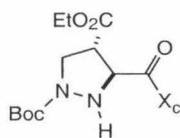


$^{13}\text{C}$  NMR  
75 MHz  
 $\text{CDCl}_3$



IR  
thin film



**83**

Product obtained (53%, two steps) as a clear, colorless oil.

$[\alpha]_{\text{D}}^{26.1} +77.5^\circ$  ( $c = 0.335$ ,  $\text{CHCl}_3$ );

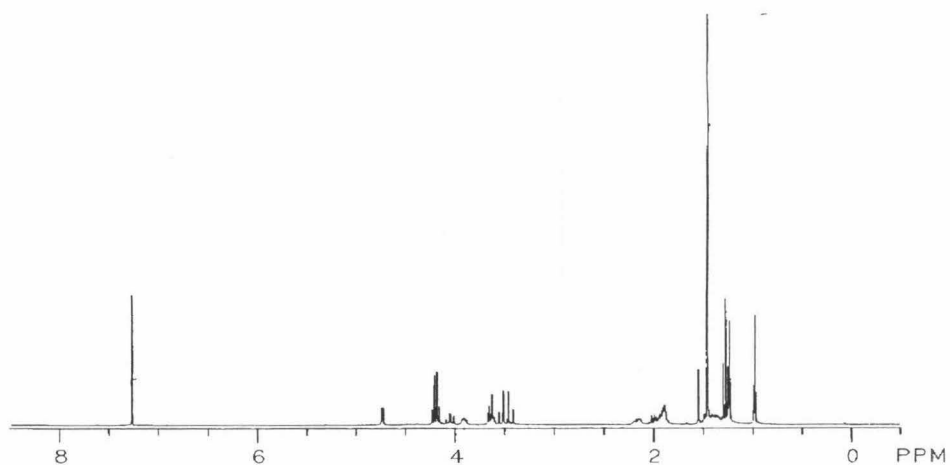
**IR** (thin film)  $\nu$  3261, 2976, 1731, 1698, 1458, 1392, 1368, 1333, 1278, 1167, 1136  $\text{cm}^{-1}$ ;

**$^1\text{H}$  NMR** (300MHz,  $\text{CDCl}_3$ ):  $\delta$  4.73 (1H, d,  $J = 2.4$  Hz), 4.18 (2H, q,  $J = 7.1$  Hz), 4.04 (1H, m), 3.86 (1H, m), 3.65 (2H, m), 3.52 (1H, d,  $J = 13.8$  Hz), 3.43 (1H, d,  $J = 13.8$  Hz), 2.14 (2H, m), 1.95 (3H, m), 1.45 (9H, s), 1.40 - 1.36 (2H, m), 1.27 (3H, t,  $J = 7.1$ Hz), 1.23 (3H, s), 0.97 (3H, s);

**$^{13}\text{C}$**  (125 MHz,  $\text{CDCl}_3$ ):  $\delta$  172.1, 168.8, 156.1, 80.8, 65.2, 62.9, 61.5, 52.9, 50.68, 48.8, 47.8, 47.7, 44.6, 37.8, 32.8, 28.2, 28.16, 2.4, 20.9, 19.9, 14.0;

**HRMS** ( $\text{CI}^+$ ) calculated for  $\text{C}_{22}\text{H}_{35}\text{N}_3\text{O}_7\text{S}$  485.2196, found 485.2184.

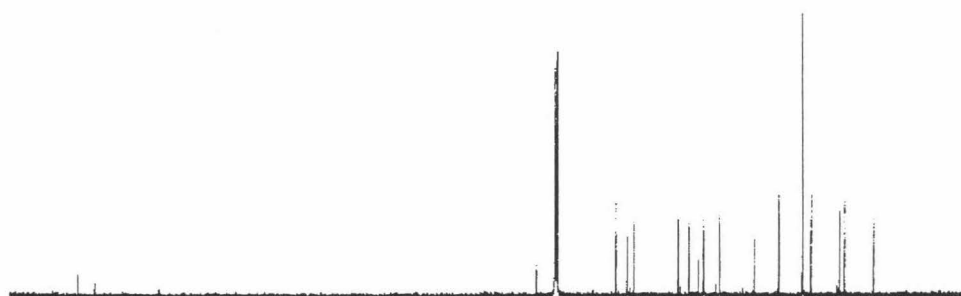
$^1\text{H}$  NMR  
300 MHz  
 $\text{CDCl}_3$



$^{13}\text{C}$  NMR

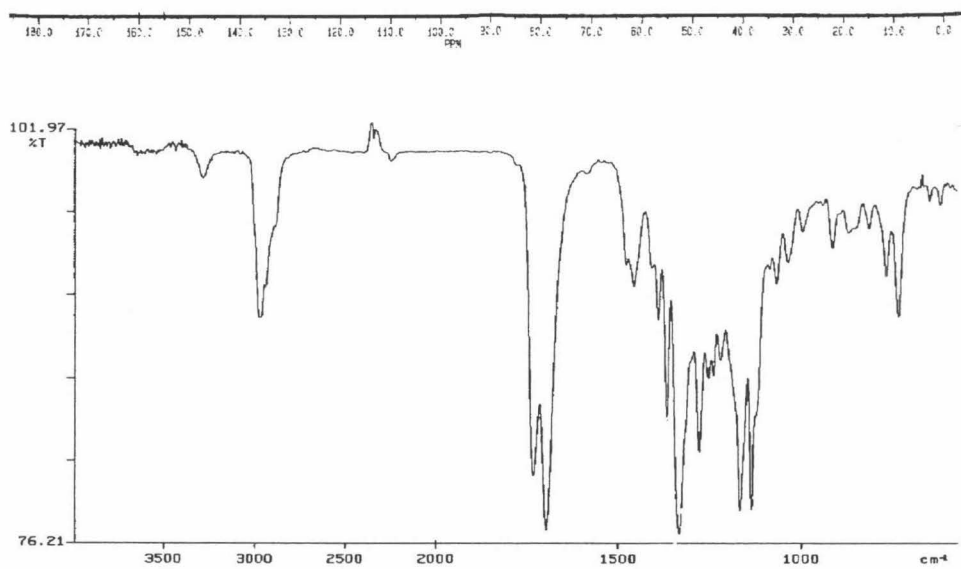
75 MHz

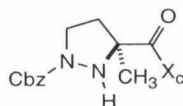
$\text{CDCl}_3$



IR

thin film



**84**

Product obtained (76%, two steps) as colorless oil.

$[\alpha]_{\text{D}}^{28.3}$  19.9 ° (c=0.37, CHCl<sub>3</sub>);

**IR** (thin film)  $\nu$  3265, 2961, 2887, 1694, 1455, 1336, 1275, 1122, 1057, 971, 735, 699, 616, 553;

**<sup>1</sup>H NMR** (CDCl<sub>3</sub>, 300 MHz):  $\delta$  7.30 (5H, m), 5.18 (1H, d,  $J$  = 12.5 Hz), 5.12 (1H, d, 12.5 Hz), 4.00 (1H, dd,  $J$  = 7.3, 4.0 Hz), 3.74 (1H, ddd,  $J$  = 10.0, 8.0, 8.0 Hz), 3.50-3.36 (3H, m), 1.48 (3H, s), 1.06 (3H, s), 0.90 (3H, s);

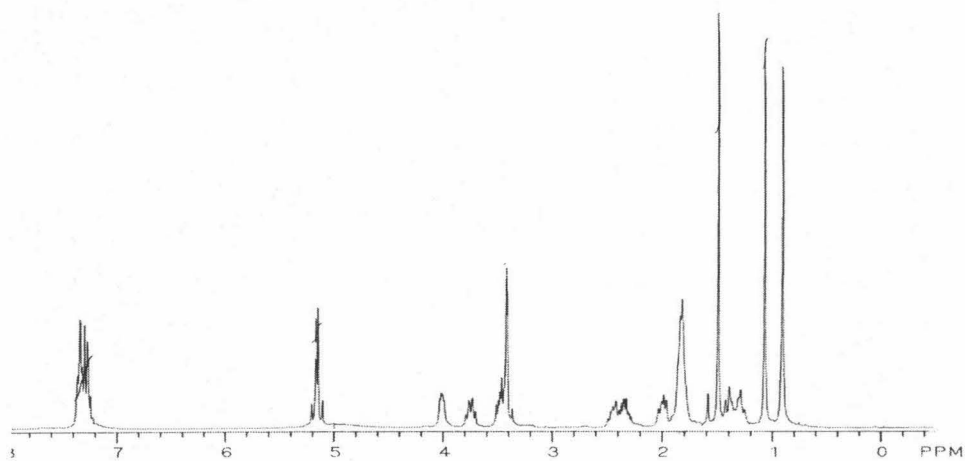
**<sup>13</sup>C NMR** (CDCl<sub>3</sub>, 75 MHz):  $\delta$  174.0, 155.6, 136.6, 128.2, 127.8, 127.8, 68.3, 67.0, 66.5, 53.2, 48.3, 47.7, 46.4, 44.2, 38.4, 36.5, 32.6, 26.4, 21.9, 20.3, 19.7;

**HRMS** (CI<sup>+</sup>) calculated for C<sub>23</sub>H<sub>30</sub>N<sub>3</sub>O<sub>5</sub>S 461.1984, found 461.1989.

$^1\text{H}$  NMR

300 MHz

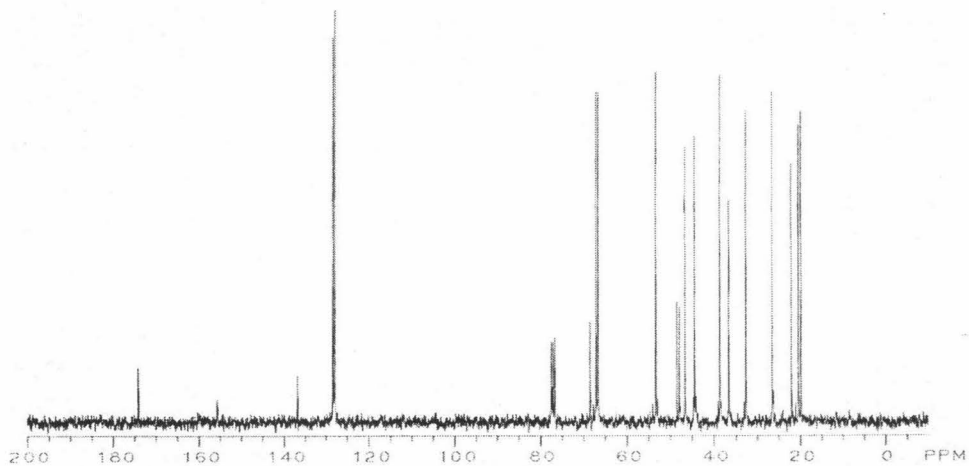
$\text{CDCl}_3$



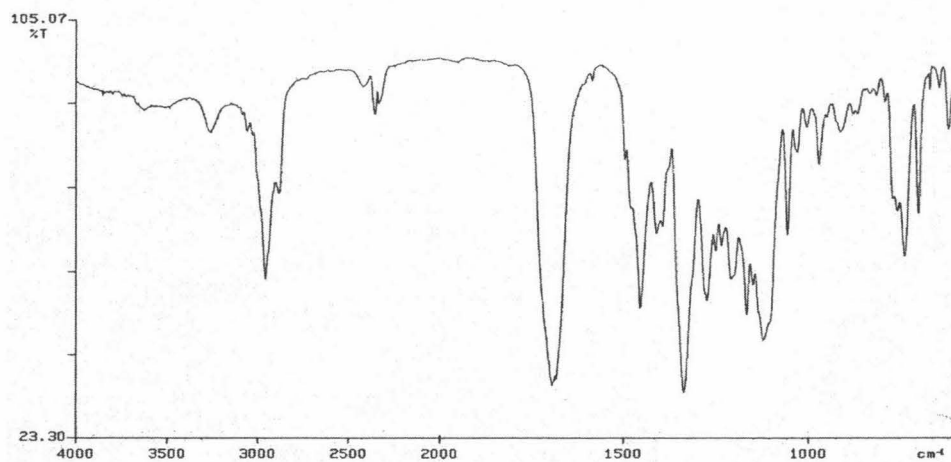
$^{13}\text{C}$  NMR

75 MHz

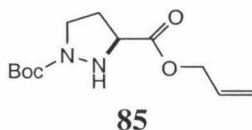
$\text{CDCl}_3$



IR  
thin film







To a stirred solution of 330  $\mu\text{L}$  of allyl alcohol (5 mmol, 10 equiv) in 1 mL dry THF under nitrogen at RT was added 19 mg lithium aluminum hydride (0.5 mmol, 1 equiv). After 5 min, 200 mg **81** (0.5 mmol, 1 equiv) was added in 0.5 mL dry THF. After 45 min, reaction was quenched by addition to brine and the aqueous layer extracted exhaustively with ethyl acetate. Removal of solvent by rotary evaporation furnished the crude product as an oil. Purification by flash chromatography to separate the allyl ester from the freeauxiliary was performed using (2:1 EtOAc/hexanes) to give **85**.

Product obtained (77%) as a clear, colorless oil.

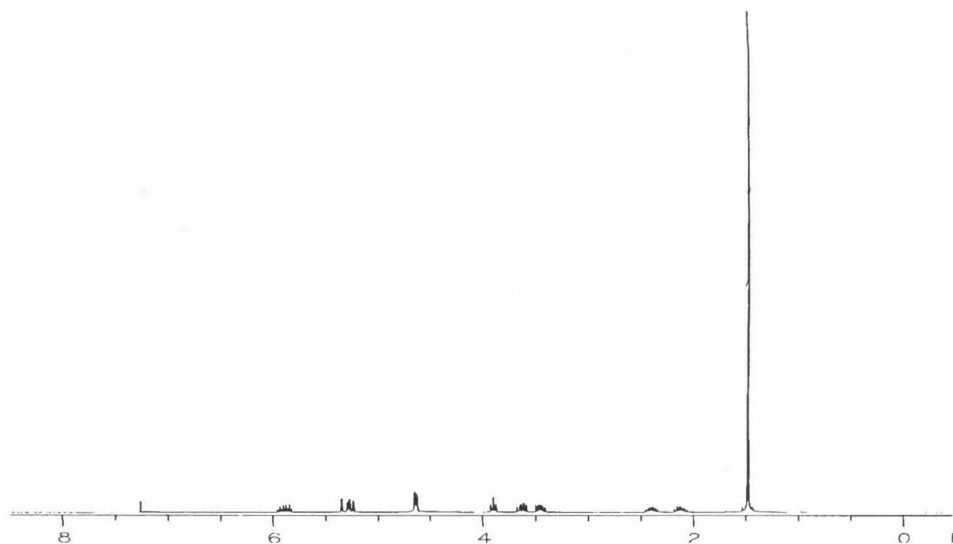
$[\alpha]_{\text{D}}^{26.7} + 0.49^\circ$  (c = 0.21,  $\text{CHCl}_3$ );

**IR** (thin film)  $\nu$  3645, 3251, 2978, 2349, 1738, 1694, 1480, 1453, 1392, 1367, 1252, 1170, 1128, 991  $\text{cm}^{-1}$ ;

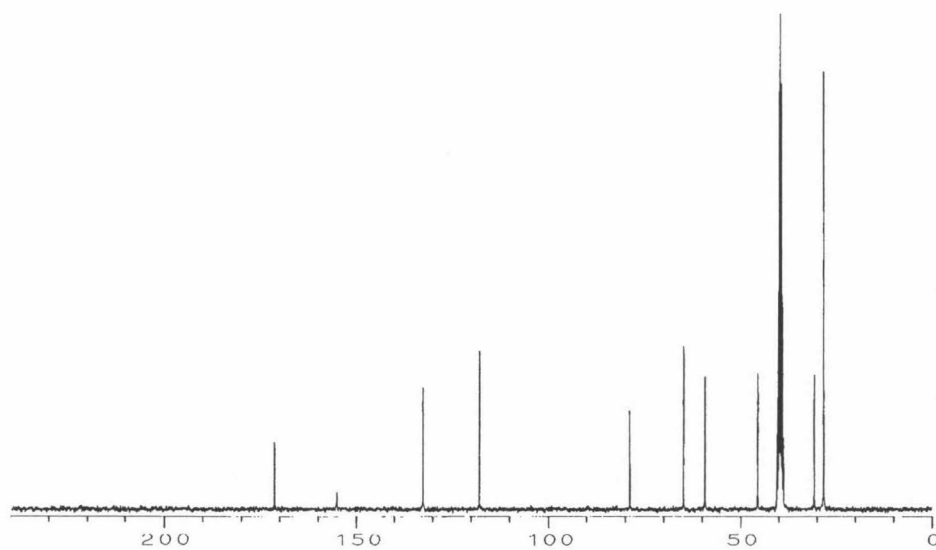
**$^1\text{H}$  NMR** (300 MHz,  $\text{CDCl}_3$ ):  $\delta$  5.89 (1H, m), 5.35 (2H, m), 4.63 (2H, m), 3.90 (1H, t, J = 7.2 Hz), 3.62 (1H, m), 3.45 (1H, m), 2.38 (1H, m), 2.13 (1H, m), 1.47 (9H, s);

**$^{13}\text{C}$  NMR** (75 MHz,  $d_6$ -DMSO):  $\delta$  171.3, 154.9, 132.3, 117.6, 78.6, 64.6, 59.1, 45.4, 30.5, 28.1.

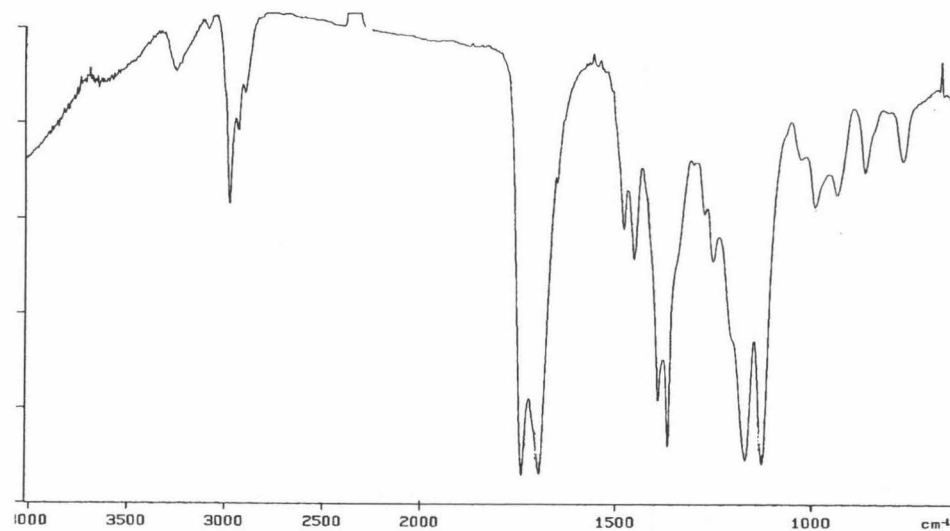
$^1\text{H}$  NMR  
300 MHz  
 $\text{CDCl}_3$

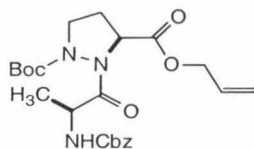


$^{13}\text{C}$  NMR  
75 MHz  
 $\text{CDCl}_3$



IR  
thin film





86

Product obtained (59%) as a clear, colorless oil:

$[\alpha]_{\text{D}}^{30.3}$   $-36.1^\circ$  ( $c = 1.24$ ,  $\text{CHCl}_3$ ); IR (thin film)  $\nu$  3332, 3065, 3033, 2981, 2938, 2252, 1727, 1587, 1522, 1455, 1393, 1369, 1342, 1316, 1251, 1184, 1157, 1115, 1070, 1027, 916  $\text{cm}^{-1}$ ;

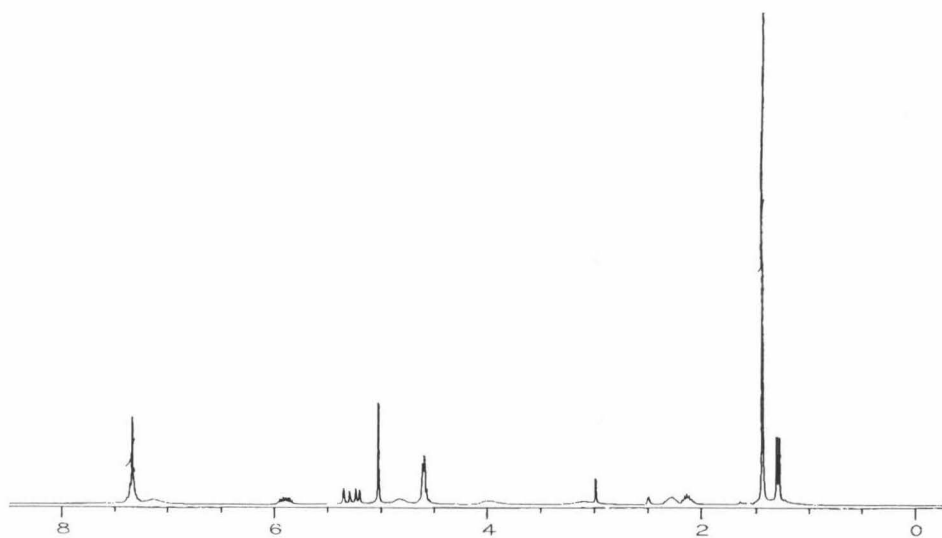
$^1\text{H NMR}$  (300 MHz,  $\text{d}_6$ -DMSO,  $100^\circ\text{C}$ ):  $\delta$  7.4-7.3 (5H, m), 5.83 (1H, m), 5.3-5.2 (2H, m), 5.05 (2H, s), 4.85 (1H, bm), 4.64 (3H, m), 3.97 (1H, m), 2.5 (1H, m), 2.25 (1H, m), 1.4 (9H, s), 1.32 (3H, d,  $J = 6.8$  Hz);

$^{13}\text{C NMR}$  (75 MHz,  $\text{CDCl}_3$ ,  $65^\circ\text{C}$ ):  $\delta$  176.7, 176.6, 169.7, 169.6, 156.7, 155.4, 136.5, 131.6, 128.3, 127.7, 118.21, 82.6, 66.6, 65.7, 57.6, 47.4, 47.1, 46.7, 29.1, 27.8, 18.4, 18.0.

$^1\text{H}$  NMR

300 MHz

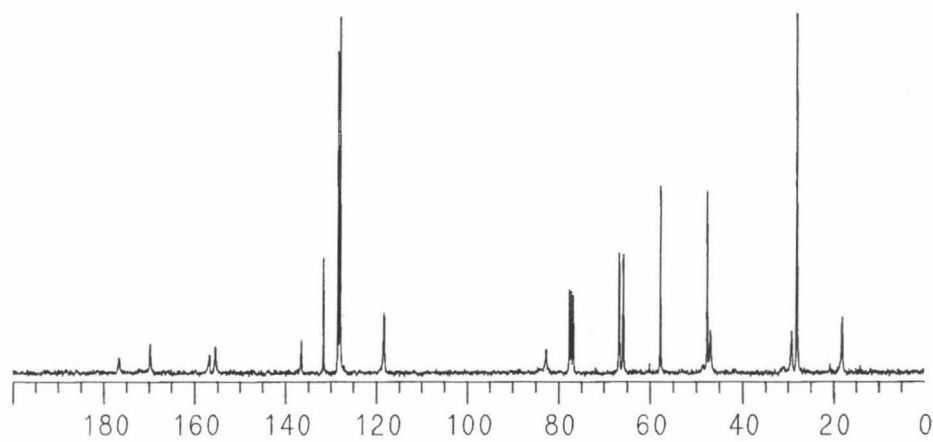
$d_6$ -DMSO



$^{13}\text{C}$  NMR

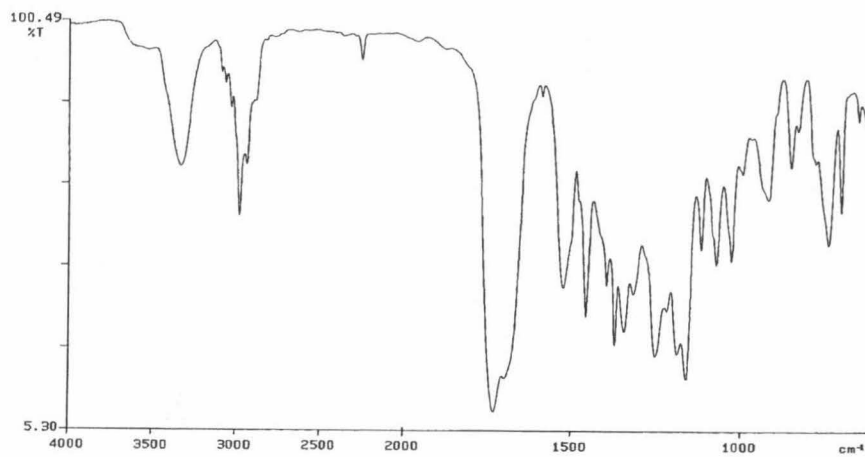
75 MHz

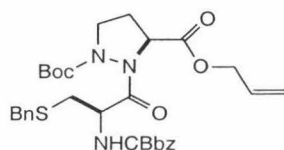
$d_6$ -DMSO



IR

thin film





## 87

Product obtained (50%) as a clear, colorless oil.

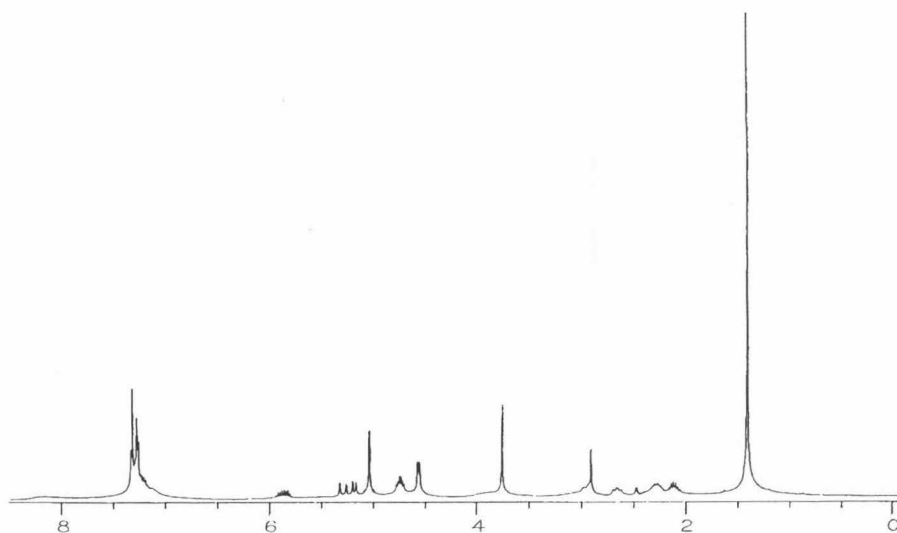
$[\alpha]_D^{30.0}$  - 47.176 ° (c = 1.335, CHCl<sub>3</sub>);

**IR** (thin film)  $\nu$  3333, 3028, 2978, 1731, 1693, 1682, 1514, 1496, 1454, 1370, 1338, 1312, 1255, 1155, 1054, 1028, 937 cm<sup>-1</sup>;

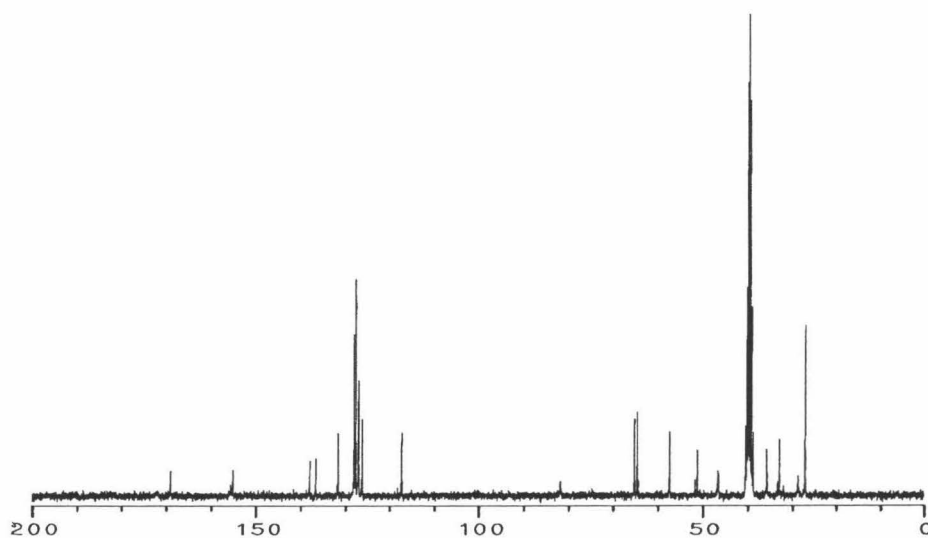
**<sup>1</sup>H NMR** (300 MHz, d<sub>6</sub>-DMSO, 110° C: carbamate rotomers in proton spectrum prevented rigorous characterization by this means);

**<sup>13</sup>C NMR** (75 MHz, DMSO, 110 ° C):  $\delta$  168.9, 155.6, 155.1, 137.8, 136.5, 131.7, 131.5, 128.2, 128.0, 127.6, 127.3, 127.0, 126.1, 117.2, 81.7, 65.1, , 64.5, 64.2, 57.2, 51.7, 51.1, 46.6, 35.7, 33.3, 32.9, 31.9, 28.7, 28.5, 27.1.

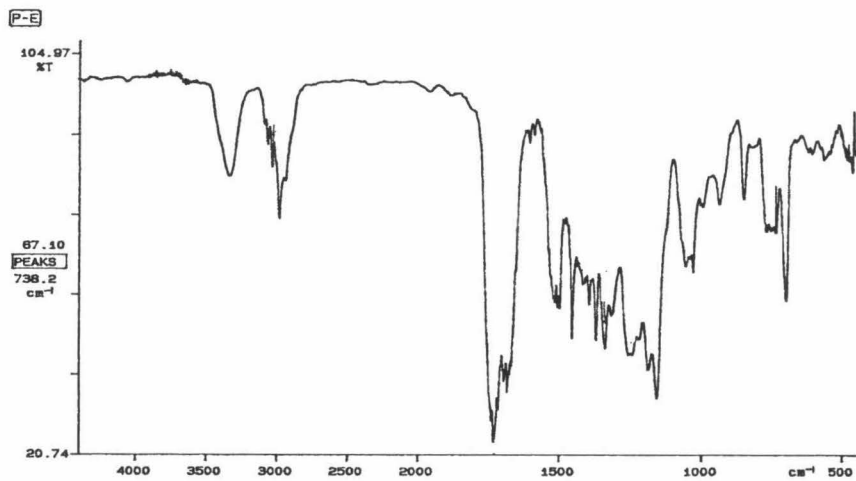
$^1\text{H}$  NMR  
300 MHz  
 $\text{d}_6$ -DMSO

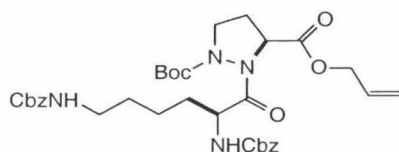


$^{13}\text{C}$  NMR  
75 MHz  
 $\text{d}_6$ -DMSO



IR  
thin film



**88**

Product obtained (45%) as a clear, colorless oil:

$[\alpha]_D^{30.3} -23.5^\circ$  ( $c = 0.490$ ,  $\text{CHCl}_3$ );

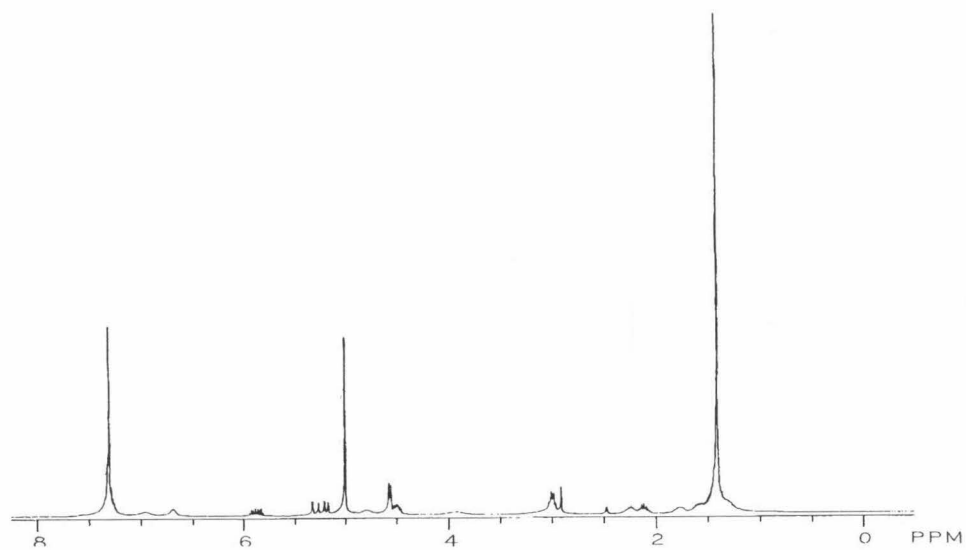
**IR** (thin film)  $\nu$  3322, 3032, 2937, 1723, 1524, 1454, 1393, 1369, 1339, 1247, 1156, 1027, 938, 738  $\text{cm}^{-1}$ ;

**$^1\text{H}$  NMR** (300 MHz,  $d_6$ -DMSO,  $100^\circ\text{C}$ :rotomers as in **87** prevented rigorous characterization by proton NMR);

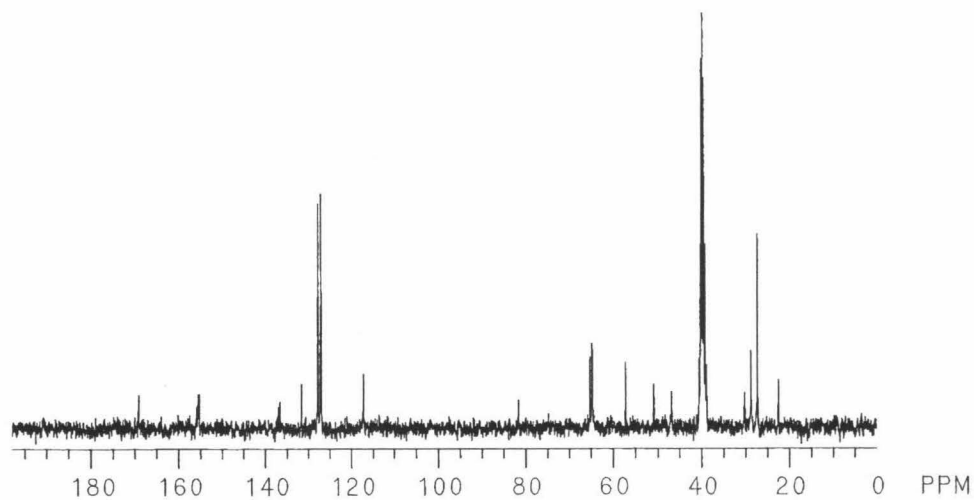
**$^{13}\text{C}$  NMR** (75 MHz,  $d_6$ -DMSO,  $100^\circ\text{C}$ )  $\delta$  169.1, 155.7, 155.4, 155.2, 136.9, 136.5,

131.5, 127.6, 127.2, 127.0, 126.9, 117.1, 81.4, 65.0, 64.7, 64.6, 64.5, 64.3, 57.1, 50.7, 50.6, 46.6, 30.1, 30.0, 28.6, 28.4.

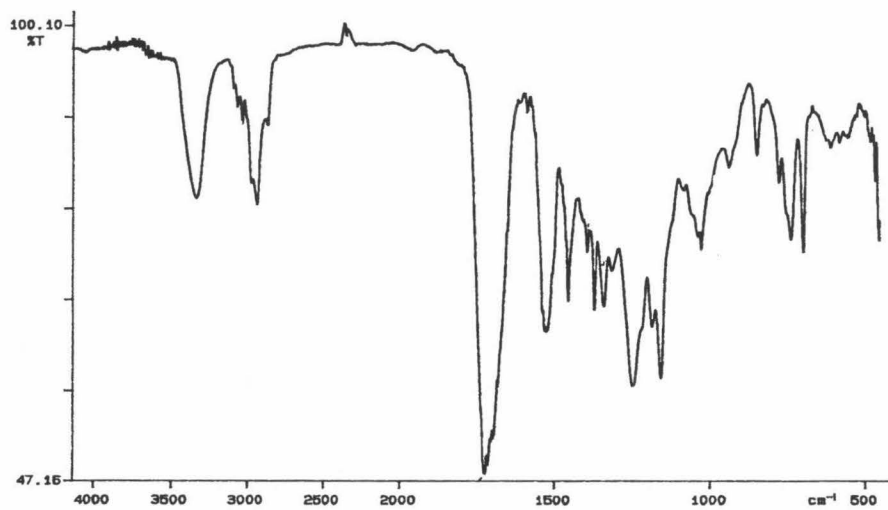
$^1\text{H}$  NMR  
300 MHz  
 $\text{d}_6\text{-DMSO}$



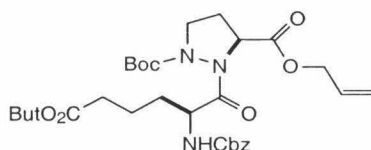
$^{13}\text{C}$  NMR  
75 MHz  
 $\text{d}_6\text{-DMSO}$



IR  
thin film





**89**

Product obtained (74%) as a clear, colorless oil.

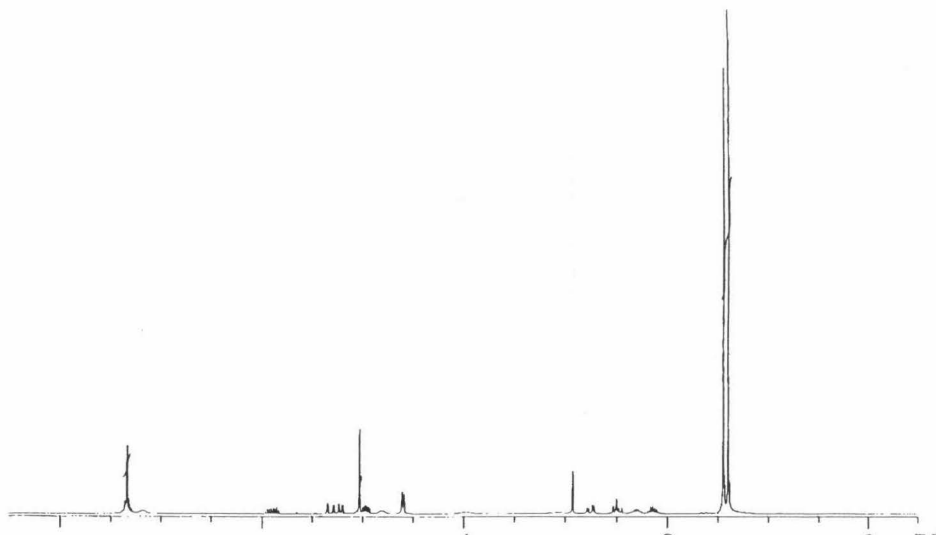
$[\alpha]_{\text{D}}^{25.5} -34.08^{\circ}$  ( $c = 0.502$ ,  $\text{CHCl}_3$ );

**IR** (thin film)  $\nu$  3338, 2979, 1737, 1716, 1704, 1519, 1455, 1393, 1369, 1338, 1249, 1158, 1049, 947, 848, 740  $\text{cm}^{-1}$ ;

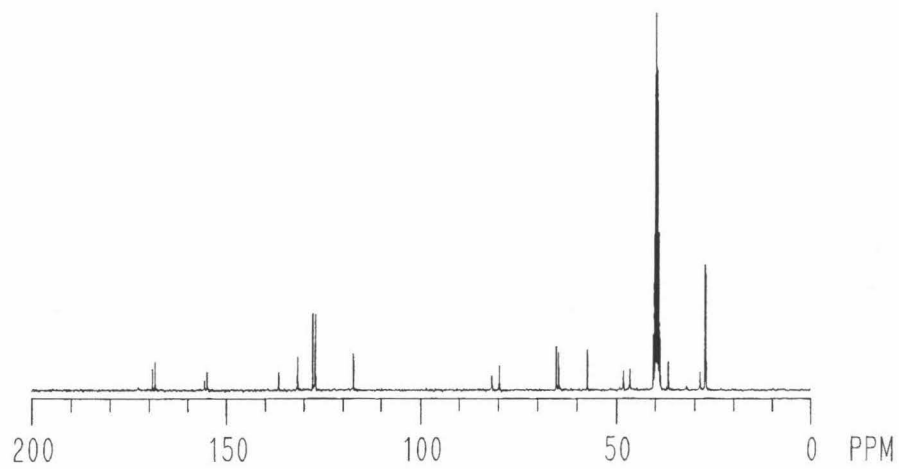
**$^1\text{H}$  NMR** (300 MHz,  $\text{d}_6$ -DMSO, 110 ° C)  $\delta$ : 7.4-7.3 (5H, m), 5.86 (1H, m), 5.3-5.2 (2H, m), 5.02 (2H, s), 4.90 (1H, m), 4.58 (2H,m), 2.91 (1H, s), 2.74 (1H, dd,  $J = 16.0, 3.9$  Hz), 2.54 (1H, m), 2.32 (1H,m), 2.20 (1H,m), 1.44 (9H, s), 1.39 (9H,s);

**$^{13}\text{C}$  NMR** (75 MHz,  $\text{d}_6$ -DMSO, 110 ° C):  $\delta$  169.0, 168.3, 155.5, 154.8, 136.4, 131.5, 127.6, 127.0, 126.9, 117.1, 81.5, 79.6, 65.1, 64.5, 57.2, 48.0, 46.3, 36.6, 28.5, 27.2, 27.0.

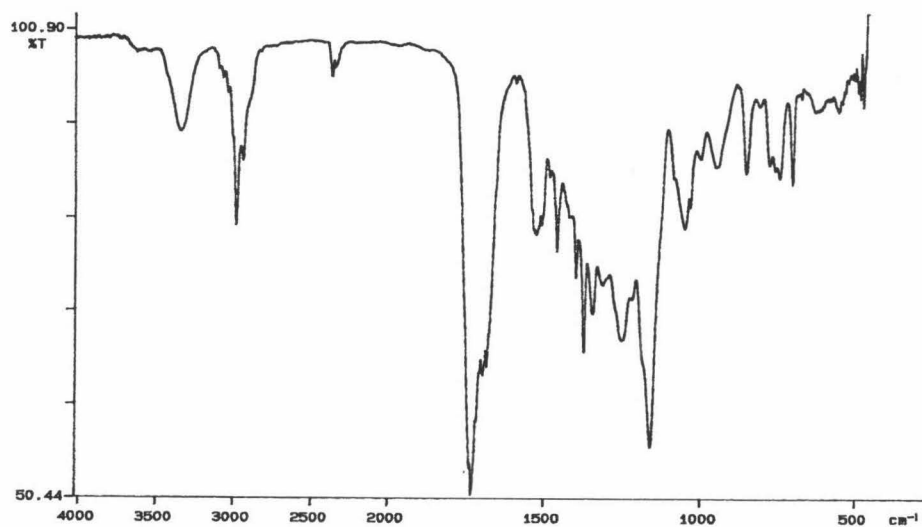
$^1\text{H}$  NMR  
300 MHz  
 $\text{d}_6\text{-DMSO}$

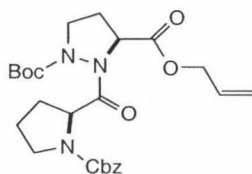


$^{13}\text{C}$  NMR  
75 MHz  
 $\text{d}_6\text{-DMSO}$



IR  
thin film



**90**

Product obtained (60%) as a clear, colorless oil.

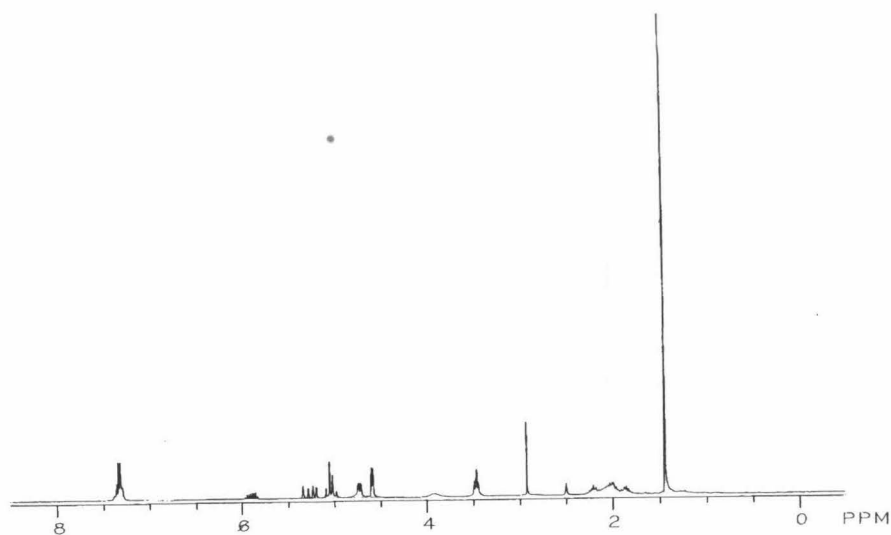
$[\alpha]_{\text{D}}^{26.6}$   $-46.4^\circ$  ( $c = 1.45$ ,  $\text{CHCl}_3$ );

**IR** (thin film)  $\nu$  2978, 2361, 1712, 1694, 1416, 1356, 1246, 1159, 1119, 992  $\text{cm}^{-1}$ ;

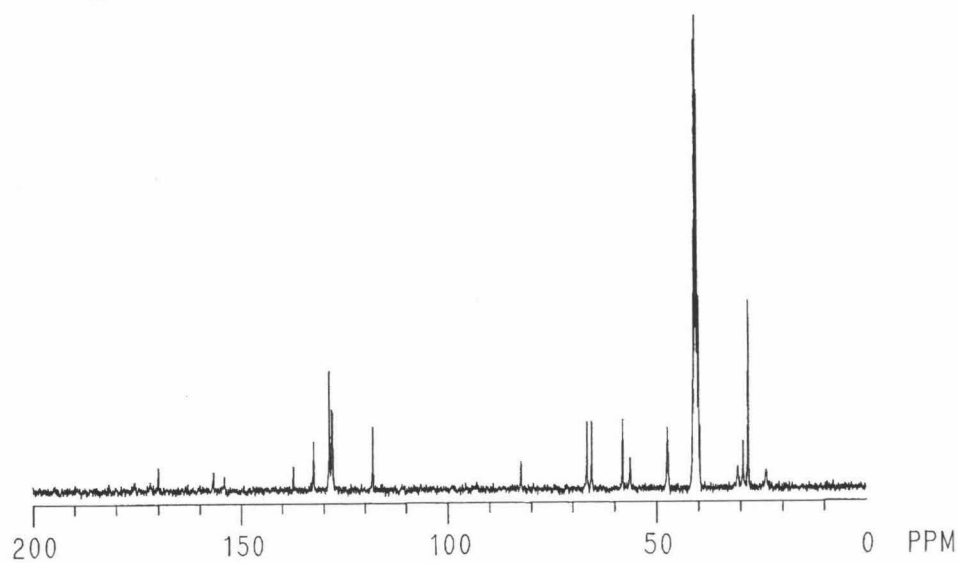
**$^1\text{H}$  NMR** (300 MHz,  $d_6$ -DMSO,  $100^\circ\text{C}$ )  $\delta$  : 7.4-7.3 (5H, m), 5.85 (1H, m), 5.02 (2H, dd,  $J = 15.0, 12.0$  Hz), 4.70 (2H, m), 4.58 (2H, d,  $J = 5.4$  Hz), 4.0-3.7 (1H, bs), 3.45 (2H, m), 2.22 (1H, m), 2.1-1.8 (4H, m), 1.45 (9H, s);

**$^{13}\text{C}$  NMR** (75 MHz,  $d_6$ -DMSO,  $100^\circ\text{C}$ ):  $\delta$  169.0, 155.8, 153.1, 136.4, 131.5, 127.6, 127.1, 126.9, 117.1, 81.5, 65.5, 64.4, 57.0, 46.4, 46.1, 28.4, 27.1.

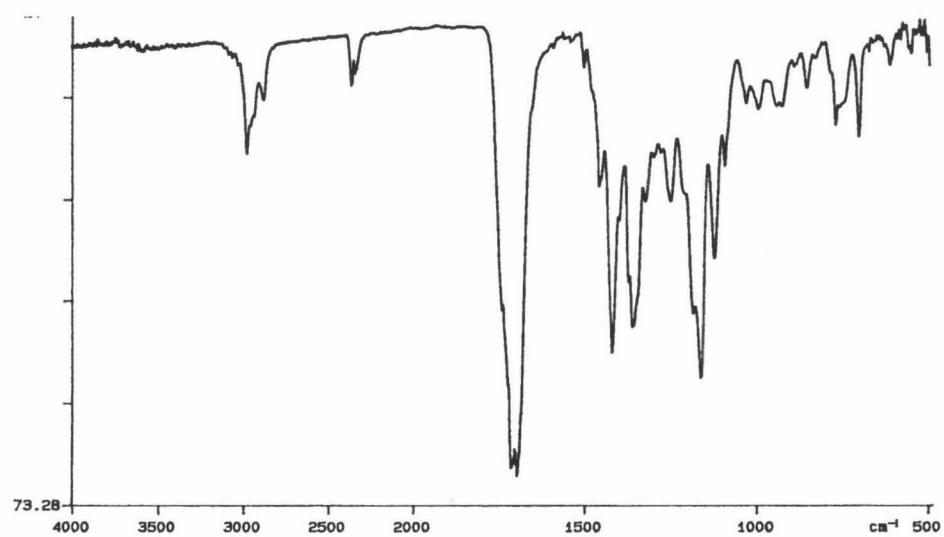
$^1\text{H}$  NMR  
300 MHz  
 $\text{d}_6\text{-DMSO}$

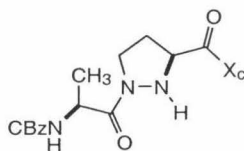


$^{13}\text{C}$  NMR  
75 MHz  
 $\text{d}_6\text{-DMSO}$



IR  
thin film



**91**

Product obtained (49%) as a clear, colorless oil:

$[\alpha]_{\text{D}}^{26.4} +57.0^{\circ}$  ( $c = 0.735$ ,  $\text{CHCl}_3$ );

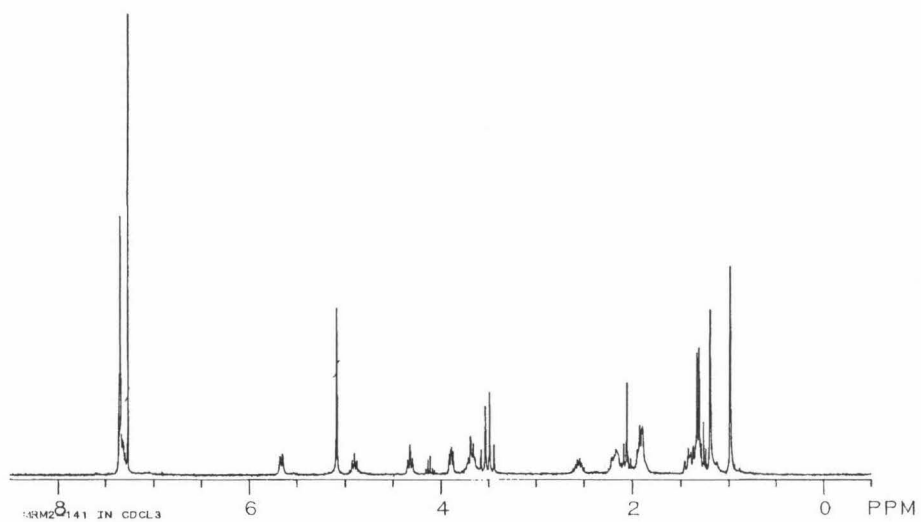
**IR** (thin film)  $\nu$  3418, 3248, 2961, 1717, 1694, 1650, 1497, 1453, 1413, 1332, 1281, 1240, 1221, 1167, 1136, 1117, 1065, 913  $\text{cm}^{-1}$ ;

**$^1\text{H}$  NMR** (300 MHz,  $\text{CDCl}_3$ )  $\delta$ : 7.4-7.3 (5H, m), 5.66 (1H, d,  $J = 7.8$  Hz), 5.08 (2H, s), 4.89 (1H, m), 4.31 (1H, t,  $J = 7.5$  Hz), 3.88 (1H, q,  $J = 3.0$  Hz), 3.64-3.70 (2H, m), 3.50 (1H, d,  $J = 13.8$  Hz), 3.48 (1H, d,  $J = 13.8$  Hz), 2.53 (1H, m), 2.20-1.88 (5H, m), 1.5-1.25 (5H, m), 1.18 (3H, s), 0.98 (3H, s);

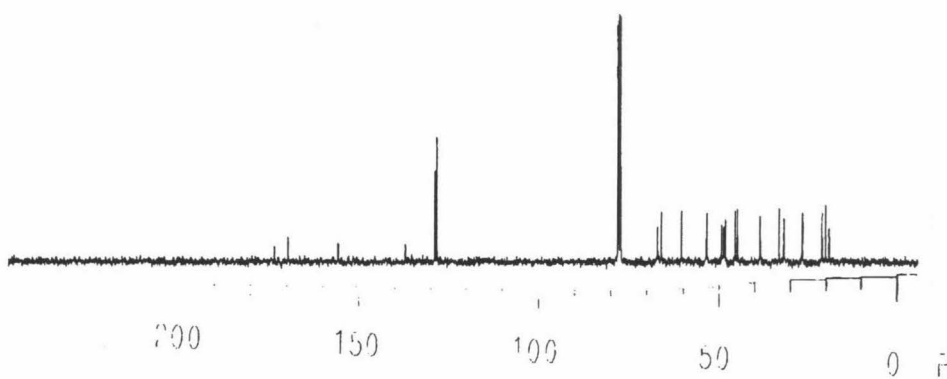
**$^{13}\text{C}$  NMR** (75 MHz,  $\text{CDCl}_3$ ):  $\delta$  173.2, 169.4, 155.4, 136.6, 128.4, 127.9, 66.5, 65.4, 59.9, 53.0, 48.9, 48.3, 47.9, 45.2, 44.5, 38.2, 32.8, 31.5, 26.4, 20.8, 19.8, 18.8.

**$^1\text{H}$  NMR**

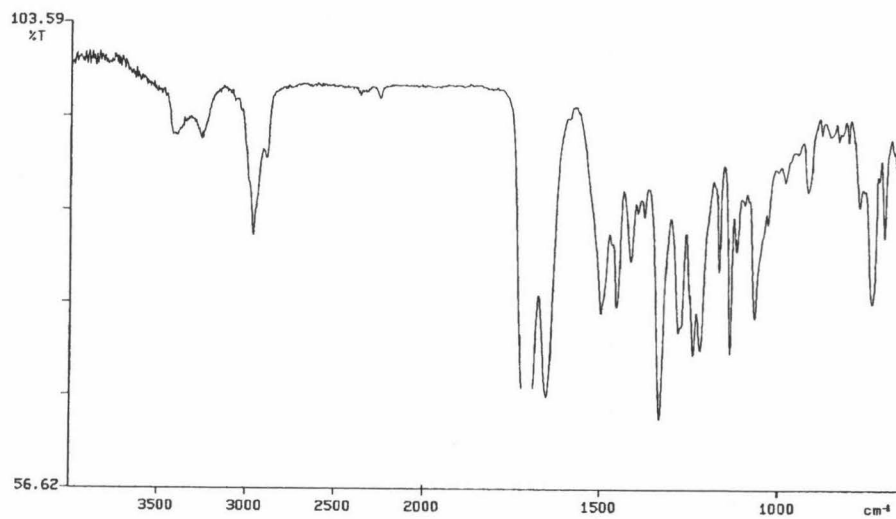
300 MHz

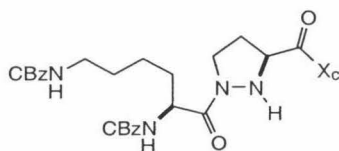
 $\text{CDCl}_3$  **$^{13}\text{C}$  NMR**

75 MHz

 $\text{CDCl}_3$ **IR**

thin film



**92**

Product obtained (74%) as a clear, colorless oil.

$[\alpha]_D^{25.0} +58.6^\circ$  ( $c = 0.30$ ,  $\text{CHCl}_3$ );

**IR** (thin film)  $\nu$  3401, 3337, 3368, 3033, 2958, 2248, 1705, 1648, 1518, 1455, 1413, 1376, 1332, 1272, 1241, 1166, 1136, 1065, 913  $\text{cm}^{-1}$ ;

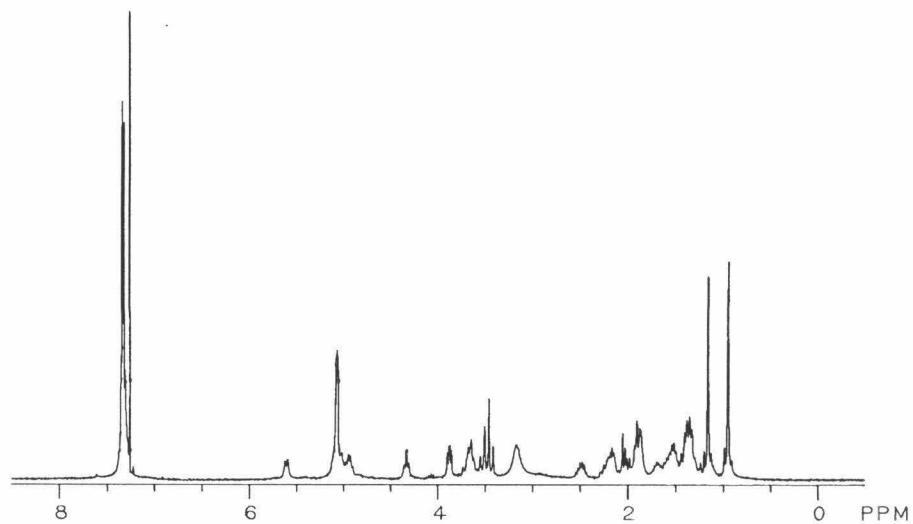
**$^1\text{H}$  NMR** (300 MHz,  $\text{CDCl}_3$ )  $\delta$ : 7.4-7.3 (10H, m), 5.60 (1H, d,  $J = 8.7$  Hz), 5.11-4.91 (5H, m), 4.32 (1H, t,  $J = 6.6$  Hz), 3.88 (1H, q,  $J = 3.0$  Hz), 3.75-3.6 (2H, m), 3.50 (1H, d,  $J = 13.8$  Hz), 3.48 (1H, d,  $J = 13.8$  Hz), 2.70 (2H, m), 3.25-3.10 (2H, bs), 2.53 (1H, m), 2.3-2.1 (2H, m), 2.05-1.88 (4H, m), 1.75-1.25 (5H, m), 1.15 (3H,s), 0.94 (3H,s);

**$^{13}\text{C}$  NMR** (75 MHz,  $\text{CDCl}_3$ ): 172.5, 169.2, 156.4, 155.8, 136.6, 136.5, 128.4, 127.9, 127.8, 66.5, 66.4, 65.3, 59.8, 52.9, 51.6, 48.8, 47.7, 45.0, 44.5, 40.4, 38.1, 32.7, 32.5, 31.0, 29.0, 26.3, 22.0, 20.7, 19.7.

$^1\text{H}$  NMR

300 MHz

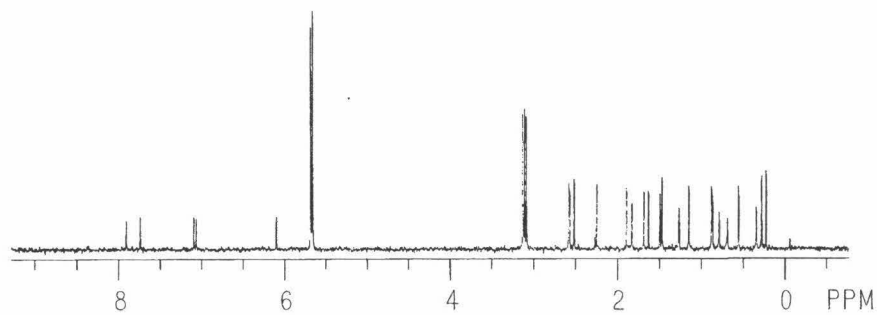
$\text{CDCl}_3$



$^{13}\text{C}$  NMR

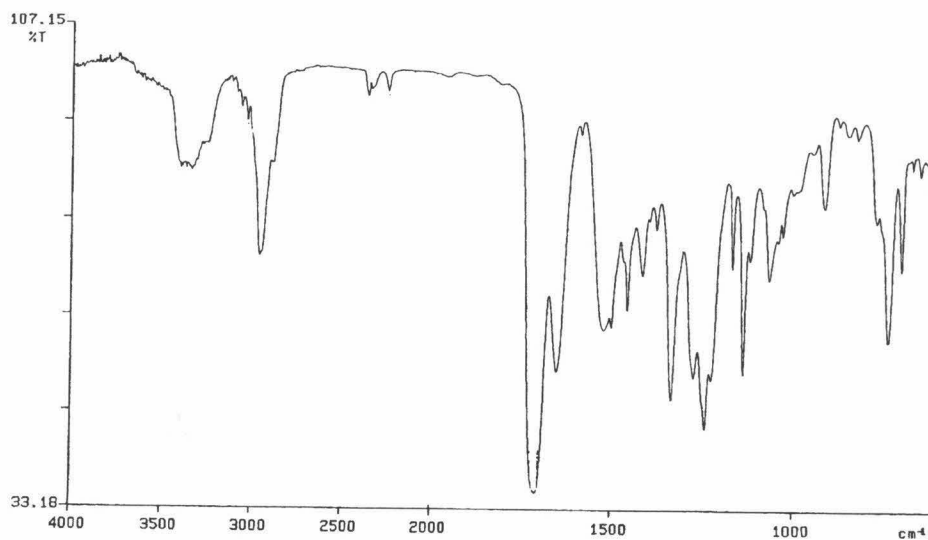
75 MHz

$\text{CDCl}_3$

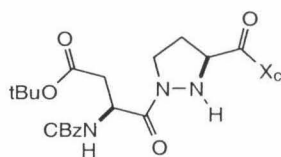


IR

thin film





**93**

Product obtained (65%) as a clear, colorless oil.

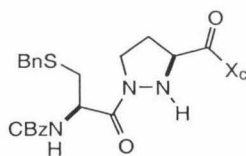
$[\alpha]_D^{28.3} +54.6^\circ$  ( $c = 1.42$ ,  $\text{CHCl}_3$ );

**IR** (thin film)  $\nu$  3410, 3252, 2963, 2251, 1724, 1652, 1498, 1455, 1414, 1393, 1368, 1335, 1281, 1241, 1222, 1167, 1137, 1065, 998, 914, 845  $\text{cm}^{-1}$ ;

**$^1\text{H}$  NMR** (300 MHz,  $\text{CDCl}_3$ )  $\delta$ : 7.4-7.3 (10H, m), 5.78 (1H, d,  $J = 8.7$  Hz), 5.13-5.07 (3H, m), 4.38 (1H, t,  $J = 6.4$  Hz), 3.88 (1H, q,  $J = 5.1$  Hz), 3.75-3.6 (2H, m), 3.55 (1H, d,  $J = 12.6$  Hz), 3.48 (1H, d,  $J = 12.6$  Hz), 2.70 (2H, d,  $J = 5.7$  Hz), 2.55 (1H, m), 2.20-1.88 (5H, m), 1.4-1.25 (11H, m), 1.18 (3H, s), 0.98 (3H, s);

**$^{13}\text{C}$  NMR** (75 MHz,  $\text{CDCl}_3$ ):  $\delta$  172.0, 170.2, 156.4, 136.5, 129.0, 128.5, 128.0, 81.0, 66.8, 65.5, 59.8, 49.6, 48.0, 46.0, 44.5, 38.4, 33.0, 31.5, 28.0, 26.5, 21.0, 20.4.



**94**

Product obtained (50%) as a clear, colorless oil.

$[\alpha]_{\text{D}}^{26.1} +63.1^\circ$  ( $c = 1.12$ ,  $\text{CHCl}_3$ );

**IR** (thin film)  $\nu$  3400, 3253, 2960, 2424, 2361, 1691, 1648, 1496, 1454, 1412, 1333,

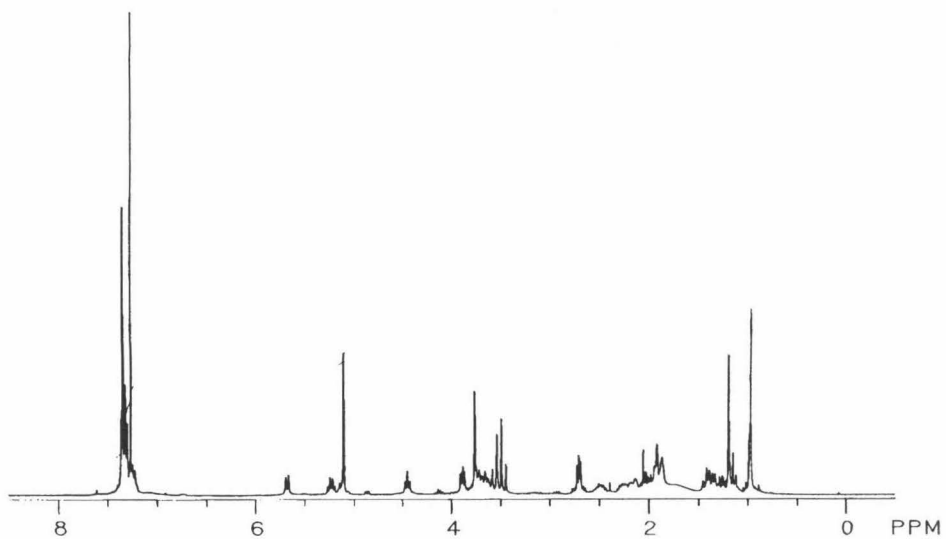
1273, 1240, 1221, 1167, 1135, 1062, 996  $\text{cm}^{-1}$ ;

**$^1\text{H NMR}$**  (300 MHz,  $\text{CDCl}_3$ )  $\delta$ : 7.4-7.3 (10H, m), 5.67 (1H, d,  $J = 8.4$  Hz), 5.22 (1H, q,  $J = 8.1$  Hz), 5.1 (2H, s), 4.45 (1H, t,  $J = 6.9$  Hz), 3.88 (1H, q,  $J = 3.0$  Hz), 3.75-3.6 (4H, m), 3.50 (1H, d,  $J = 13.8$  Hz), 3.48 (1H, d,  $J = 13.8$  Hz), 2.70 (2H, m), 2.53 (1H, m), 2.20-1.88 (5H, m), 1.5-1.25 (5H, m), 1.18 (3H, s), 0.98 (3H, s);

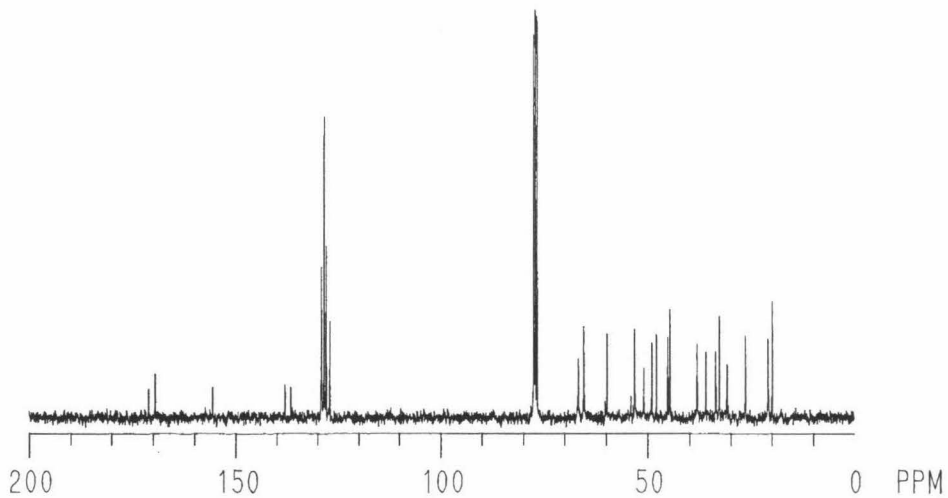
**$^{13}\text{C NMR}$**  (75 MHz,  $\text{CDCl}_3$ ):  $\delta$  171.0, 169.5, 155.5, 138.0, 136.5, 129.1,

128.4, 127.9, 126.9, 66.6, 65.3, 59.7, 53.0, 50.8, 48.9, 47.8, 45.1, 44.5, 38.1, 38.06, 36.0, 33.6, 32.8, 30.9, 26.3, 20.9, 19.8.

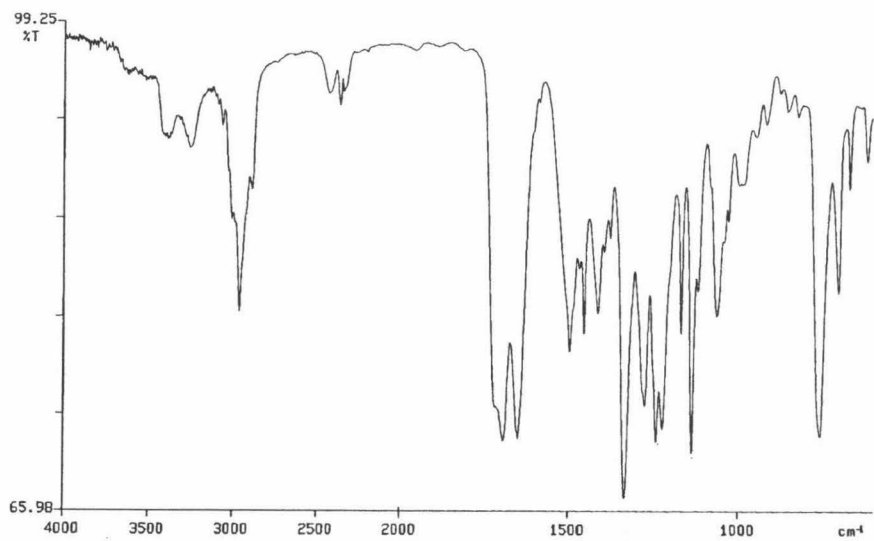
$^1\text{H}$  NMR  
300 MHz  
 $\text{CDCl}_3$

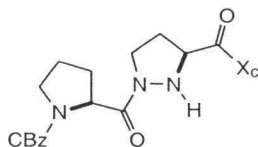


$^{13}\text{C}$  NMR  
75 MHz  
 $\text{CDCl}_3$



IR  
thin film



**95**

Product obtained (58%) as a clear, colorless oil.

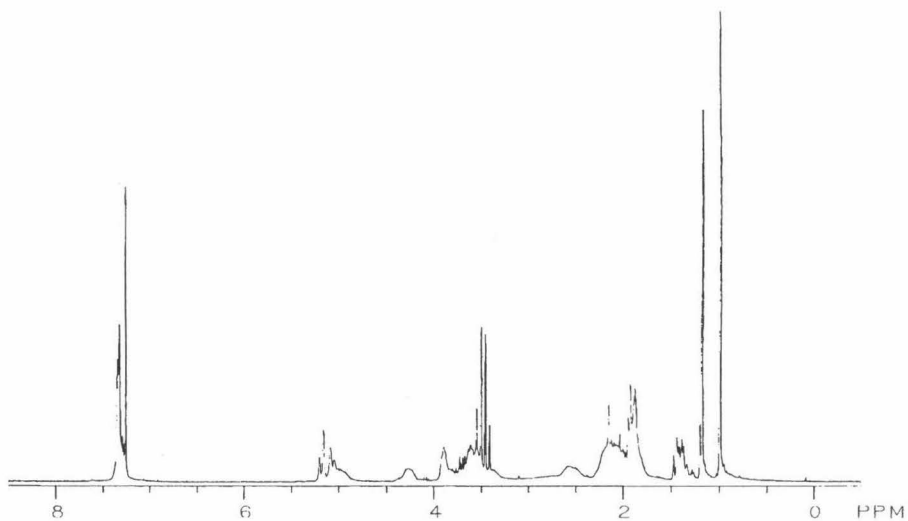
$[\alpha]_{\text{D}}^{28.5} +76.1^\circ$  ( $c = 1.03$ ,  $\text{CHCl}_3$ );

**IR** (thin film)  $\nu$  3468, 3246, 2960, 2883, 2360, 2341, 1698, 1448, 1416, 1359, 1333, 1273, 1240, 1220, 1167, 1135, 1118, 1068, 1038, 983, 917  $\text{cm}^{-1}$ ;

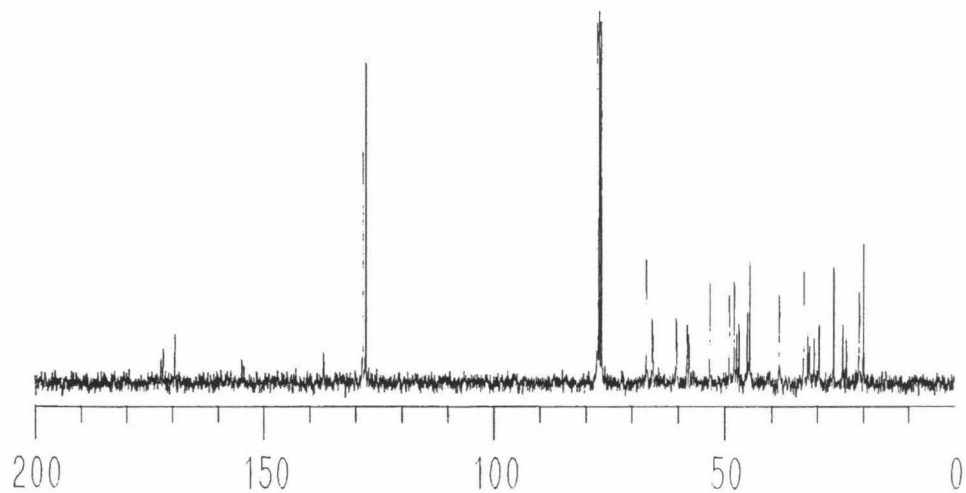
**$^1\text{H}$  NMR** (300 MHz,  $\text{CDCl}_3$ , rotomers present prevented rigorous spectral characterization by this means);

**$^{13}\text{C}$  NMR** (75 MHz,  $\text{CDCl}_3$ ): $\delta$  172.4, 171.9, 169.4, 154.8, 136.9, 136.9, 128.3, 127.7, 66.7, 65.5, 65.4, 60.3, 60.2, 57.9, 57.5, 53.0, 48.9, 47.8, 47.3, 46.8, 45.1, 44.5, 38.2, 32.8, 32.0, 31.6, 30.5, 29.5, 26.3, 24.3, 23.6, 20.8, 19.8.

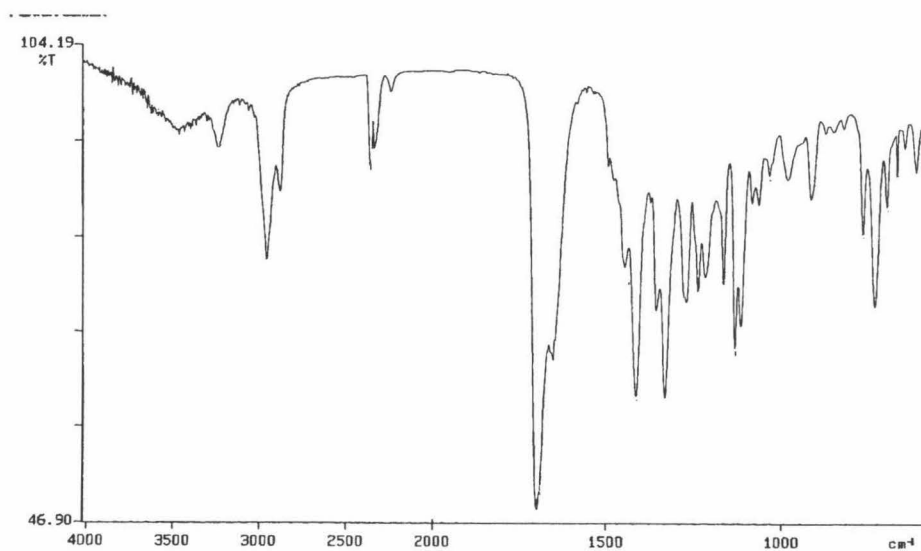
**$^1\text{H}$  NMR**  
**300 MHz**  
 **$\text{CDCl}_3$**



**$^{13}\text{C}$  NMR**  
**75 MHz**  
 **$\text{CDCl}_3$**

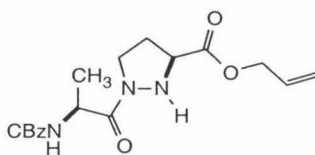


**IR**  
**thin film**



**General Procedure for the Synthesis of Allyl-Ester Derived Dipeptides 96-100**

To a stirred solution of 330  $\mu\text{L}$  of allyl alcohol (5 mmol, 10 equiv) in 1 mL dry THF under nitrogen at RT was added 19 mg lithium aluminum hydride (0.5 mmol, 1 equiv). After 5 min, 0.5 mmol (1 equiv) of the dipeptide was added in 0.5 mL dry THF. After 45 min, reaction was quenched by addition to brine and the aqueous layer extracted exhaustively with ethyl acetate. Removal of solvent by rotary evaporation furnished the crude product as an oil. Purification by flash chromatography to separate the allyl ester from the freeauxiliary was performed using (2:1 EtOAc/hexanes) to give dipeptides **96-100** as their respective allyl esters.



Allyl Ester **96**, isolated as a clear oil, 76%.

$[\alpha]_D^{24.6^\circ} +17.2^\circ$  ( $c=0.73$ ,  $\text{CHCl}_3$ );

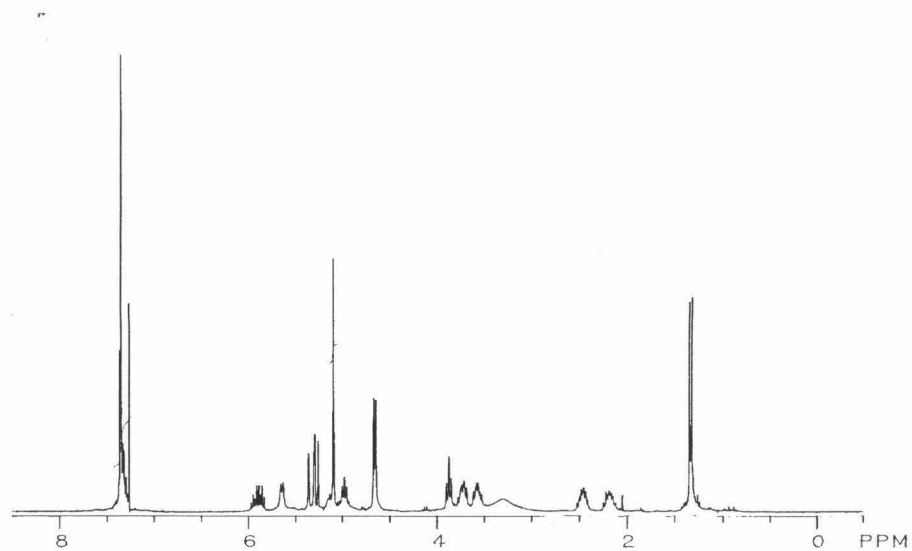
**$^1\text{H}$  NMR** (300 MHz,  $\text{CDCl}_3$ )  $\delta$  7.36-7.30 (5H, m), 5.94-5.85 (1H, m), 5.64 (1H, d,  $J = 7.7$  Hz), 5.32 (2H, m), 5.08 (2H, s), 4.94 (1H, m), 4.65 (2H, d,  $J = 15.2$  Hz), 3.86 (1H, m), 3.75 (1H, m), 3.60 (1H, m), 3.5-3.2 (1H, bs), 2.43 (1H, m), 2.19 (1H, m), 1.31 (9H, s);

**IR** (thin film)  $\nu$  3410, 3249, 2960, 2359, 1738, 1714, 1644, 1504, 1455, 1415, 1372, 1337, 1209, 1145, 1095, 988  $\text{cm}^{-1}$ ;

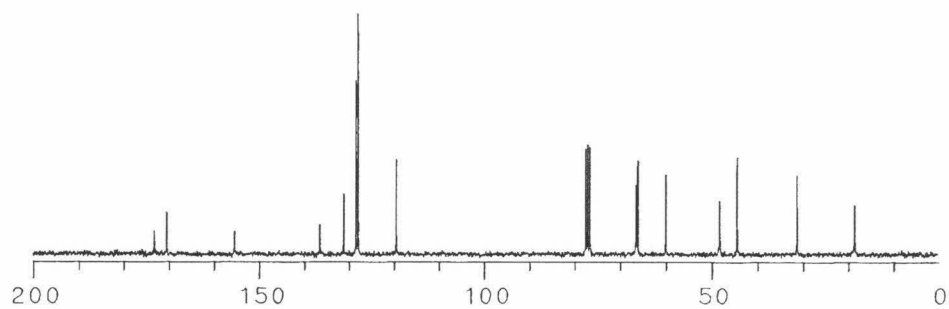
**$^{13}\text{C}$  NMR** (75 MHz,  $\text{CDCl}_3$ ):  $\delta$  173.2, 170.4, 155.4, 136.5, 131.1, 128.3, 127.9, 119.3, 66.5, 66.1, 59.9, 48.2, 44.32, 31.33, 18.6



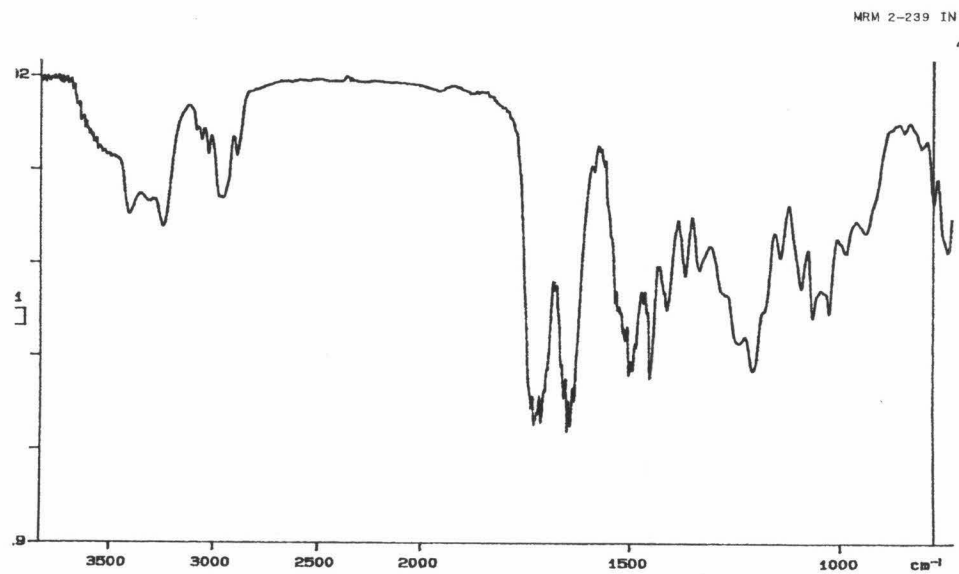
$^1\text{H}$  NMR  
300 MHz  
 $\text{CDCl}_3$

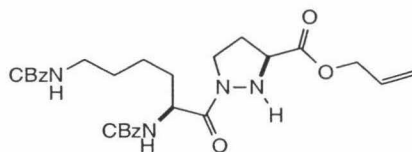


$^{13}\text{C}$  NMR  
75 MHz  
 $\text{CDCl}_3$



IR  
thin film





Allyl ester **97**, isolated as a clear oil, 62%.

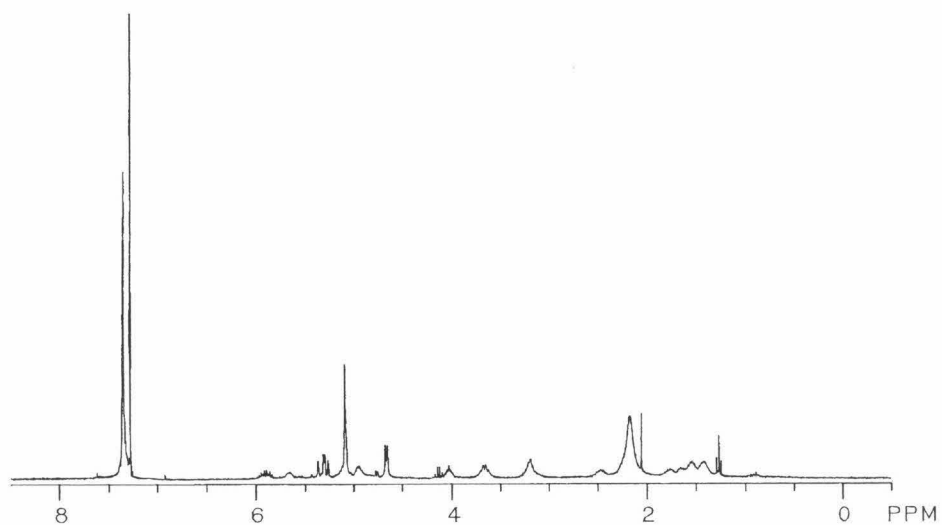
$[\alpha]_{\text{D}}^{28.5} + 8.48^\circ$  ( $c = 1.2$  in  $\text{CHCl}_3$ );

**$^1\text{H}$  NMR** (300 MHz,  $\text{CDCl}_3$ )  $\delta$  7.45, (10H, m), 5.81 (1H, m), 5.72 (1H, d,  $J = 7.2$  Hz), 5.34 (2H, m), 5.12 (4H, s), 4.96 (1H, m), 4.64 (2H, d,  $J = 8.2$  Hz), 4.12 (1H, m) 3.66 (1H, m), 3.20 (1H, m), 2.48 (1H, m) 2.3 (6H, bs), 1.78-1.35 (8H, m);

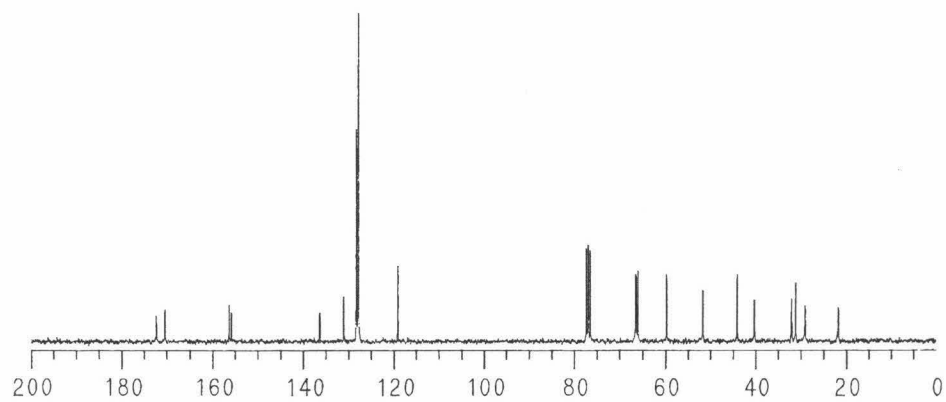
**IR** (thin film)  $\nu$  3331, 3032, 2942, 1722, 1713, 1651, 1644, 1537, 1504, 1454, 1415, 1248, 1139, 1027  $\text{cm}^{-1}$ ;

**$^{13}\text{C}$  NMR** (75 MHz,  $\text{CDCl}_3$ ):  $\delta$  1172.4, 170.5, 156.4, 155.9, 136.5, 131.1, 128.4, 127.9, 119.2, 66.6, 66.4, 66.1, 59.9, 51.8, 44.2, 40.4, 32.1, 29.1, 21.8.

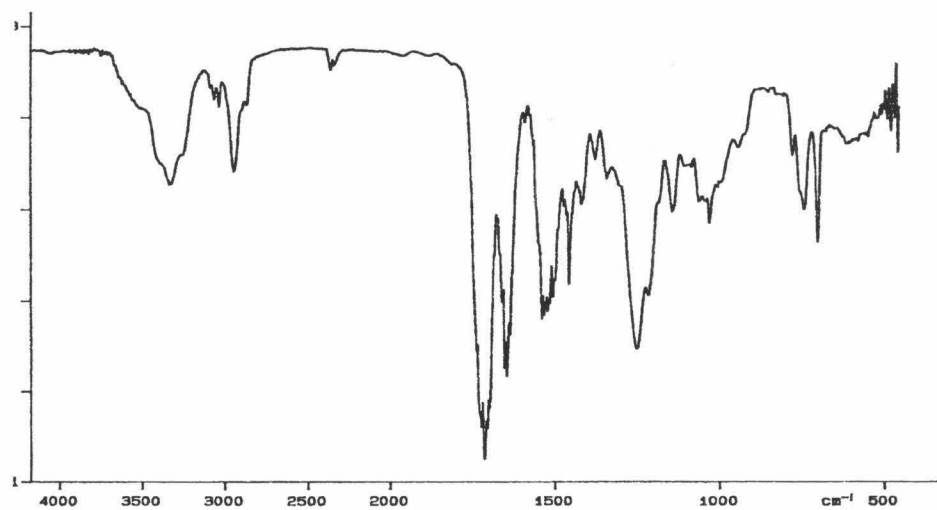
**$^1\text{H}$  NMR**  
300 MHz  
 $\text{CDCl}_3$

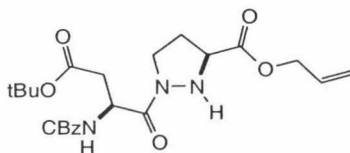


**$^{13}\text{C}$  NMR**  
75 MHz  
 $\text{CDCl}_3$



**IR**  
thin film





Allyl ester **98**, isolated as a clear oil, 45%.

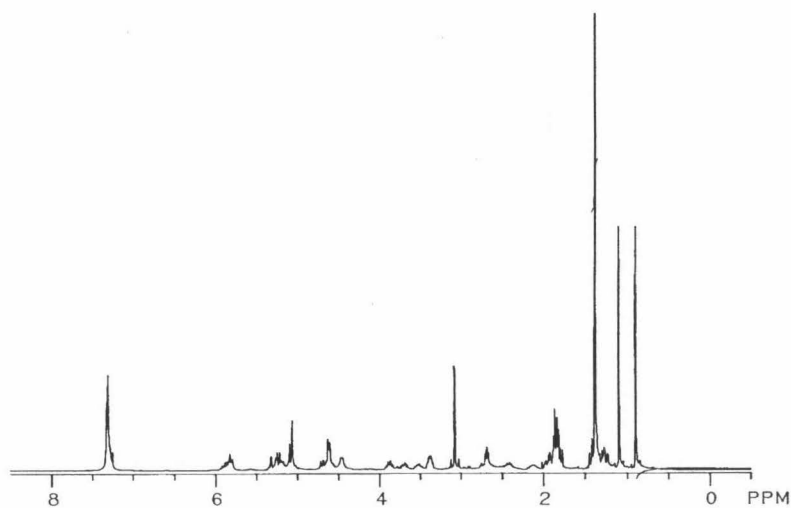
$[\alpha]_D^{27.7}$ ; +8.5° (c=1.59, CHCl<sub>3</sub>),

**<sup>1</sup>H NMR** (300 MHz, CDCl<sub>3</sub>) δ 7.45-7.25 (10H,m), 5.92 (1H, m), 5.82 (1H, d, J = 8.2 Hz), 5.45-5.21 (3H, m), 5.18 (4H, s), 4.72 (2H, d, J= 9.5 Hz), 3.91 (1H, m), 3.78 (1H, m), 3.62 (1H, m), 2.74 (2H, d, J = 3.2 Hz), 2.60-2.15 (6H, m), 1.44 (9H, s);

**IR** (thin film) ν cm<sup>-1</sup>; 3402, 3252, 2977, 1724, 1652, 1505, 1497, 1455, 1412, 1366, 1252, 1209, 1157, 1059;

**<sup>13</sup>C NMR** (75 MHz, CDCl<sub>3</sub>):δ 170.7, 170.6, 169.7, 155.5, 136.4, 131.2, 128.4, 127.9, 119.4, 81.1, 66.7, 66.2, 59.8, 49.5, 44.6, 38.2, 31.4, 27.9.

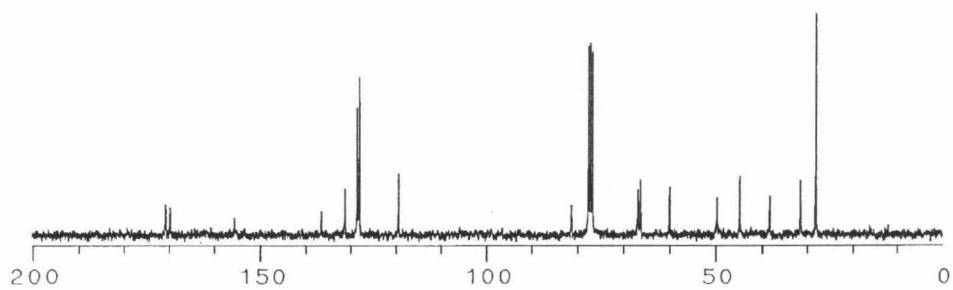
$^1\text{H}$  NMR  
300 MHz  
 $\text{CDCl}_3$



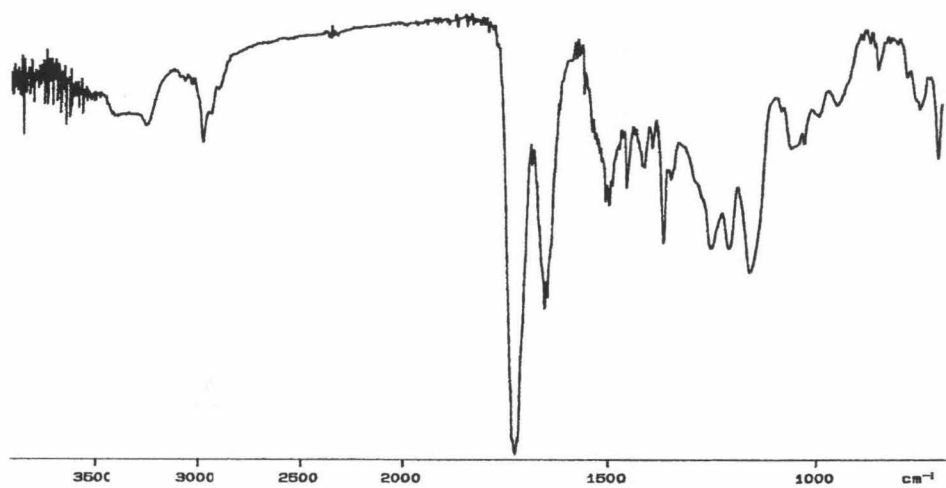
$^{13}\text{C}$  NMR

75 MHz

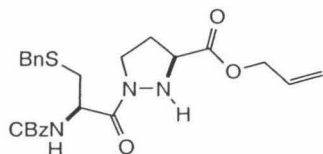
$\text{CDCl}_3$



IR



**thin film**



Allyl ester **99**, isolated as a clear oil, 64%.

$[\alpha]_D^{27.7}$ ;  $-3.9^\circ$  ( $c=1.59$ ,  $\text{CDCl}_3$ );

$^1\text{H NMR}$  (300 MHz,  $\text{CDCl}_3$ )  $\delta$  7.35-7.20 (10H, m), 5.89 (1H, m), 5.69 (1H, d,  $J = 8.5$  Hz), 5.35 (2H, m), 5.11 (2H, s), 4.65 (2H, d,  $J = 5.8$  Hz), 3.85-3.65 (4H, m), 3.55 (1H, m), 2.77 (2H, m), 2.41 (1H, m), 2.35-1.92 (6H, bm);

**IR** (thin film)  $\nu$  3392, 3246, 2952, 1718, 1647, 1495, 1453, 1411, 1207, 1027  $\text{cm}^{-1}$ ;

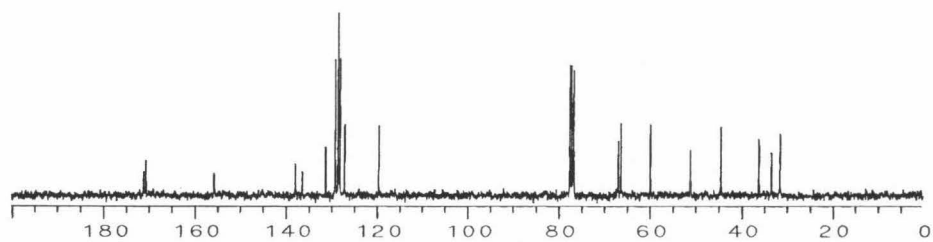
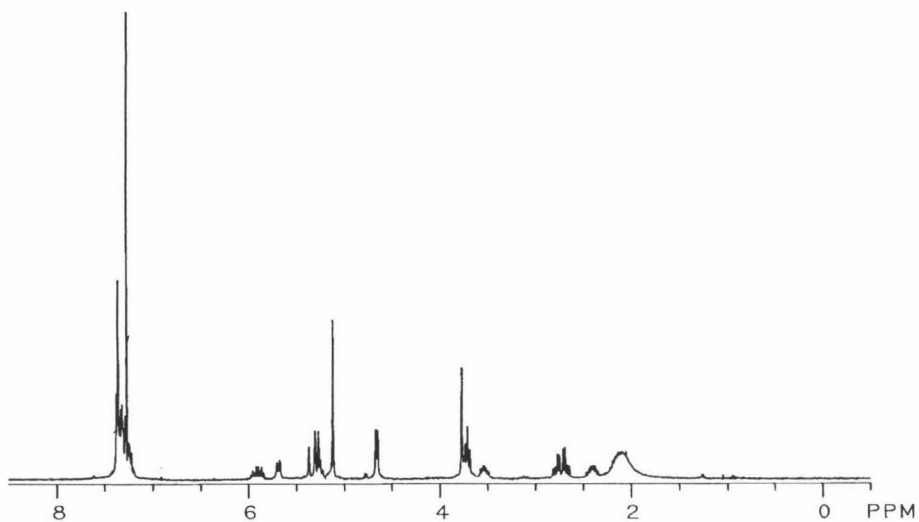
$^{13}\text{C NMR}$  (75 MHz,  $\text{CDCl}_3$ ):  $\delta$  170.9, 170.5, 155.6, 137.9, 136.4, 131.1, 129.0, 128.4,

128.35, 127.9, 127.0, 119.4, 66.7, **66.1**, **59.7**, **50.9**, **44.3**, **36.0**, 33.3, **31.3**.

$^1\text{H NMR}$

300 MHz

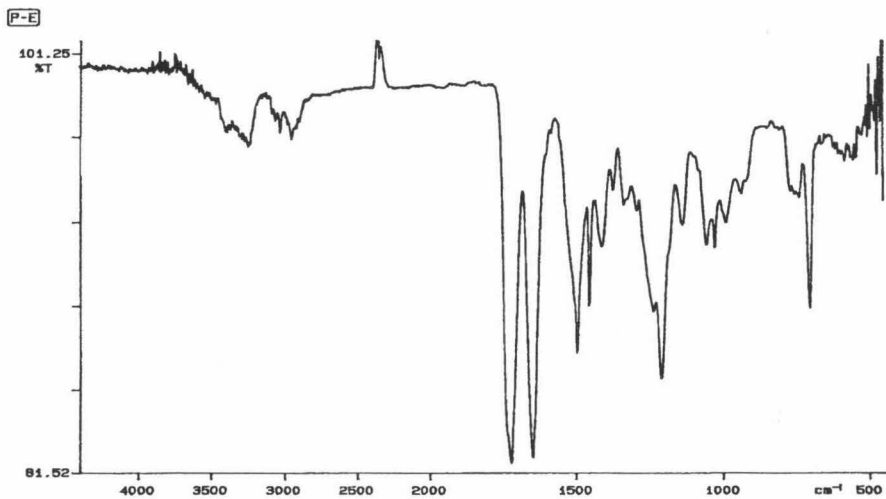
$\text{CDCl}_3$



$^{13}\text{C NMR}$

75 MHz

$\text{CDCl}_3$





**IR**

**thin film**

**Allyl ester 100, isolated as a clear oil., 74%.**

$[\alpha]_{\text{D}}^{25.4} + 11.8^{\circ}$  ( $c = 0.87$ ,  $\text{CHCl}_3$ );

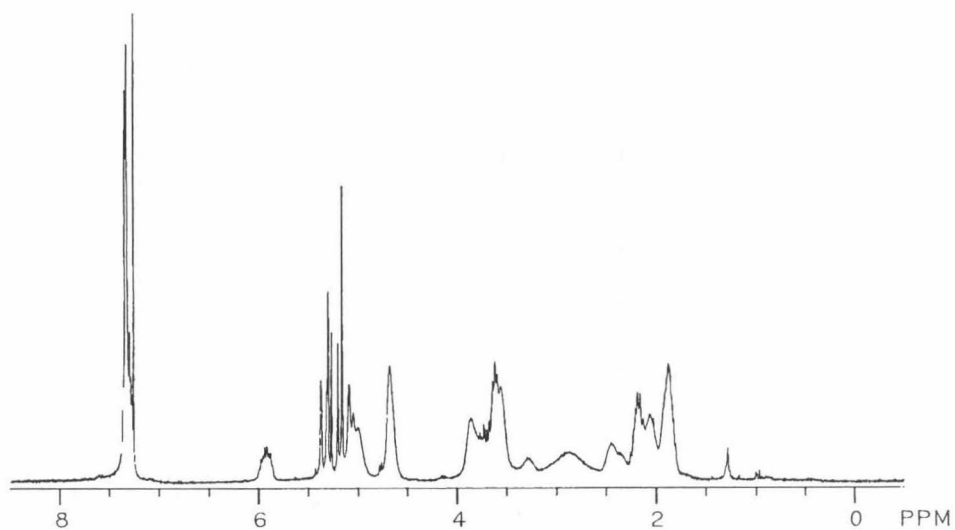
**$^1\text{H}$  NMR** (300 MHz,  $\text{CDCl}_3$ ) rotomers are observed at temperatures up to 75 C;

**IR** (thin film)  $\nu$  3232, 2954, 2884, 1738, 1694, 1644, 1497, 1453, 1416, 1360, 1271, 1204, 1119, 1029, 989, 769  $\text{cm}^{-1}$ ;

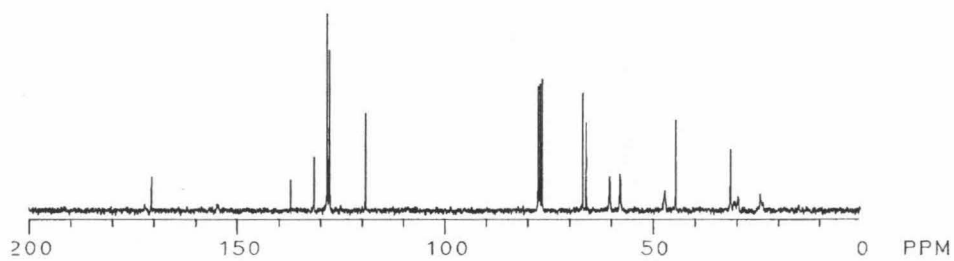
**$^{13}\text{C}$  NMR** (75 MHz,  $\text{CDCl}_3$ ):  $\delta$  170.3, 137.1, 131.5, 128.3, 127.7, 119.0, 66.8, 66.0, 57.8,

47.1, 47.0, 46.9, 44.4, 31.4, 29.7, 29.6, 24.3

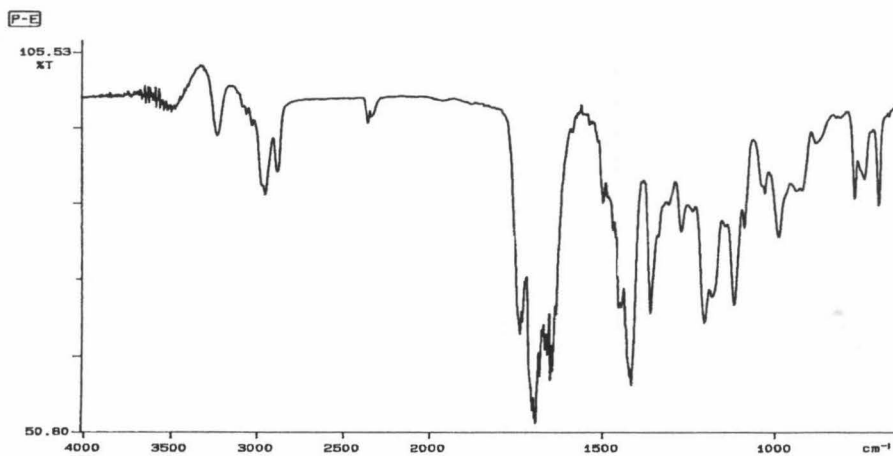
$^1\text{H}$  NMR  
300 MHz  
 $\text{CDCl}_3$



$^{13}\text{C}$  NMR  
75 MHz  
 $\text{CDCl}_3$

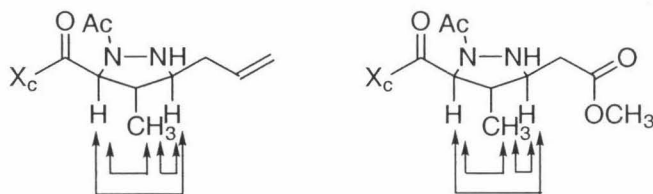


IR  
thin film



### Assignment of pyrazolidine stereochemistry

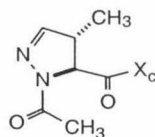
In the case of pyrazolidine **130**, the stereochemistry of addition was determined by single crystal X-ray analysis. In the cases of pyrazolidines **127** and **131**, the nOe enhancements shown below were observed. Assignment of the stereochemistry of addition for additional products was made by analogy.



nOe Enhancements observed in pyrazolidines **127** and **131**.

### General Procedure for the synthesis of N-acetylated pyrazolidines **126**, **128**, **129**

To a 0.05 M solution of the pyrazolidine in CH<sub>2</sub>Cl<sub>2</sub> at 23° C is added 10.0 eq. dry acetic anhydride, followed by 0.10 eq toluenesulfonic acid monohydrate. The reaction is stirred under N<sub>2</sub> at 23° C. Upon completion of the reaction (2 h-6 h), the reaction mixture is poured into a volume of saturated sodium bicarbonate solution equal to the volume of CH<sub>2</sub>Cl<sub>2</sub> used. After stirring for 30 min, this mixture is extracted 3x with CH<sub>2</sub>Cl<sub>2</sub> and dried over Na<sub>2</sub>SO<sub>4</sub>. Solvent removal gives the unpurified product as a white powder. Flash chromatography (2:1 hexanes/EtOAc) furnishes the N-acetylated product as a crystalline solid.



*N*-Acetyl Pyrazoline **126**, obtained as a crystalline solid, 94%.

**m.p.** = 174-175°C;

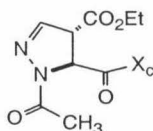
$[\alpha]_D^{23.1} +100.5^\circ$  ( $c = 0.49$ ,  $\text{CHCl}_3$ );

**$^1\text{H}$  NMR** (300 MHz,  $\text{CDCl}_3$ )  $\delta$  6.73 (1H, s), 4.95 (1H, d,  $J = 4.5$  Hz), 3.85 (1H, dd,  $J = 7.7, 4.8$  Hz) 3.53 (1H, d,  $J=13.7$  Hz), 3.41 (1H, d,  $J = 13.7$  Hz), 3.28 (1H,m), 2.27 (3H,s), 2.2 (1H, m) 2.05-1.85 (4H, bm) 1.52-1.32 (8H, m) 0.93 (3H,s);

**$^{13}\text{C}$  NMR**(75 MHz,  $\text{CDCl}_3$ ) 168.9, 168.3, 149.8, 65.1, 62.8, 52.9, 49.1, 47.8, 46.8, 44.2, 37.5, 32.4, 26.4, 21.1, 20.2, 19.8, 16.8;

**IR** (thin film,  $\text{cm}^{-1}$ ) 2961, 2883, 1698, 1667, 1604, 1410, 1330, 1284, 1216, 1167, 1136, 1066, 735, 538;

**HRMS** calcd. for  $\text{C}_{17}\text{H}_{25}\text{N}_3\text{O}_4\text{S}$  ( $\text{M}+1$ )<sup>+</sup> 368.1644, found 368.1642.



*N*-Acetyl pyrazoline **128**, obtained as a crystalline solid, 76 %.

**m.p** = 158-160° C

$[\alpha]_D^{26.0} + 321.3^\circ$  (c = 0.81, CHCl<sub>3</sub>);

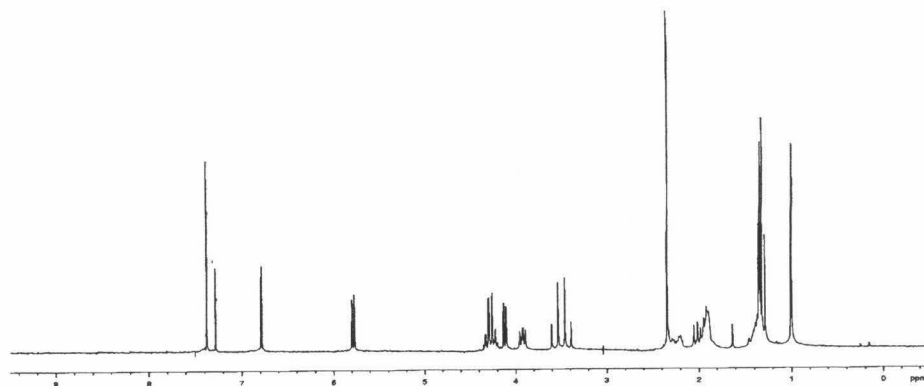
<sup>1</sup>H NMR (200 MHz, CDCl<sub>3</sub>) : δ 6.90 (d, 1H, *J* = 2.0 Hz), δ 5.79 (d, 1H, *J* = 5.8 Hz), δ 4.27 (1H, d, *J* = 5.0 Hz), δ 4.16 (1H, δ, *J* = 5.8 Hz), δ 3.93 (1H, dd, *J* = 7.9, 5.0), δ 3.57 (1H, d, *J* = 13.7) δ 3.50 (1H, d, *J* = 13.7), δ 2.35 (3H, s), δ 2.3-1.8 (6H, m), δ 1.7-1.2 (8H, m), δ 1.00 (s, 3H);

<sup>13</sup>C NMR (75 MHz, CDCl<sub>3</sub>) : δ 168.7, 167.2, 166.4, 140.7, 65.40, 62.56, 59.45, 57.70, 53.09, 49.31, 47.95, 44.73, 37.82, 32.82, 26.48, 21.20, 20.69, 19.93, 14.07;

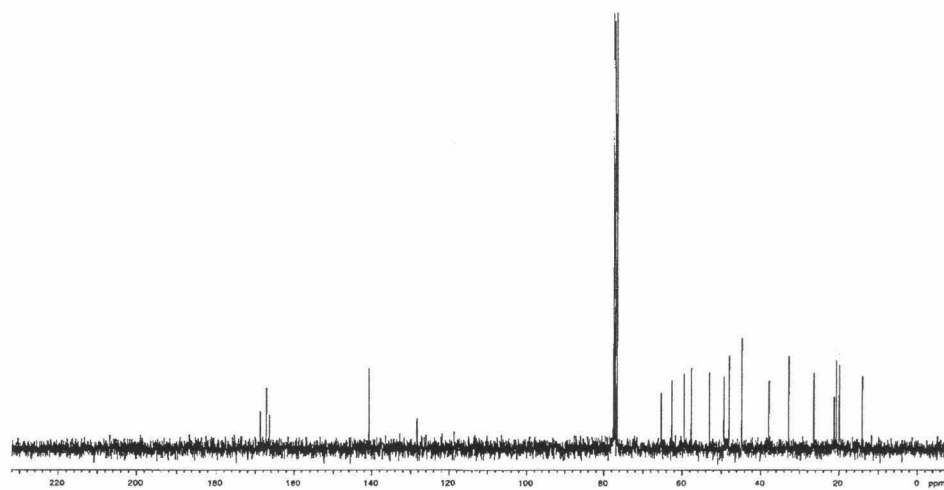
IR (thin film, cm<sup>-1</sup>) : 2961, 2248, 1744, 1701, 1672, 1595, 1409, 1369, 1242, 1213, 1185, 1166, 1136, 1120, 993, 963, 646;

HRMS calc. for C<sub>19</sub>H<sub>27</sub>O<sub>6</sub>S Anal. calcd. for C<sub>19</sub>H<sub>27</sub>N<sub>3</sub>O<sub>6</sub>S (M + Na) 448.1518, found : 448.1515.

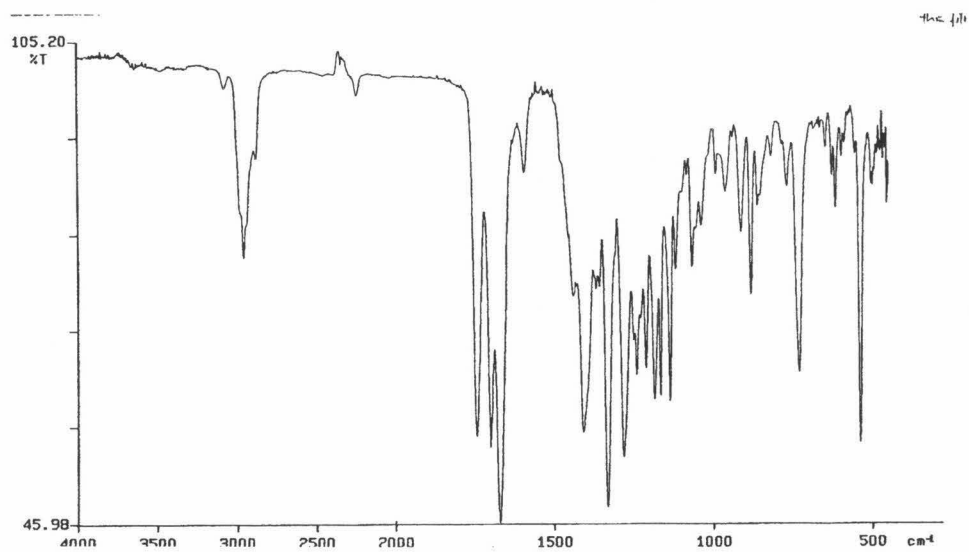
$^1\text{H}$  NMR  
300MHz  
 $\text{CDCl}_3$

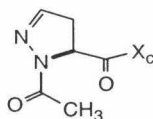


$^{13}\text{C}$   
NMR  
75 MHz  
 $\text{CDCl}_3$



IR  
thin film





*N*-Acetyl pyrazoline **129**, obtained as a crystalline solid, 80%.

**m.p.** = 168 °C;

$[\alpha]_D^{29.3} + 17.9^\circ$  ( $c = 0.09$ ,  $\text{CHCl}_3$ );

**$^1\text{H}$  NMR** (200 MHz,  $\text{CDCl}_3$ )  $\delta$  6.851 (1H, t,  $J = 1.6$  Hz), 5.33 (1H, dd,  $J = 12.0, 7.4$  Hz) 3.91 (1H, m), 3.51 (1H, d,  $J = 13.7$  Hz) 3.40 (1H, d,  $J = 13.7$  Hz) 3.16 (1H, ddd,  $J = 18.6, 11.6, 1.6$  Hz) 2.97 (1H, ddd,  $J = 18.6, 7, 1.6$  Hz), 2.33 (3H, s), 2.24 (1H, m), 2.1-1.85 (5H, m), 1.48-1.31 (4H, m), 1.00 (3H, s);

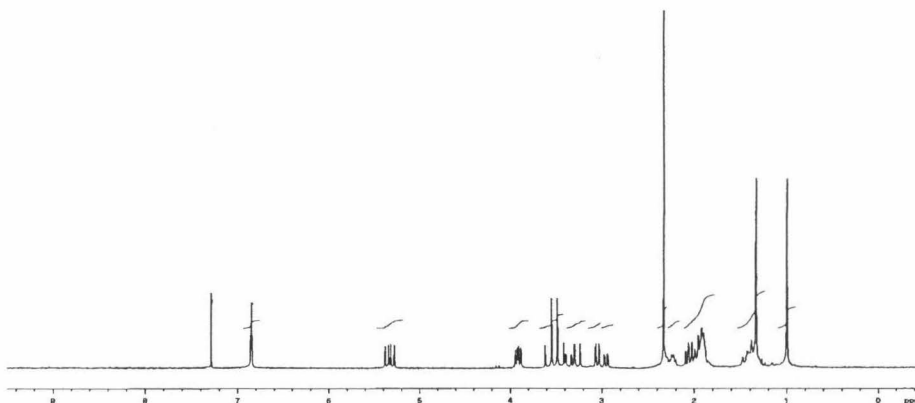
**$^{13}\text{C}$  NMR** (75 MHz,  $\text{CDCl}_3$ )  $\delta$  186.9, 166.4, 142.7, 62.9, 53.5, 50.6, 46.7, 45.5, 42.1, 36.9, 35.8, 35.3, 31.0, 30.2, 29.1, 24.1, 18.7, 18.1, 17.4;

**IR** (thin film,  $\text{cm}^{-1}$ ) 2960, 2358, 2244, 1702, 1661, 1605, 1412, 1358, 1329, 1272, 1237, 1221, 1166, 1119, 1067, 976, 668, 483;

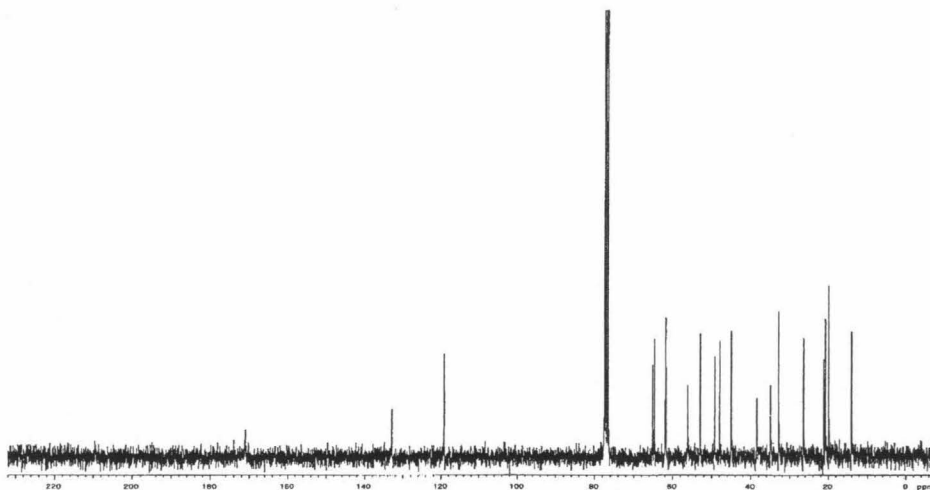
**HRMS** calcd. for  $\text{C}_{16}\text{H}_{23}\text{N}_3\text{O}_4\text{S}$  (M + Na) 376.1307, found 376.1302.



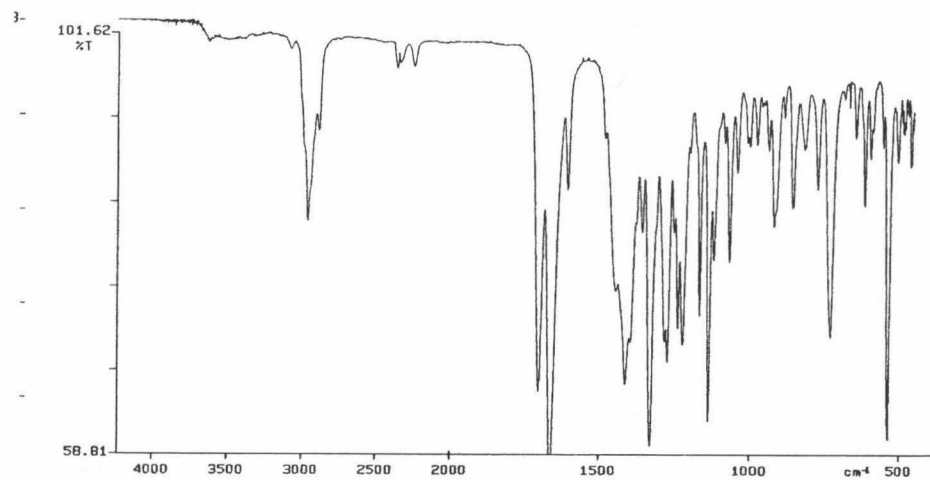
$^1\text{H}$  NMR  
300MHz  
 $\text{CDCl}_3$



$^{13}\text{C}$  NMR  
75 MHz  
 $\text{CDCl}_3$

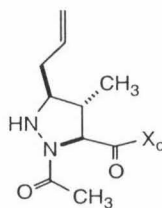


IR  
thin film



**General Procedure for the  $\text{TiCl}_4$ -promoted addition of nucleophiles to *N*-acetyl pyrazolines 126-129 to give *N*-acetyl pyrazolidines 127, 130-137 .**

To a 0.05 to 0.10 M solution of the *N*-acetyl pyrazoline in  $\text{CH}_2\text{Cl}_2$  or toluene, cooled to  $-78\text{ }^\circ\text{C}$ , under an atmosphere of  $\text{N}_2$  is added via syringe 1.2 eq  $\text{TiCl}_4$  as a 1.0 M solution in  $\text{CH}_2\text{Cl}_2$ . The cold bath is removed and the reaction is allowed to stir for a period of 15 min. The reaction is recooled to  $-78\text{ }^\circ\text{C}$  and 2.1 to 4.0 eq of nucleophile is added neat to the reaction solution via syringe. The cold bath is removed and the reaction is allowed to reach  $23\text{ }^\circ\text{C}$  with stirring. Upon warming, the yellow color of the reaction solution turns dark brown. The reaction is monitored by TLC for progression to the product which is, in all cases studied, of lower  $R_f$  than the starting *N*-acetyl pyrazoline. After completion of the reaction, (4-24 h), the reaction is diluted with additional reaction solvent and washed with aq. sodium bicarbonate solution. The aq. layer is extracted with additional reaction solvent, and the combined organic layers are washed with brine and dried over  $\text{Na}_2\text{SO}_4$ . Solvent is removed by rotary evaporation and the residue subjected to flash chromatography on silica gel (1:1 hexanes/EtOAc to 2:1 hexanes/EtOAc) to provide the pure *N*-acetyl pyrazolidine products.



Pyrazolidine **127**, obtained as a colorless oil, 71%.

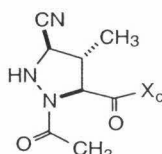
$[\alpha]_D^{23.1}$  100.5 ° (c = 0.49, CHCl<sub>3</sub>);

**<sup>1</sup>H NMR** (300 MHz, CDCl<sub>3</sub>) δ 5.81 (1H, m), 5.15 (1H, d, *J* = 16.2 Hz), 5.11 (1H, d, *J* = 9.3 Hz), 4.75 (1H, d, *J* = 6.1 Hz), 3.97 (1H, dd, *J* = 7.6, 4.9 Hz), 3.52 (1H, d, *J* = 13.7 Hz) 3.42 (1H, d, *J* = 13.7 Hz), 2.81 (1H, ddd, *J* = 7.6, 7.6, 5.1 Hz), 2.52-2.13 (3H, bm), 2.14 (3H, s), 1.94-1.8 (3H, bm), 1.5-1.25 (8H, bm), 0.97 (3H, s);

**<sup>13</sup>C NMR** (75 MHz, CDCl<sub>3</sub>) δ 172.4, 169.9, 133.4, 118.1, 66.8, 65.3, 65.1, 53.0, 48.9, 47.9, 46.8, 44.5, 44.5, 38.4, 34.5, 32.7, 26.5, 21.2, 20.4, 19.9, 16.3;

**IR** (thin film, cm<sup>-1</sup>) : 3242, 3071, 2959, 1690, 1651, 1483, 1393, 1333, 1275, 1237, 1214, 1167, 1136, 1066, 1041, 992, 918, 857, 763, 733;

**HRMS** calcd. for C<sub>20</sub>H<sub>31</sub>N<sub>3</sub>O<sub>4</sub>S (M+1)<sup>+</sup> 410.2113, found 410.2115.



Pyrazolidine **130**, obtained as a crystalline solid, 87%.

**m.p.** =124 °C;

$[\alpha]_{\text{D}}^{32.4} + 60.0^{\circ}$  (c=2.15, CHCl<sub>3</sub>);

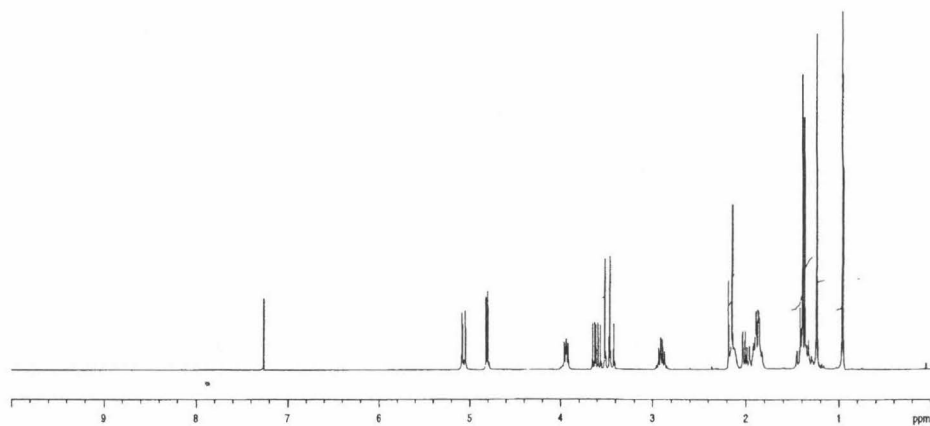
**<sup>1</sup>H NMR** (300 MHz, CDCl<sub>3</sub>) δ 5.07 (1H, d, *J* = 10.8 Hz), 4.81 (1H, d, *J* = 4.8 Hz), 3.94 (1H, m), 3.62 (1H, dd, *J* = 10.5, 7.2 Hz), 3.54 (1H, d, *J* = 13.8 Hz), 3.44 (1H, d, *J* = 13.8 Hz), 2.90 (1H, m), 2.18-1.82 (7H, m), 1.34-1.23 (5H, m), 1.24 (3H, s), 0.96 (3H,s);

**<sup>13</sup>C NMR** (75 MHz, CDCl<sub>3</sub>) δ 170.2, 170.0, 116.2, 65.4, 63.9, 55.6, 53.2, 49.1, 48.0, 47.97, 44.5, 38.0, 32.7, 26.5, 21.3, 20.5, 20.0, 16.5;

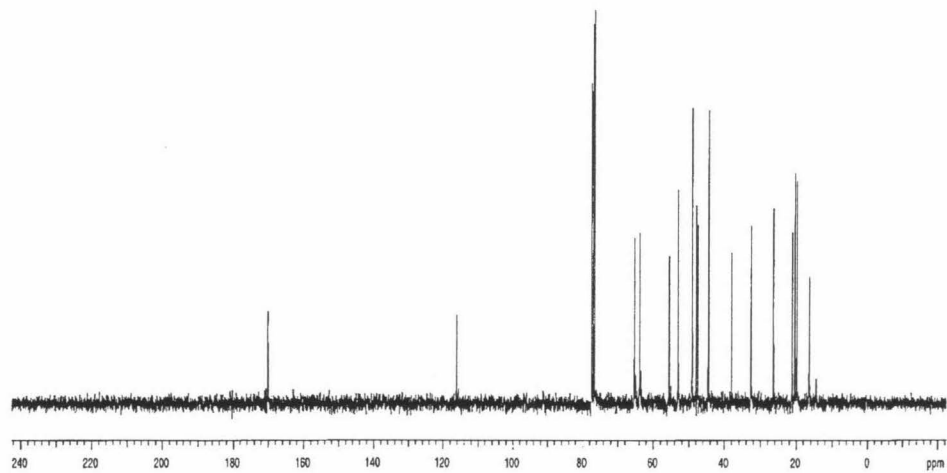
**IR** (thin film, cm<sup>-1</sup>) 3246, 2962, 2251, 1702, 1650, 1469, 1393, 1327, 1276, 1215, 1135, 1063, 913, 732;

**Combustion analysis** : anal. calcd. for C<sub>18</sub>H<sub>26</sub>N<sub>4</sub>O<sub>4</sub>S: C, 54.80, H, 6.64, N, 14.20. Found : C, 54.78, H, 6.69, N, 14.04.

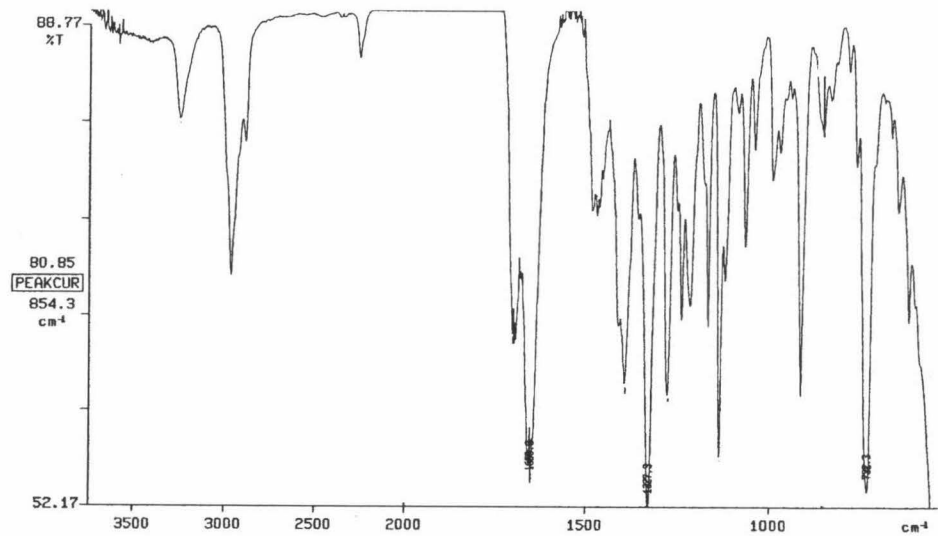
**$^1\text{H}$  NMR**  
**300MHz**  
 **$\text{CDCl}_3$**

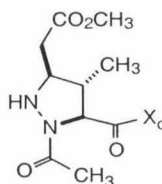


**$^{13}\text{C}$**   
**NMR**  
**75 MHz**  
 **$\text{CDCl}_3$**



**IR**  
**thin film**





Pyrazolidine **131** obtained as a colorless oil, 75%.

$[\alpha]_{\text{D}}^{32.4} +45.0$  (c=1.09,  $\text{CHCl}_3$ );

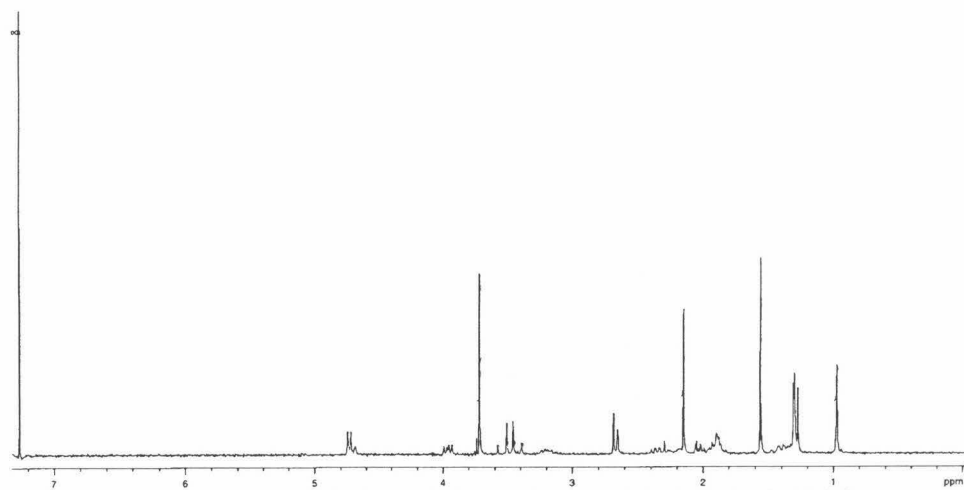
$^1\text{H NMR}$  (300 MHz,  $\text{CDCl}_3$ )  $\delta$  4.71 (2H, m), 3.94 (1H, m), 3.70 (3H, s), 3.52 (1H, d,  $J = 13.8$  Hz), 3.44 (1H, d,  $J = 13.8$  Hz), 3.18 (1H, m), 2.65 (2H, d,  $J = 6$  Hz), 2.36 (1H, m), 2.27-2.13 (4H, m), 2.02-1.86 (4H, m), 1.44-1.22 (5H, m), 0.96 (3H, s);

$^{13}\text{C NMR}$  (75 MHz,  $\text{CDCl}_3$ )  $\delta$  171.7, 171.6, 169.8, 65.43, 65.40, 65.41, 53.3, 52.0, 49.1, 48.0, 46.8, 44.6, 38.2, 35.6, 32.8, 26.6, 21.3, 20.5, 20.0, 17.0;

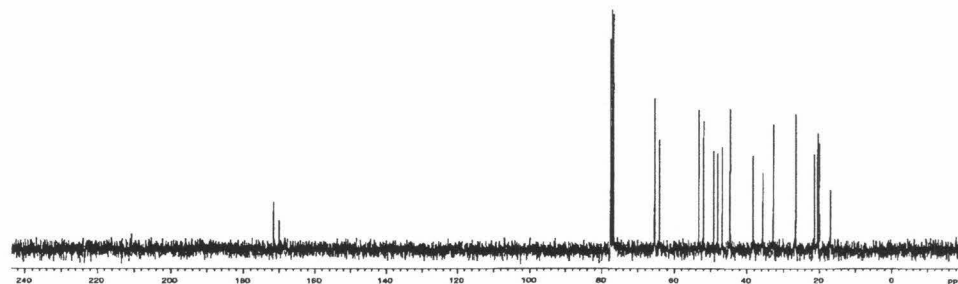
**IR** (thin film,  $\text{cm}^{-1}$ ) 3234, 2958, 2360, 2340, 1735, 1696, 1647, 1391, 1328, 1274, 1215, 1166, 1134, 1064, 993, 913, 731;

**HRMS** calcd for  $\text{C}_{20}\text{H}_{31}\text{N}_3\text{O}_4\text{S}$  (M +H) 442.2012, found : 442.2006.

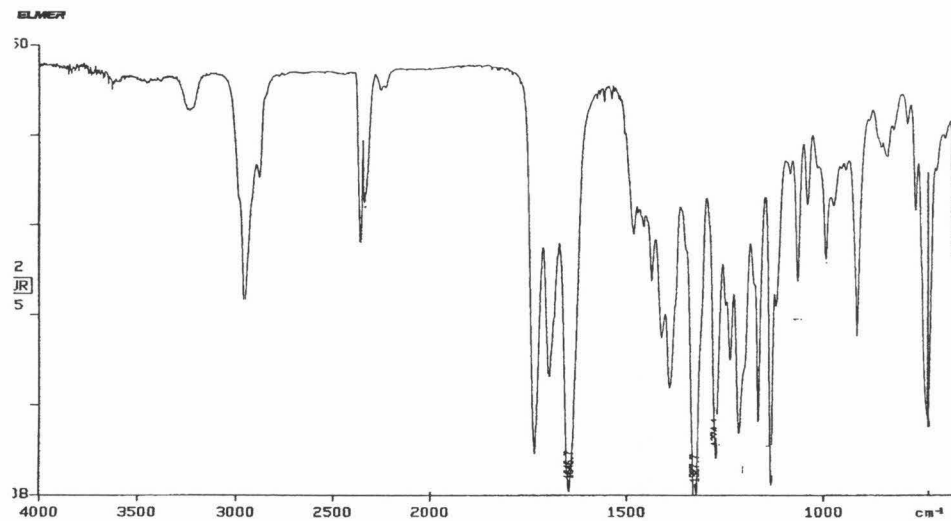
$^1\text{H}$  NMR  
300MHz  
 $\text{CDCl}_3$

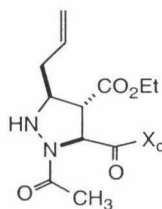


$^{13}\text{C}$  NMR  
75 MHz  
 $\text{CDCl}_3$



IR  
thin film





Pyrazolidine **132**, obtained as a colorless oil, 60%.

$[\alpha]_D^{32.2} +88.7^\circ$  (c=0.42, CHCl<sub>3</sub>);

**<sup>1</sup>H NMR** (300 MHz, CDCl<sub>3</sub>) :  $\delta$  5.80 (1H,m), 5.39 (1H, d,  $J = 5.3$  Hz), 5.20 (2H, m), 4.43 (1H, d,  $J = 11.5$  Hz), 4.20 (2H, m), 4.05 (1H,bm), 3.45 (3H,m), 3.10 (1H,m), 2.56 (2H,m), 2.22 (4H, m), 2.1-1.8 (4H, bm), 1.42-1.25 (8H, m), 0.97 (3H,s);

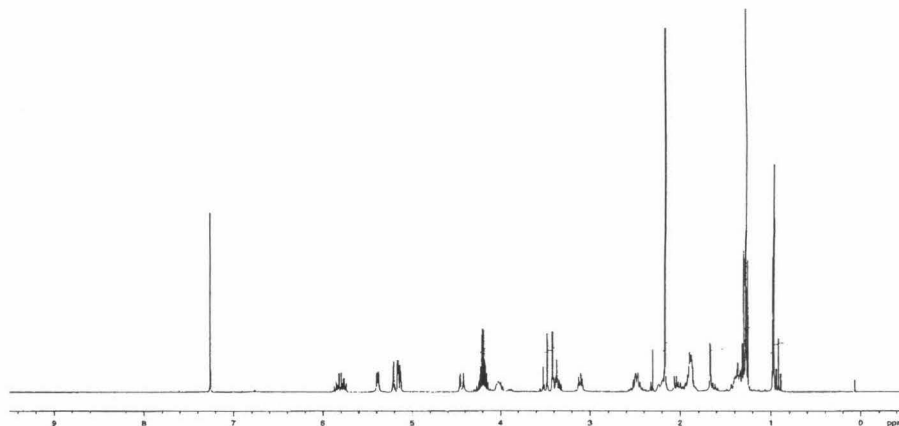
**<sup>13</sup>C NMR** (75MHz, CDCl<sub>3</sub>) :  $\delta$  174.0, 170.7, 132.9, 119.2, 64.7, 61.9, 61.0, 56.2, 54.2, 53.0, 49.4, 48.0, 45.1, 38.8, 35.9, 35.0, 33.0, 26.4, 21.4, 20.9, 20.0, 17.2;

**IR** (thin film, cm-1) 3230, 2960, 2359, 2340, 1733, 1683, 1652, 1483, 1394, 1334, 1276, 1220, 1167, 1136, 1068, 1040, 995, 913;

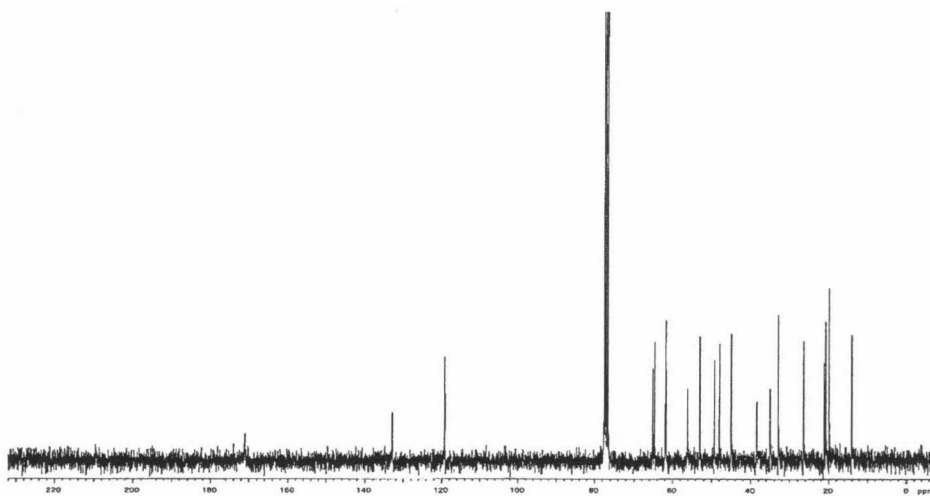
**HRMS** Calcd. for C<sub>22</sub>H<sub>33</sub>N<sub>3</sub>O<sub>6</sub>S ( M + Na) 490.1988, found 490.1983.



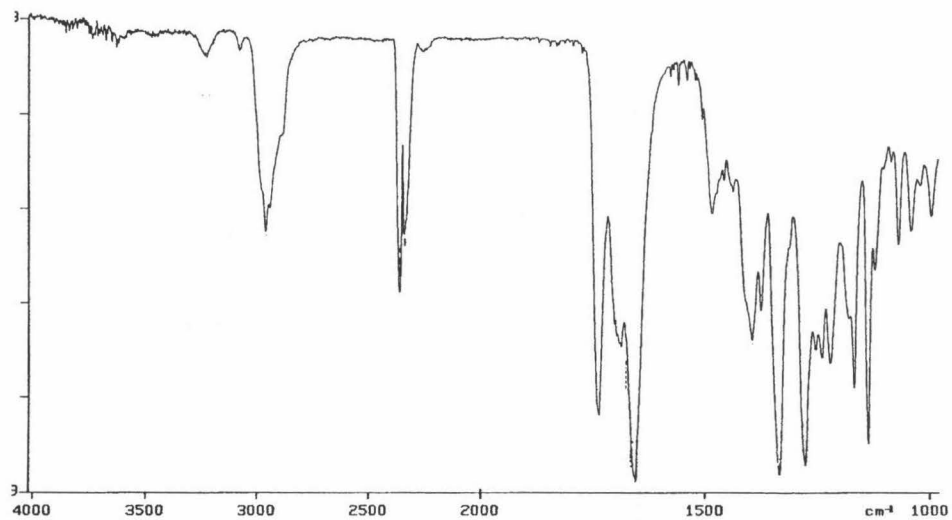
$^1\text{H}$  NMR  
300MHz  
 $\text{CDCl}_3$

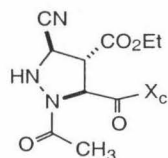


$^{13}\text{C}$  NMR  
75 MHz  
 $\text{CDCl}_3$



IR  
thin film





Pyrazolidine **133**, obtained as a colorless oil, 91%.

$[\alpha]_D^{32.4} + 79.1^\circ$  (c=1.33, CHCl<sub>3</sub>);

<sup>1</sup>H NMR (300MHz, CDCl<sub>3</sub>) : d 5.41 (1H, d, *J* = 3.9 Hz), 5.07 (1H, d, *J* = 9.3 Hz), 4.28-4.21 (3H, m), 4.00 (1H,m), 3.70 (1H,m), 3.52 (1H, d, *J* = 13.8 Hz), 3.42 (1H, d, *J* = 13.8 Hz), 2.24-2.15 (4H, bm), 2.06 (1H,m), 1.90 (2H, bm), 1.44-1.192 (8H, m), 0.97 (3H,s);

<sup>13</sup>C NMR (75 MHz, CDCl<sub>3</sub>) : δ 170.4, 169.0, 168.5, 115.5, 65.3, 62.9, 60.9, 60.5, 55.5, 53.07, 52.3, 49.3, 48.0, 44.9, 38.2, 32.9, 21.3, 20.8, 19.9, 14.0;

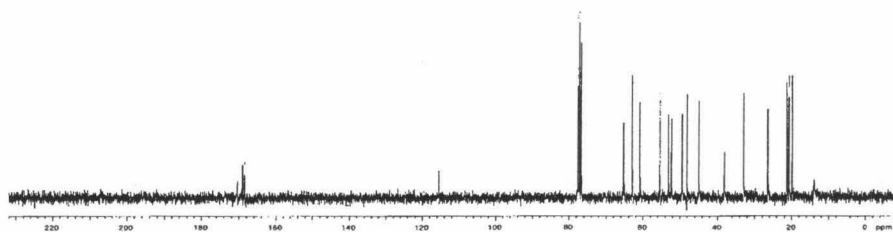
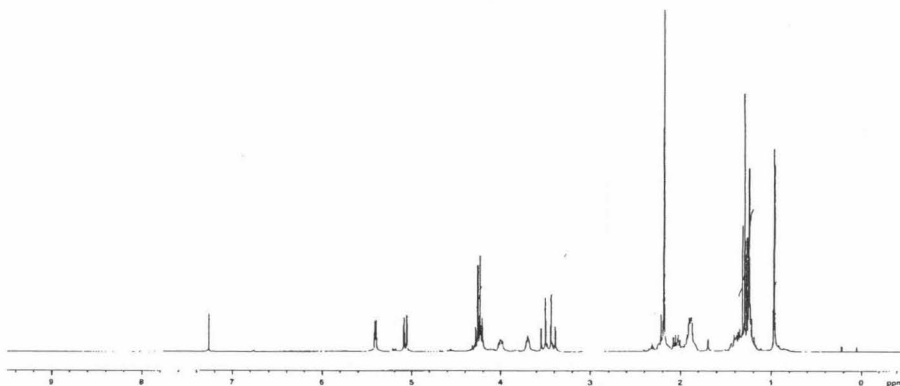
IR (thin film, cm<sup>-1</sup>) : 3240, 2963, 2362, 2254, 1738, 1703, 1661, 1470, 1393, 1373, 1332, 1275, 1215, 1195, 1167, 1136, 1067, 1039;

HRMS calcd. for C<sub>20</sub>H<sub>28</sub>N<sub>4</sub>O<sub>6</sub>S (M + Na) 475.1627, found 475.1620.

$^1\text{H}$  NMR

300MHz

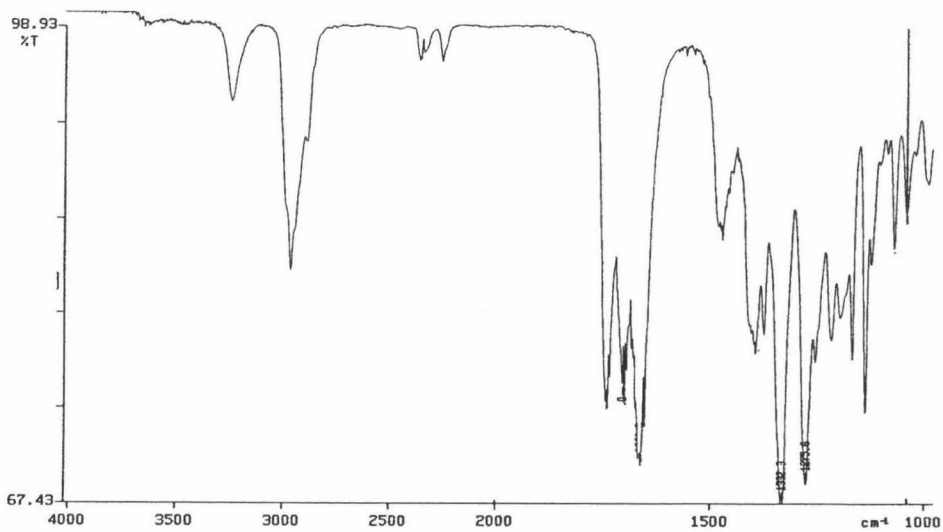
$\text{CDCl}_3$



$^{13}\text{C}$  NMR

75 MHz

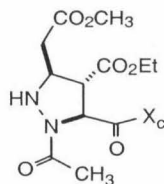
$\text{CDCl}_3$



IR

t h i n

f i l m



Pyrazolidine **134**, obtained as a colorless oil, 73%.

$[\alpha]_{\text{D}}^{32.4} +83.1$  (c=0.695,  $\text{CHCl}_3$ );

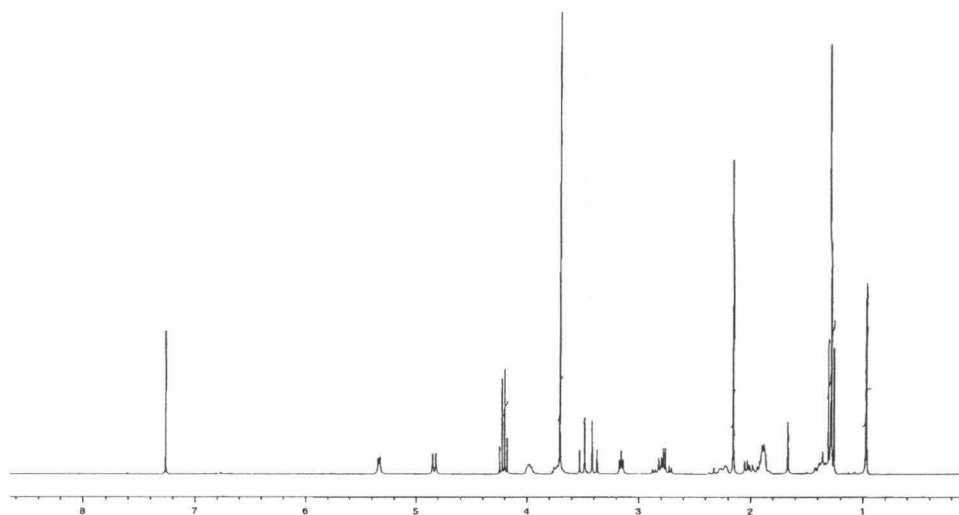
$^1\text{H NMR}$  (300 MHz,  $\text{CDCl}_3$ ) :  $\delta$  5.33 (1H, d,  $J = 4.5$  Hz), 4.83 (1H, d,  $J = 9.3$  Hz), 4.19 (2H, q,  $J = 7.2$  Hz), 3.98 (1H, m), 3.73 (4H, m), 3.50 (1H, d,  $J = 13.8$  Hz), 3.39 (1H, d,  $J = 13.8$  Hz), 3.15 (1H, m), 2.76 (2H, m), 2.00 (1H, m), 2.15 (3H, s), 2.08-1.83 (4H, m), 1.43-1.28 (8H, m), 0.97 (3H, s);

$^{13}\text{C NMR}$  (75 MHz,  $\text{CDCl}_3$ ):  $\delta$  171.2, 170.8, 169.5, 169.0, 65.2, 61.9, 61.7, 61.4, 55.7, 53.0, 52.0, 49.1, 47.914, 44.9, 38.2, 35.9, 32.9, 26.5, 21.4, 20.8, 19.9, 14.1;

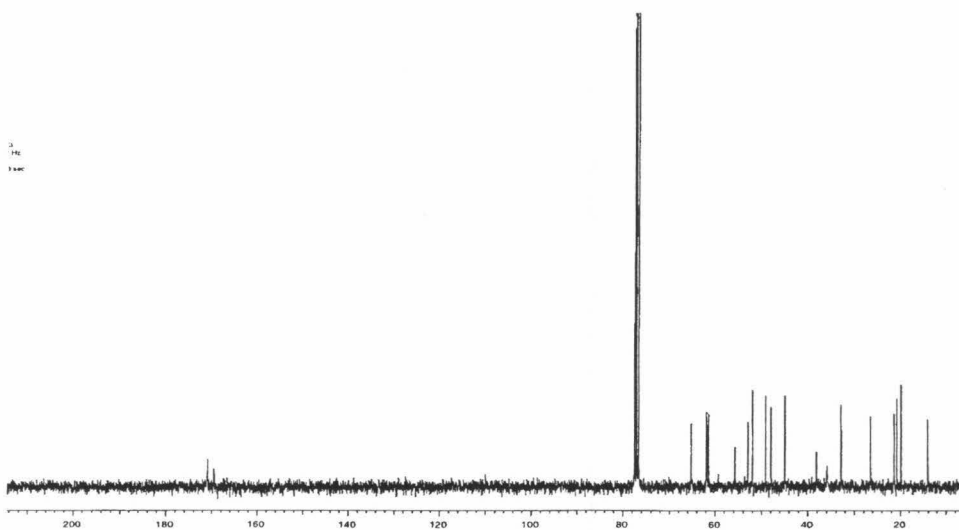
**IR** (thin film,  $\text{cm}^{-1}$ ) : 3244, 2959, 2353, 2340, 1736, 1696, 1655, 1394, 1331, 1275, 1217, 1166, 1135, 1068, 1040;

**HRMS** Calcd. for  $\text{C}_{22}\text{H}_{33}\text{N}_3\text{O}_8\text{S}$  (M + Na): 522.1886, found 522.1881.

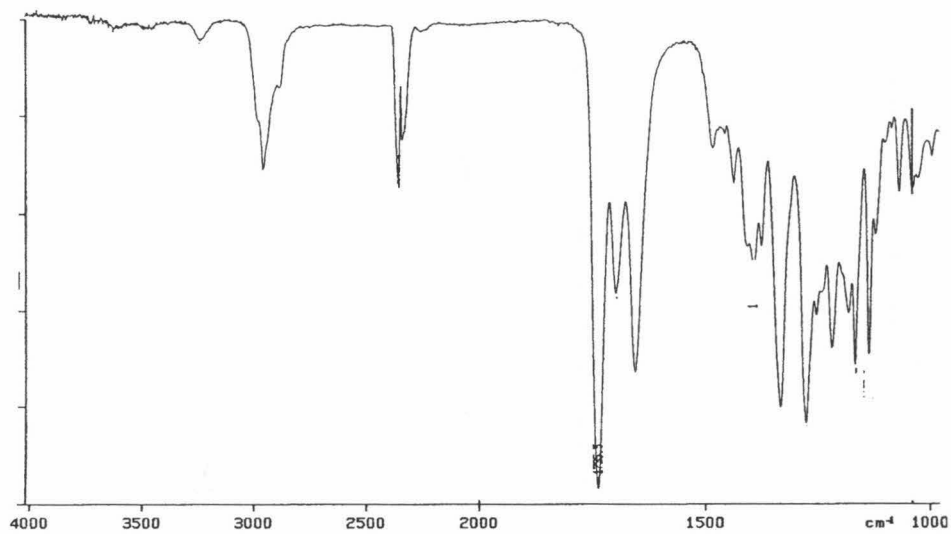
$^1\text{H}$  NMR  
300MHz  
 $\text{CDCl}_3$

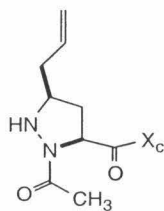


$^{13}\text{C}$  NMR  
75 MHz  
 $\text{CDCl}_3$



IR  
thin film





Pyrazolidine **135**, obtained as an inseparable mixture of diastereomers in a 1:1 ratio, 74% combined yield.

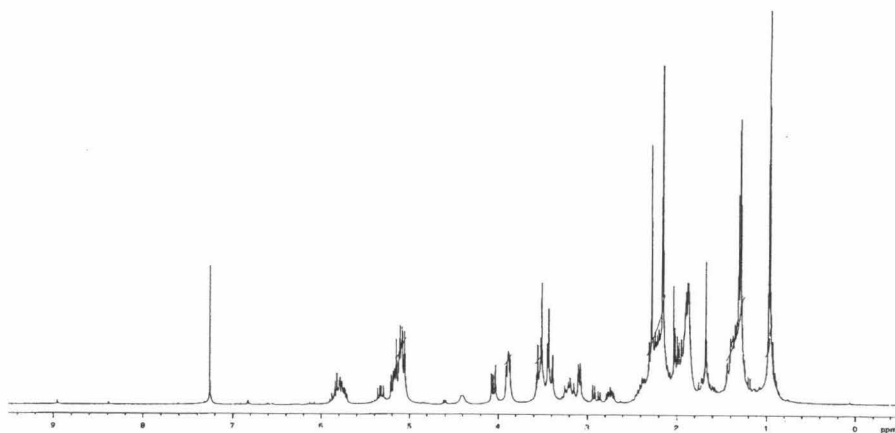
**<sup>1</sup>H NMR** (300 MHz, CDCl<sub>3</sub>): δ 5.81 (2H,m), 5.30 (1H, dd, *J* = 19.5, 12.0 Hz), 5.12 (6H,m), 4.40 (1H,bs), 4.08 (1H,m), 3.90 (3H,m), 3.50 (7H,m), 3.20 (2H,m), 3.08 (1H,d, *J*= 6.3 Hz), 2.89 (1H,m), 2.74(1H,m), 2.42-1.85 (12H, cm), 1.71(2H,m)1.31 (10H,cm), 0.96 (6H,s);

**<sup>13</sup>C NMR** (75MHz, CDCl<sub>3</sub>) δ 171.9,170.7,134.8, 133.8, 118.7, 118.1, 65.5, 60.3, 59.4, 58.2, 53.3, 49.4, 48.2, 44.9, 39.6, 38.7, 38.2, 37.0, 35.7, 33.0, 26.8, 21.6, 21.6, 20.8, 20.2 .

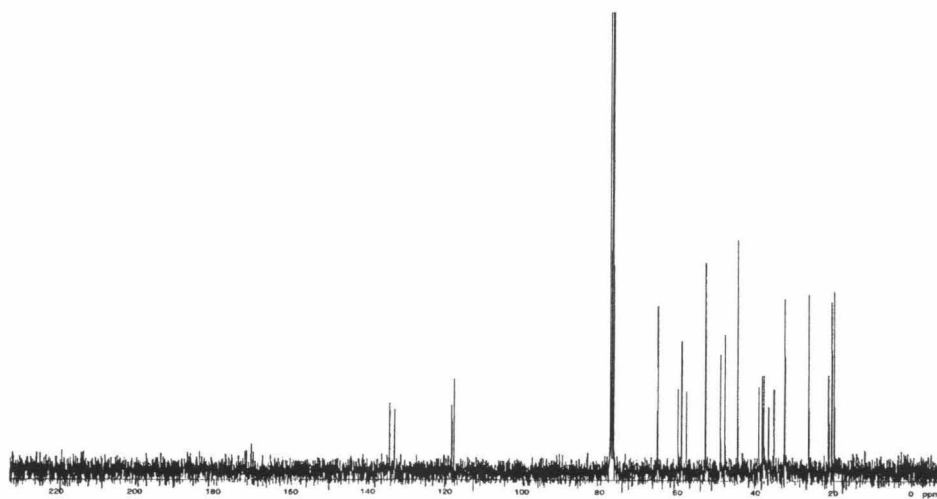
δ IR (thin film, cm<sup>-1</sup>) 3222, 2950, 2341, 1694, 1642, 1480, 1448, 1395, 1330, 1273, 1220, 1135, 1067, 917, 780, 730;

**HRMS** calcd. for C<sub>19</sub>H<sub>29</sub>N<sub>3</sub>O<sub>4</sub>S (M + Na) 418.1776, found 418.1815.

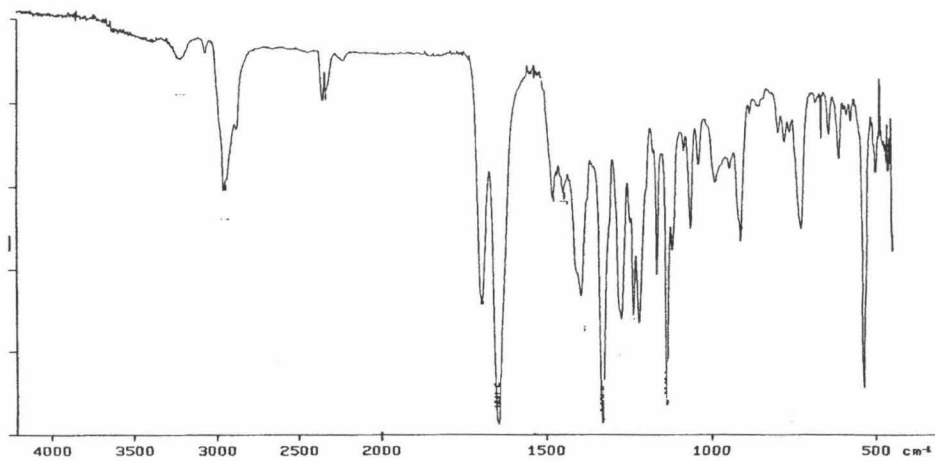
$^1\text{H}$  NMR  
300MHz  
 $\text{CDCl}_3$



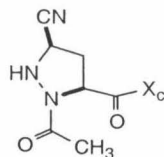
$^{13}\text{C}$  NMR  
75 MHz  
 $\text{CDCl}_3$



IR  
thin film







Pyrazolidine **136**, obtained as an inseparable mixture of diastereomers, in a 1.5:1 ratio, 79% combined yield.

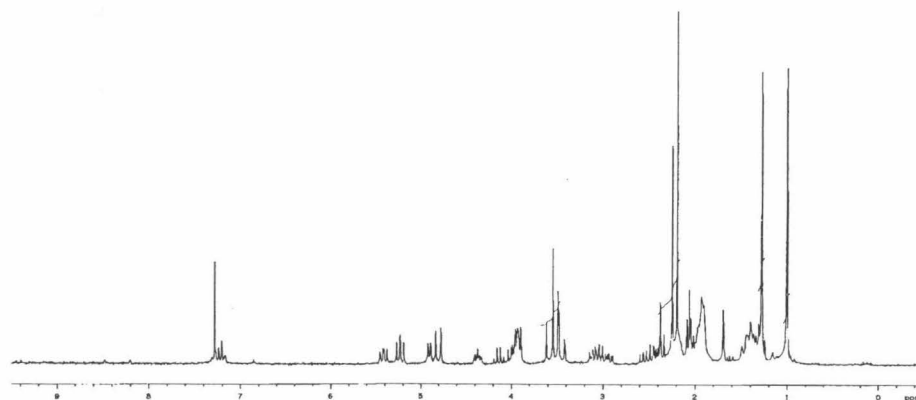
**<sup>1</sup>H NMR** (300 MHz, CDCl<sub>3</sub>) Non-integer proton values indicate a resonance belonging to or including the minor diastereomer: δ 5.37 (0.7H, dd, *J* = 8.1, 6.9 Hz), 5.21 (1H, dd, *J* = 8.7, 7.5 Hz), 4.87 (0.7H, d, *J* = 6.8 Hz), 4.79 (1H, d, *J* = 11.7 Hz), 4.34 (0.7H, m), 3.93 (2.7H, m), 3.55 (1.7H, d, *J* = 14.1 Hz), 3.43 (1.7H, m), 3.05-2.88 (1.7H, m), 2.55-2.31 (1.7H, m), 2.22-2.17 (6.8H, m), 2.05-1.88 (6H, m), 1.67-1.20 (8.2H, m), 0.976 (5.1H, s).

**<sup>13</sup>C NMR** (75 MHz, CDCl<sub>3</sub>): δ 170.8, 170.0, 117.8, 115.9, 70.9, 65.2, 64.9, 57.5, 56.6, 52.9, 52.8, 49.5, 49.2, 48.1, 47.8, 45.8, 44.6, 38.5, 38.3, 38.1, 37.8, 32.6, 26.3, 21.0, 20.5, 19.7 .

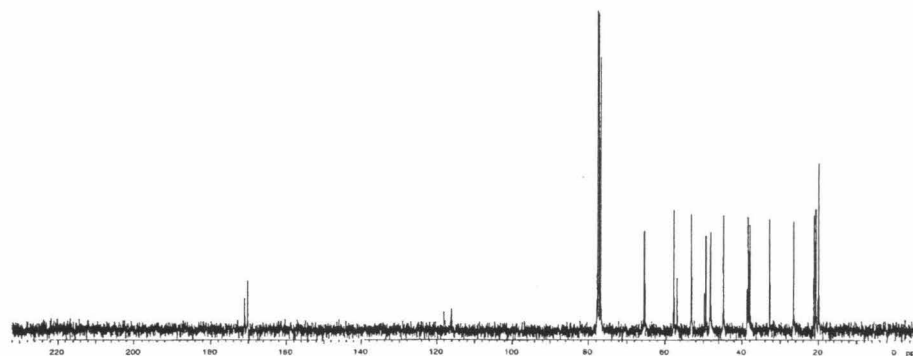
**IR** (thin film, cm<sup>-1</sup>) 3238, 2962, 2252, 1669, 1652, 1488, 1394, 1328, 1273, 1240, 1215, 1167, 1135, 1066, 913, 730.

**HRMS** calcd. for C<sub>17</sub>H<sub>24</sub>N<sub>4</sub>O<sub>4</sub>S (M + Na) 403.1416, found 403.1410.

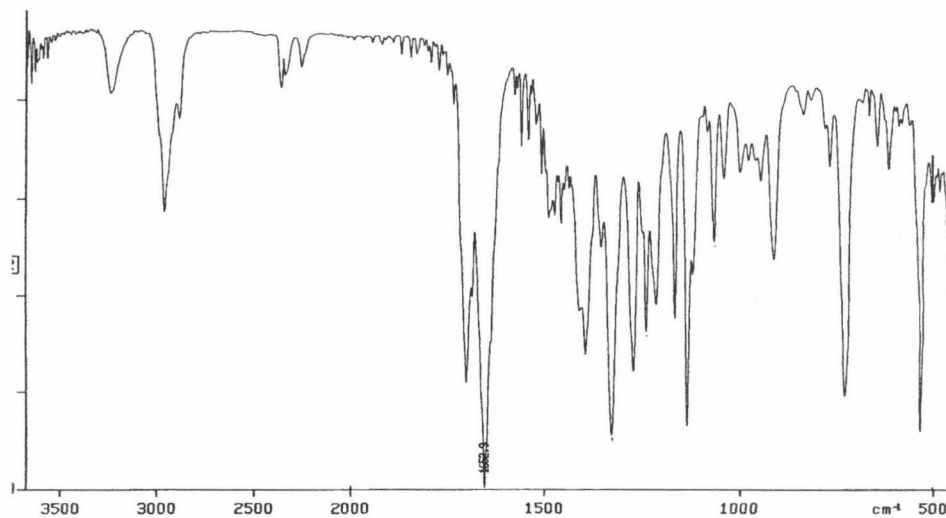
**$^1\text{H}$  NMR**  
300MHz  
 $\text{CDCl}_3$

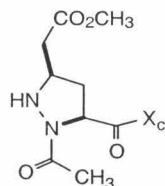


**$^{13}\text{C}$  NMR**  
75 MHz  
 $\text{CDCl}_3$



**IR**  
thin film





Pyrazoline **137**, obtained as an inseparable mixture of diastereomers in a 1.5:1 ratio, 84% combined yield.

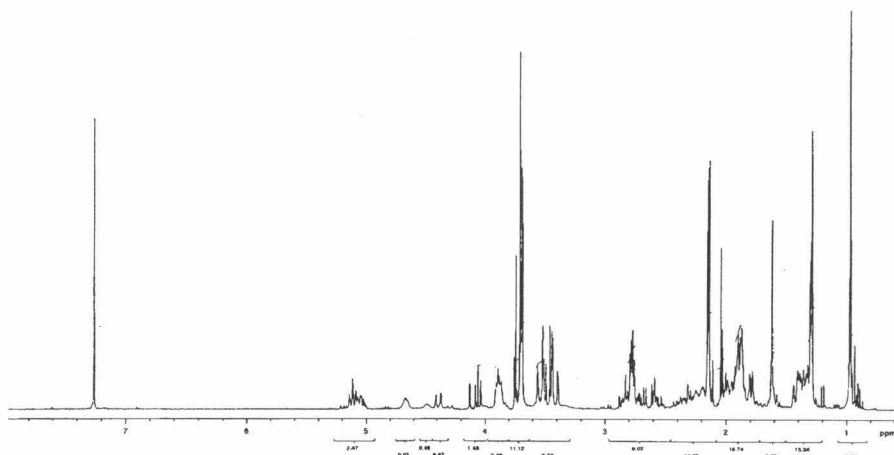
**<sup>1</sup>H NMR** (300MHz, CDCl<sub>3</sub>) Non-integer proton values indicate resonances belonging to or including the minor diastereomer : δ 5.13 (1.7H,m), 4.67(0.7H, d, *J* = 9.6 Hz), 4.38(1H,d, *J* = 16.4 Hz), 3.90 (1.7H, m), 3.75-3.65 (5.1H,m), 3.58-3.41 (3.4H, m), 2.92-2.61 (6H,m), 2.45-2.10 (8H,m), 2.05-1.74(8H,m), 1.55-1.20(9H,m), 0.97(5.1H,s).

**<sup>13</sup>C NMR** (75MHz, CDCl<sub>3</sub>) δ 171.6, 170.0, 65.2, 65.0, 59.1, 57.6, 56.9, 56.4, 53.1, 52.1, 49.2, 48.1, 45.7, 39.2, 38.5, 37.6, 37.5, 35.8, 32.7, 28.6, 26.6, 22.9, 21.2, 20.6, 20.0;

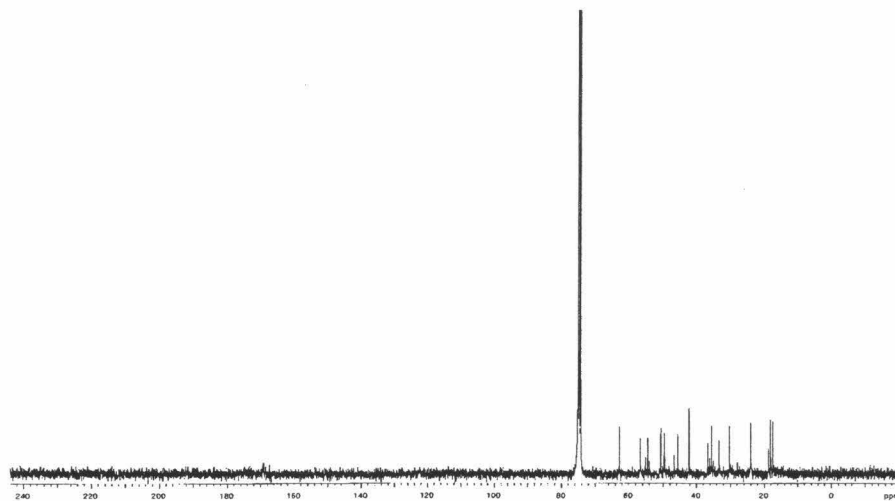
**IR** (thin film, cm<sup>-1</sup>) 3244, 2954, 1736, 1696, 1664, 1480, 1435, 1396, 1291, 1274, 1235, 1216, 1166, 1135, 1065, 999.2, 978.5, 916.2;

**HRMS** calcd for C<sub>19</sub>H<sub>29</sub>N<sub>3</sub>O<sub>6</sub>S (M + Na) 450.1675, found 450.1668.

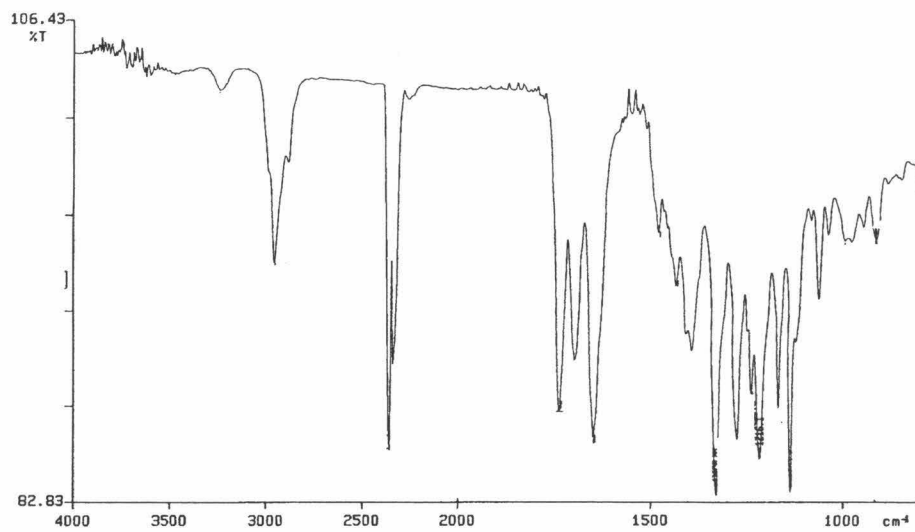
**$^1\text{H}$  NMR**  
300MHz  
 $\text{CDCl}_3$

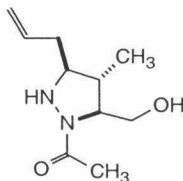


**$^{13}\text{C}$  NMR**  
75 MHz  
 $\text{CDCl}_3$



**IR**  
thin film



**Reductive auxiliary removal with NaBH<sub>4</sub> to give the free alcohol 138.**

To a solution of 200 mg (1.0 eq, 0.47 mmol) N-acetyl pyrazolidine **127** in 5 ml of a 10:1 solution of THF/CH<sub>3</sub>OH is added 9 mg (0.5 eq, 0.2 mmol) NaBH<sub>4</sub>. After 2 h, TLC showed that an approximately 1:1 ratio of starting material to lower R<sub>f</sub> spot existed as judged by visualization with CAM stain. An additional 9.0 mg NaBH<sub>4</sub> was added and after an additional 1 h, the reaction was seen to be complete via TLC analysis. The reaction was diluted with 50 ml diethyl ether and washed with 10 ml sodium bicarbonate solution. The aq. layer was extracted with 2x25 ml diethyl ether, and the combined organics washed with brine and dried over Na<sub>2</sub>SO<sub>4</sub>. Solvent removal via rotary evaporation followed by flash chromatography (EtOAc) furnished 77mg of the alcohol (84%) as a colorless oil.

$[\alpha]_D^{26.2} = -85.0^\circ$  (c = 1.1, CHCl<sub>3</sub>);

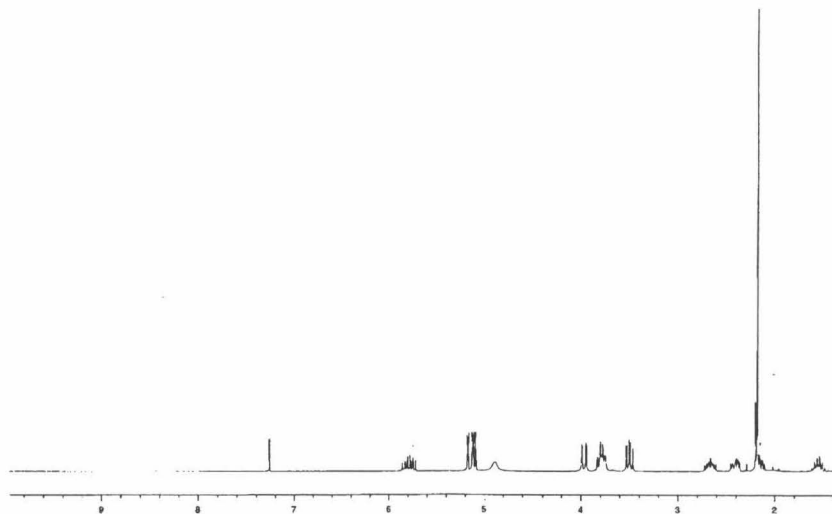
<sup>1</sup>H NMR (300MHz, CDCl<sub>3</sub>) δ 5.78 (1H,m), 5.11 (2H, m), 4.88 (1H,bs), 3.96 (1H, d, J = 12.9 Hz), 3.77 (2H,m), 3.50 (1H, dd, J = 11.1 , 8.1 Hz), 2.66 (1H,m), 2.40 (1H,m), 2.16 (4H,m), 1.54 (1H,m), 1.11 (3H, d, J = 6.3 Hz);

<sup>13</sup>C NMR (75MHz, CDCl<sub>3</sub>) d 174.2, 133.18, 118.3, 69.0, 65.3, 64.8, 44.4, 33.9, 21.5, 14.9;

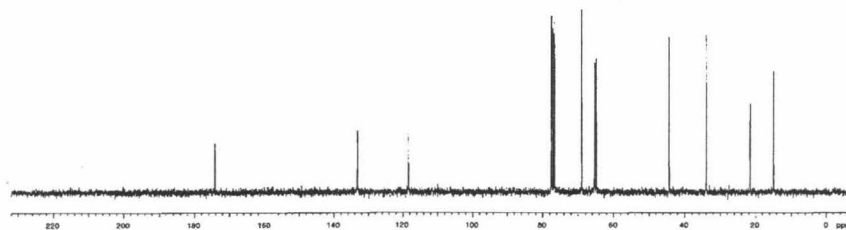
IR (thin film, cm<sup>-1</sup>) 3375, 3219, 2958, 2929, 2875, 1623, 1495, 1435, 1417, 1184, 1072.2, 1041, 995, 968, 915, 668;

HRMS calcd for C<sub>10</sub>H<sub>18</sub>N<sub>2</sub>O<sub>2</sub> (M + H) 199.1447, found 199.1445.

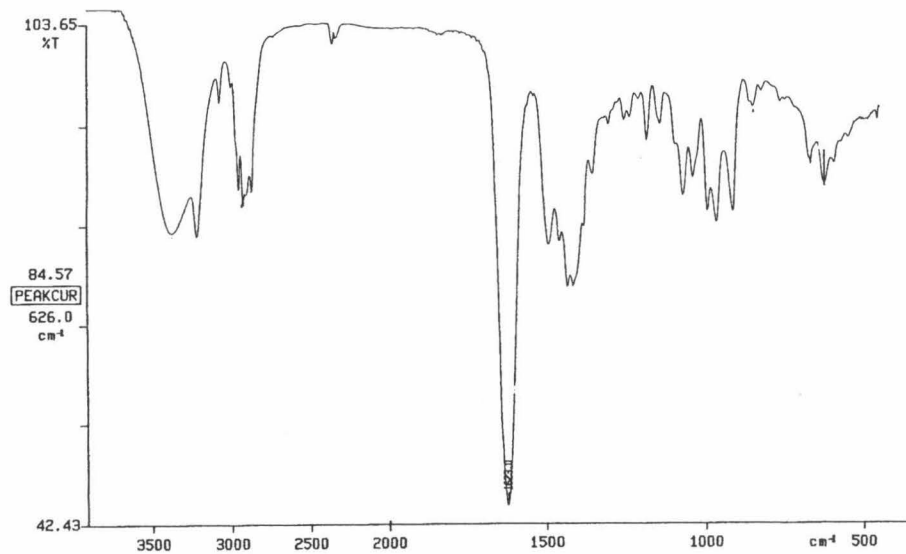
$^1\text{H}$  NMR  
300MHz  
 $\text{CDCl}_3$

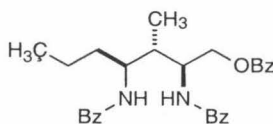


$^{13}\text{C}$   
NMR  
75 MHz  
 $\text{CDCl}_3$



IR  
thin film





### Hydrogenation and Benzoylation to give diamine **139**.

To 7.0 mg (0.029 mmol, 1.0 eq) of the alcohol **138** in 2 ml of a 1.6 M solution of aqueous HCl in methanol is added a weight equivalent of PtO<sub>2</sub>. The open reaction flask is placed in a high pressure reaction apparatus which is charged with 5 atm H<sub>2</sub> and the heterogeneous reaction mixture stirred rapidly at 23 °C. The reaction is allowed to continue in this manner for a period of 18 h to insure complete reaction has taken place. After this time, the reaction mixture is removed from the hydrogenation apparatus and filtered through celite. The filtrate is concentrated to furnish the presumed intermediate diammonium salt as a white solid. To this material is added CH<sub>2</sub>Cl<sub>2</sub> (2 ml) and 6.0 eq (0.18 mmol, 25 μL) triethylamine followed by 3.0 eq. (0.09 mmol, 10 μL) benzoyl chloride. The reaction is monitored via TLC, and after 1.5 h the reaction mixture is diluted with 10 ml CH<sub>2</sub>Cl<sub>2</sub> and washed with 10 ml 1M aq. HCl solution, and then washed with 10 ml sat. aq. Na<sub>2</sub>(CO<sub>3</sub>)<sub>2</sub> solution. The organic layer is dried over Na<sub>2</sub>SO<sub>4</sub> and solvent removed via rotary evaporation and high vacuum to give product as a white solid. Flash chromatography (3:1 hexanes/EtOAc) gives 11 mg pure product, 79%.

$[\alpha]_D^{25.2} = -2.19$  (c=2.16, CHCl<sub>3</sub>);

<sup>1</sup>H NMR (CDCl<sub>3</sub>, 300 MHz) δ 8.00 (5H,cm), 7.45 (6H,cm), 7.02 (1H, d, *J* = 11.3 Hz), 4.75 (2H,m), 4.45 (1H,m), 4.28 (1H,m), 2.14 (1H,m), 1.66 (1H,m), 1.5-1.25 (4H, bm), 1.10 (3H, d, *J* = 6.9 Hz), 0.87 (3H, t, *J* = 13 Hz);

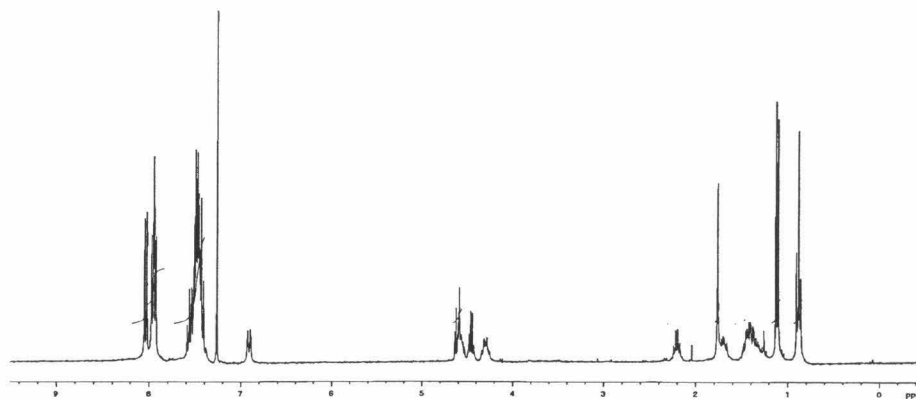
**<sup>13</sup>C NMR** (75 MHz, CDCl<sub>3</sub>) δ 167.9, 167.88, 167.6, 134.2, 134.1, 133.3, 131.7, 131.65, 129.8, 129.6, 128.7, 128.66, 128.5, 127.3, 127.1, 65.6, 51.9, 51.8, 38.6, 34.3, 19.6, 15.0, 13.9;

**IR** (thin film, cm<sup>-1</sup>) 3300, 3064, 2961, 2873, 1721, 1635, 1538, 1490, 1452, 1385, 1315, 1275, 1114, 1072, 1028, 911, 711;

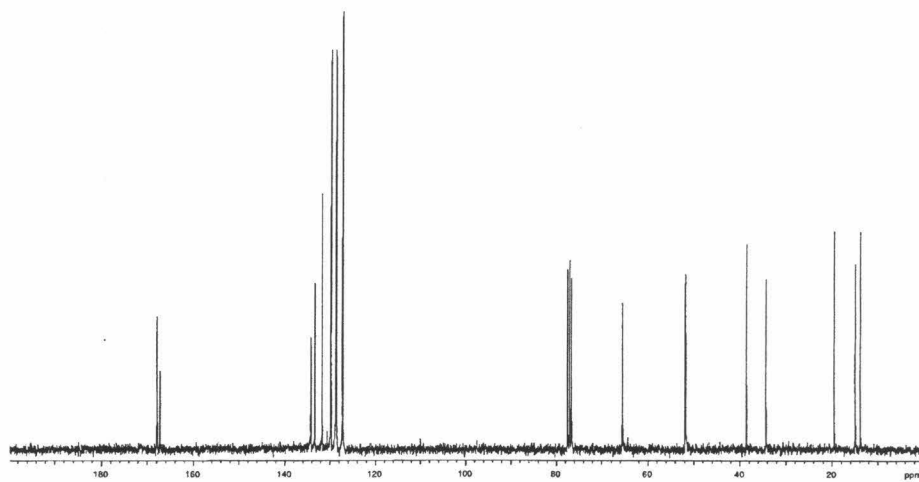
**HRMS** calcd for C<sub>29</sub>H<sub>32</sub>N<sub>2</sub>O<sub>4</sub> (M + Na) 492.2260, found 492.2272.



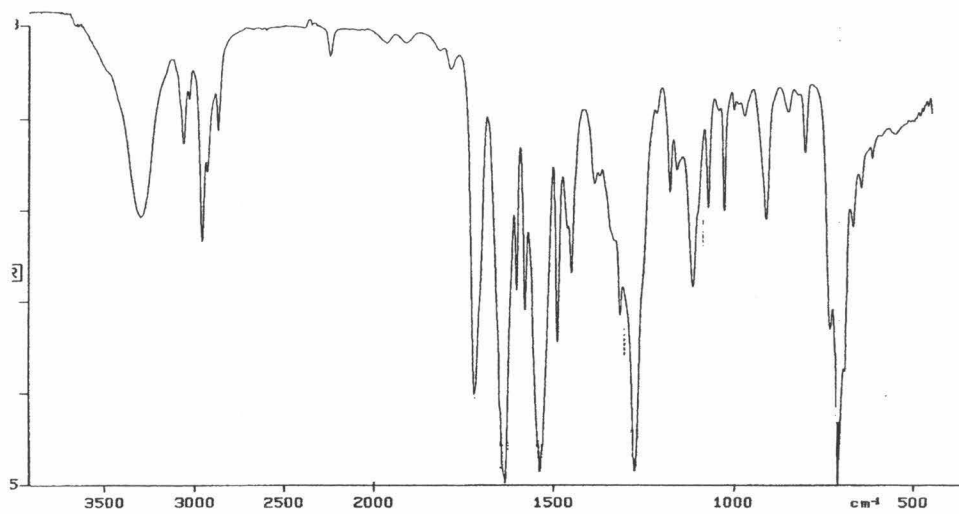
**$^1\text{H}$  NMR**  
300MHz  
 $\text{CDCl}_3$



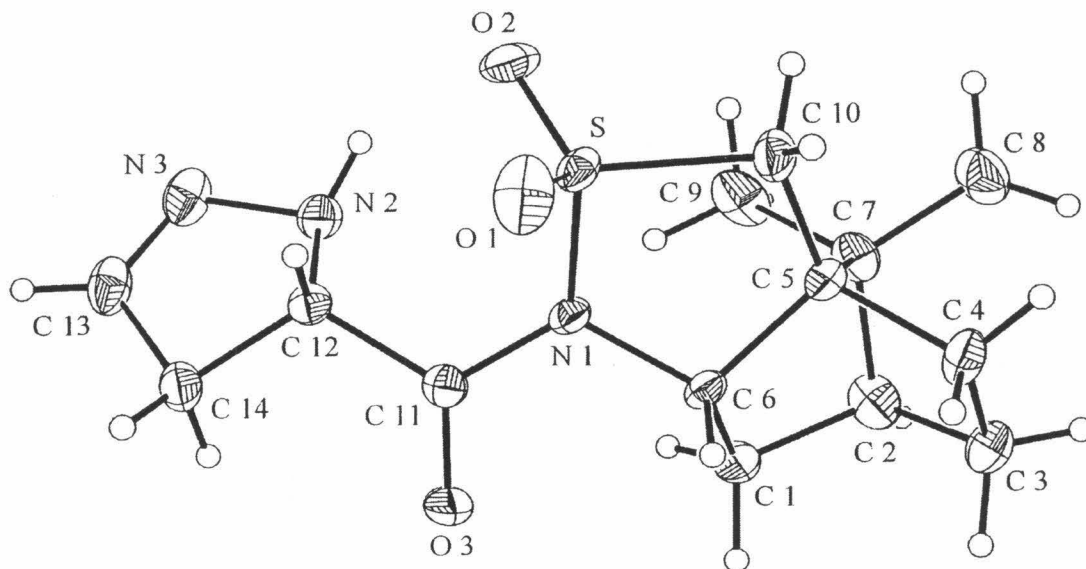
**$^{13}\text{C}$  NMR**  
75 MHz  
 $\text{CDCl}_3$



**IR**  
thin film



**Appendix I : X-Ray Crystal Data for Pyrazoline 60**

**Figure 1.** ORTEP diagram of Pyrazoline **60**, displaying 50 % probability ellipsoids**Table 1.** Crystal data and structure refinement for Pyrazoline **60**

Empirical formula	$C_{14}H_{21}N_3O_3S$
Formula weight	311.40
Crystallization solvent	Hexanes/ethyl acetate
Crystal shape	Fragment
Crystal size	0.38 x 0.33 x 0.26 mm
Crystal color	Colorless

#### Data Collection

Preliminary photos	None
Type of diffractometer	CAD-4
Wavelength	0.710731 Å MoK $\alpha$
Data collection temperature	160 K
Lattice determination from	25 reflections
Theta range for reflections used in lattice determination	13.4 to 18.9°

Unit cell dimensions	$a = 7.211(2)$ Å $\alpha = 90^\circ$
	$b = 9.361(2)$ Å $\beta = 90^\circ$
	$c = 21.913(6)$ Å $\gamma = 90^\circ$
Volume	$1479.2(7)$ Å <sup>3</sup>
Z	4

Crystal system and space group	Orthorhombic P2(1)2(1)2(1)
Density (calculated)	1.398 g/cm <sup>3</sup>

**Table 1.** Continued

Absorption coefficient 0.233 mm<sup>-1</sup>  
 F(000) 664

Theta range for data collection 1.9 to 27.5°

Index ranges -10'=h'=0, -13'=k'=0, -28'=l'=28

Data collection scan type Omega scans

Reflections collected 8804

Independent reflections 1968 [R(merge) = 0.034 GOF(merge) = 1.27 ]

Number of standards 3 reflections measured every 60 min.

Variation of standards zero, within counting statistics.

- Structure solution and refinement

Structure solution program SHELXS-86 (Sheldrick, 1990)

Primary solution method Direct methods

Secondary solution method Difference Fourier map

Hydrogen placement Difference Fourier map

Structure refinement program SHELXL-93 (Sheldrick, 1993)

Refinement method Full matrix least-squares on F<sup>2</sup>

Data / restraints / parameters 1965 / 0 / 276

Treatment of hydrogen atoms No restraints

Goodness-of-fit on F<sup>2</sup> 2.034

Final R indices [I>2sigma(I)] R1 = 0.0271, wR2 = 0.0579

R indices (all data) R1 = 0.0306, wR2 = 0.0591

Max shift/error -0.003

Average shift/error 0.000

Absolute structure parameter 0.25(9)

Extinction coefficient 0.0113(10)

Largest diff. peak and hole 0.239 and -0.266 e.Å<sup>-3</sup>

**Special Notes -**

Refinement on F<sup>2</sup> for ALL reflections except for 3 with very negative F<sup>2</sup> or flagged by the user for potential systematic errors. Weighted R-factors wR and all goodnesses of fit S are based on F<sup>2</sup>, conventional R-factors R are based on F, with F set to zero for negative F<sup>2</sup>. The observed criterion of F<sup>2</sup> > 2sigma(F<sup>2</sup>Å) is used only for calculating \_R\_factor\_obs, etc. and is not relevant to the choice of reflections for refinement. R-factors based on F<sup>2</sup> are statistically about twice as large as those based on F, and Rfactors based on ALL data will be even larger.

All esds (except the esd in the dihedral angle between two l.s. planes) are estimated using the full covariance matrix. The cell esds are taken into account individually in the estimation of esds in distances, angles and torsion angles; correlations between esds in cell parameters are only used when they are defined by crystal symmetry. An

approximate (isotropic) treatment of cell esds is used for estimating esds involving I.s. planes.

**Table 2.** Atomic coordinates ( $\times 10^4$ ) and equivalent isotropic displacement parameters ( $\text{\AA}^2 \times 10^3$ ) for 1.  $U(\text{eq})$  is defined as one-third of the trace of the orthogonalized  $U_{ij}$  tensor.

	x	y	z	U(eq)
S	10038(1)	8229(1)	6037(1)	19(1)
O(1)	9935(3)	9221(2)	5542(1)	35(1)
O(2)	9523(2)	8741(2)	6627(1)	32(1)
O(3)	15253(2)	8025(1)	5931(1)	27(1)
N(1)	12217(2)	7549(2)	6070(1)	17(1)
N(2)	13122(3)	9452(2)	7147(1)	22(1)
N(3)	13777(3)	10624(2)	7497(1)	29(1)
C(1)	13738(3)	5082(2)	5974(1)	23(1)
C(2)	12473(3)	3773(2)	6059(1)	28(1)
C(3)	11813(3)	3281(2)	5426(1)	33(1)
C(4)	10340(3)	4417(2)	5250(1)	26(1)
C(5)	10438(2)	5459(2)	5791(1)	17(1)
C(6)	2350(3)	6197(2)	5728(1)	17(1)
C(7)	10713(3)	4422(2)	6341(1)	23(1)
C(8)	9108(4)	3364(3)	6421(1)	35(1)
C(9)	11011(4)	5160(3)	6957(1)	34(1)
C(10)	8931(3)	6577(2)	5846(1)	25(1)
C(11)	13777(3)	8404(2)	6140(1)	18(1)
C(12)	3541(3)	9784(2)	6499(1)	18(1)
C(13)	14975(4)	11298(2)	7180(1)	28(1)
C(14)	5297(3)	10675(2)	6558(1)	25(1)

-

**Table 3.** Bond lengths [ $\text{\AA}$ ] and angles [ $^\circ$ ] for **60**

S-O(2)	1.4283(14)	C(2)-C(3)	1.537(3)
S-O(1)	1.4291(14)	C(2)-C(7)	1.537(3)
S-N(1)	1.697(2)	C(2)-H(2)	0.91(2)
S-C(10)	1.790(2)	C(3)-C(4)	1.552(3)
O(3)-C(11)	1.211(2)	C(3)-H(3A)	0.97(3)
N(1)-C(11)	1.389(2)		
N(1)-C(6)	1.473(2)	C(3)-H(3B)	0.99(3)
N(2)-N(3)	1.420(2)	C(4)-C(5)	1.537(2)
N(2)-C(12)	1.486(2)	C(4)-H(4A)	0.92(2)
N(2)-H(N)	0.88(2)	C(4)-H(4B)	0.95(2)
N(3)-C(13)	1.275(3)	C(5)-C(10)	1.513(3)
C(1)-C(2)	1.538(3)	C(5)-C(6)	1.549(3)
C(1)-C(6)	1.543(3)	C(5)-C(7)	1.561(3)
C(1)-H(1A)	0.96(2)		
C(1)-H(1B)	1.01(2)	<b>Table 3.</b> Continued	
		C(6)-H(6)	0.98(2)

C(7)-C(9)	1.532(3)	C(2)-C(3)-H(3B)	109(2)
C(7)-C(8)	1.534(3)	C(4)-C(3)-H(3B)	114(2)
C(8)-H(8A)	0.94(3)	H(3A)-C(3)-H(3B)	108(2)
C(8)-H(8B)	0.95(2)	C(5)-C(4)-C(3)	102.3(2)
C(8)-H(8C)	1.00(3)	C(5)-C(4)-H(4A)	111.5(13)
C(9)-H(9A)	0.93(3)	C(3)-C(4)-H(4A)	112.0(14)
C(9)-H(9B)	0.98(3)	C(5)-C(4)-H(4B)	111.8(12)
C(9)-H(9C)	0.98(3)	C(3)-C(4)-H(4B)	113.6(12)
C(10)-H(10A)	0.95(3)	H(4A)-C(4)-H(4B)	106(2)
C(10)-H(10B)	0.93(3)	C(10)-C(5)-C(4)	117.9(2)
C(11)-C(12)	1.522(3)	C(10)-C(5)-C(6)	109.8(2)
C(12)-C(14)	1.522(3)	C(4)-C(5)-C(6)	104.9(2)
C(12)-H(12)	0.91(2)	C(10)-C(5)-C(7)	117.3(2)
C(13)-C(14)	1.501(3)	C(4)-C(5)-C(7)	101.9(2)
C(13)-H(13)	0.91(3)	C(6)-C(5)-C(7)	103.42(14)
C(14)-H(14A)	0.99(2)	N(1)-C(6)-C(1)	116.5(2)
C(14)-H(14B)	0.92(3)	N(1)-C(6)-C(5)	106.27(14)
O(2)-S-O(1)	117.06(9)	C(1)-C(6)-C(5)	104.2(2)
O(2)-S-N(1)	109.11(8)	N(1)-C(6)-H(6)	109.4(12)
O(1)-S-N(1)	108.98(10)	C(1)-C(6)-H(6)	110.6(12)
O(2)-S-C(10)	112.64(11)	C(5)-C(6)-H(6)	109.5(12)
O(1)-S-C(10)	111.20(10)	C(9)-C(7)-C(8)	107.2(2)
N(1)-S-C(10)	95.67(9)	C(9)-C(7)-C(2)	114.7(2)
C(11)-N(1)-C(6)	119.9(2)	C(8)-C(7)-C(2)	114.5(2)
C(11)-N(1)-S	122.56(12)	C(9)-C(7)-C(5)	114.7(2)
C(6)-N(1)-S	111.15(12)	C(8)-C(7)-C(5)	113.2(2)
N(3)-N(2)-C(12)	106.7(2)	C(2)-C(7)-C(5)	92.26(14)
N(3)-N(2)-H(N)	110.5(14)	C(7)-C(8)-H(8A)	111(2)
C(12)-N(2)-H(N)	112.6(14)	C(7)-C(8)-H(8B)	116(2)
C(13)-N(3)-N(2)	108.3(2)	H(8A)-C(8)-H(8B)	103(2)
C(2)-C(1)-C(6)	101.3(2)	C(7)-C(8)-H(8C)	113(2)
C(2)-C(1)-H(1A)	113.8(13)	H(8A)-C(8)-H(8C)	106(2)
C(6)-C(1)-H(1A)	111.7(13)	H(8B)-C(8)-H(8C)	106(2)
C(2)-C(1)-H(1B)	115.5(13)	C(7)-C(9)-H(9A)	110(2)
C(6)-C(1)-H(1B)	110.4(12)	C(7)-C(9)-H(9B)	115.0(13)
H(1A)-C(1)-H(1B)	104(2)	H(9A)-C(9)-H(9B)	106(2)
C(3)-C(2)-C(7)	103.1(2)	C(7)-C(9)-H(9C)	111.1(13)
C(3)-C(2)-C(1)	108.2(2)	H(9A)-C(9)-H(9C)	106(2)
C(7)-C(2)-C(1)	102.9(2)	H(9B)-C(9)-H(9C)	108(2)
C(3)-C(2)-H(2)	109(2)	C(5)-C(10)-S	107.21(14)
C(7)-C(2)-H(2)	114(2)	C(5)-C(10)-H(10A)	120(2)
C(1)-C(2)-H(2)	118(2)	S-C(10)-H(10A)	105(2)
C(2)-C(3)-C(4)	103.3(2)	<b>Table 3.</b> Continued	
C(2)-C(3)-H(3A)	113.3(14)	C(5)-C(10)-H(10B)	115(2)
C(4)-C(3)-H(3A)	109(2)	S-C(10)-H(10B)	105(2)
		H(10A)-C(10)-H(10B)	104(2)

O(3)-C(11)-N(1)	120.1(2)	N(3)-C(13)-H(13)	119(2)
O(3)-C(11)-C(12)	122.8(2)	C(14)-C(13)-H(13)	127(2)
N(1)-C(11)-C(12)	117.1(2)	C(13)-C(14)-C(12)	99.4(2)
N(2)-C(12)-C(14)	101.6(2)	C(13)-C(14)-H(14A)	115.5(13)
N(2)-C(12)-C(11)	109.8(2)	C(12)-C(14)-H(14A)	115.6(14)
C(14)-C(12)-C(11)	114.6(2)	C(13)-C(14)-H(14B)	110~2)
N(2)-C(12)-H(12)	110.8(12)	C(12)-C(14)-H(14B)	109(2)
C(14)-C(12)-H(12)	110.4(12)	H(14A)-C(14)-H(14B)	107(2)
C(11)-C(12)-H(12)	109.4(12)		
N(3)-C(13)-C(14)	114.0(2)		

**Table 4.** Anisotropic displacement parameters ( $\text{\AA}^2 \times 10^2$ ) for 60. The anisotropic displacement factor exponent takes the form:  $-2 \pi^2 [ h^2 a^*2 U11 + \dots + 2 h k a^* b^* U12 ]$

	U11	U22	U33	U23	U13	U12
S	17(1)	18(1)	23(1)	-7(1)	-6(1)	5(1)
O(1)	42(1)	25(1)	38(1)	4(1)	-20(1)	3(1)
O(2)	18(1)	44(1)	33(1)	-21(1)	0(1)	6(1)
O(3)	19(1)	23(1)	41(1)	-4(1)	10(1)	1(1)
N(1)	16(1)	16(1)	20(1)	-4(1)	1(1)	4(1)
N(2)	23(1)	24(1)	20(1)	-3(1)	-2(1)	-1(1)
N(3)	34(1)	28(1)	25(1)	-7(1)	13(1)	1(1)
C(1)	19(1)	17(1)	33(1)	-1(1)	2(1)	4(1)
C(2)	25(1)	17(1)	43(1)	9(1)	-3(1)	4(1)
C(3)	34(1)	18(1)	49(1)	-10(1)	7(1)	(1)
C(4)	34(1)	21(1)	24(1)	-7(1)	-2(1)	-2(1)
C(5)	20(1)	15(1)	17(1)	-2(1)	0(1)	2(1)
C(6)	21(1)	5(1)	14(1)	-2(1)	4(1)	2(1)
C(7)	26(1)	23(1)	22(1)	6(1)	-1(1)	-5(1)
C(8)...	36(1)	33(1)	37(1)	5(1)	5(1)	-11(1)
C(9) ...	35(1)	47(2)	18(1)	8(1)	0(1)	-13(1)
C(10)	19(1)	20(1)	36(1)	-8(1)	-7(1)	1(1)
C(11)	19(1)	6(1)	20(1)	4(1)	1(1)	1(1)
C(12)	16(1)	16(1)	21(1)	1(1)	-2(1)	3(1)
C(13)	28(1)	21(1)	35(1)	-5(1)	-13(1)	-1(1)
C(14)	19(1)	19(1)	36(1)	-2(1)	-1(1)	-1(1)

**Table 5.** Hydrogen coordinates ( $\times 10^4$ ) and isotropic displacement parameters ( $\text{\AA}^2 \times 10^3$ ) for 60

	x	y	z	U(eq)
H(N)	11925(34)	9313(24)	7213(9)	22(6)
H(1A)	14320(29)	5397(24)	6343(9)	23(5)
H(1B)	14801(32)	4952(23)	5677(9)	28(6)
H(2)	12928(34)	3013(25)	6265(10)	34(7)
H(3A)	11245(36)	2346(26)	5429(10)	35(6)
H(3B)	12888(40)	3255(28)	5145(12)	51(8)
H(4A)	9175(33)	4025(24)	5211(9)	25(6)
H(4B)	10589(28)	4883(22)	4871(9)	23(5)
H(6)	12595(29)	6404(21)	5299(9)	19(5)
H(8A)	9369(41)	2689(30)	6727(12)	56(9)
H(8B)	8813(36)	2790(25)	6075(11)	37(7)
H(8C)	7932(40)	3840(28)	6545(11)	46(7)
H(9A)	11334(37)	4494(31)	7252(12)	49(8)
H(9B)	12000(36)	5884(25)	6962(10)	35(7)
H(9C)	9869(35)	5608(26)	7101(10)	34(6)



**Table 5.** Continued

	x	y	z	U(eq)
H(10A)	7977(41)	6470(29)	6144(12)	54(8)
H(10B)	8279(36)	6762(27)	5487(11)	42(7)
H(12)	12615(29)	10310(20)	6329(8)	13(5)
H(13)	15586(35)	12049(27)	7350(10)	41(7)
H(14A)	15514(35)	11373(26)	6230(10)	37(7)
H(14B)	16306(35)	10082(27)	6563(10)	37(7)

**Appendix II : X-Ray Crystallographic Data for Pyrazolidine 130**

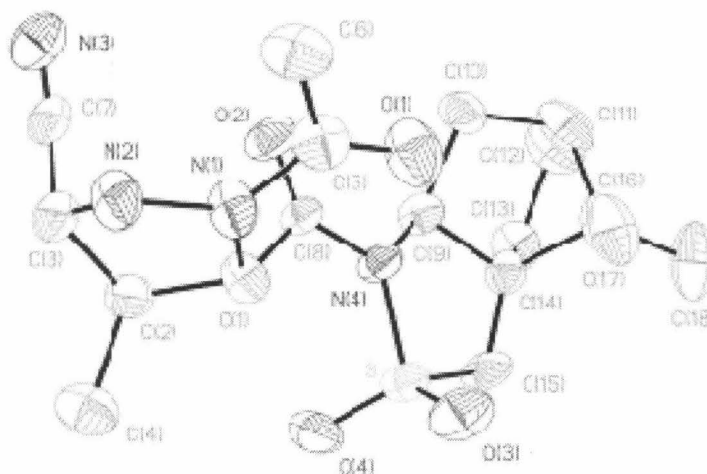


**Figure 1.** ORTEP diagram of pyrazolidine **130**, displaying 30% probability ellipsoids

**Table 1.** Crystal data and structure refinement for **130**

Identification code	mrm4-243	Index ranges	$0 \leq h \leq 17, 0 \leq k \leq 12, 0 \leq l \leq 26$
Empirical formula	$C_{18}H_{26}N_4O_4$	Reflections collected	2409
S		Independent reflections	2409 [R(int) = 0.0000]
Formula weight	394.49	Absorption correction	None
Temperature	293(2) K	Refinement method	Full-matrix least-squares on $F^2$
Wavelength	1.54178 Å	Data / restraints / parameters	2409 / 0 / 488
Crystal system	Tetragonal	Goodness-of-fit on $F^2$	1.042
Space group	$P4(1)2(1)2$	Final R indices [ $I > 2\sigma(I)$ ]	R1 = 0.0508, wR2 = 0.1324
Unit cell dimensions		R indices (all data)	R1 = 0.0703, wR2 = 0.1484
a = 17.342(9) Å	alpha = 90 deg.	Absolute structure parameter	-0.01(4)
b = 17.342(9) Å	beta = 90 deg.	Extinction coefficient	0.00008(6)
c = 26.57(2) Å	gamma = 90 deg.	Largest diff. peak and hole	0.254 and -0.230 e.Å <sup>-3</sup>
Volume	7989(8) Å <sup>3</sup>		
Z	16		
Density (calculated)	1.312 Mg/m <sup>3</sup>		
Absorption coefficient	1.705 mm <sup>-1</sup>		
F(000)	3360		
Crystal size	0.4 x 0.3 x 0.2 mm		
Theta range for data collect.	3.04 to 50.01 deg.		

**Table 2.** Atomic coordinates (x 10<sup>4</sup>) and equivalent isotropic

**Table 2.** Atomic coordinates ( $\times 10^4$ ) and equivalent isotropic displacement parameters ( $\text{Å}^2 \times 10^3$ ) for **130**.  $U(\text{eq})$  is defined as one-third of the trace of the orthogonalized  $U_{ij}$  tensor.

	x	y	z	$U(\text{eq})$
S	5839(1)	6685(1)	1133(1)	63(1)
O(1)	7106(4)	4759(4)	1561(2)	94(2)
N(1)	7961(4)	5342(4)	1066(3)	69(2)
C(1)	7405(4)	5911(5)	874(3)	54(2)
O(2)	6653(3)	4983(3)	431(2)	73(2)
N(2)	8678(4)	5383(4)	813(3)	72(2)
C(2)	7809(4)	6245(5)	413(3)	64(2)
C(3)	8475(5)	5673(5)	324(3)	71(2)
O(3)	6119(3)	6715(4)	1640(2)	88(2)
N(3)	8122(5)	4503(6)	-251(3)	98(3)
N(4)	5964(3)	5804(3)	898(2)	54(2)
O(4)	6154(3)	7236(3)	796(2)	79(2)
C(4)	8129(5)	7060(5)	506(4)	82(3)
C(5)	7746(6)	4766(5)	1382(3)	68(2)
C(6)	8355(5)	4158(5)	1494(3)	80(3)
C(7)	8260(5)	5028(6)	5(4)	75(2)
C(8)	6649(5)	5508(4)	715(3)	55(2)
C(9)	5230(4)	5454(4)	720(3)	57(2)
C(10)	5117(5)	4590(5)	810(4)	78(3)
C(11)	4363(5)	4572(6)	1100(4)	84(3)
C(12)	3716(6)	4823(6)	748(4)	100(3)
C(13)	3852(5)	5701(6)	703(3)	78(3)
C(14)	4582(4)	5837(4)	1014(3)	55(2)
C(15)	4800(4)	6651(5)	1111(3)	70(2)
C(16)	4455(4)	5265(6)	1462(3)	77(3)
C(17)	5119(5)	5189(7)	1830(3)	96(3)
C(18)	3738(6)	5471(8)	1765(4)	128(5)
S'	2017(1)	5126(1)	-647(1)	73(1)
N(1')	1286(4)	7345(4)	43(2)	65(2)
O(1')	228(3)	6621(4)	42(2)	82(2)
C(1')	1784(4)	6723(5)	-140(3)	62(2)
O(2')	1612(4)	6009(3)	614(2)	82(2)
N(2')	1696(4)	8036(4)	130(3)	78(2)
C(2')	2612(5)	7064(5)	-76(3)	76(3)
O(3')	1649(4)	5522(3)	-1039(2)	82(2)
N(3')	2587(8)	7533(8)	1214(4)	150(5)
C(3')	2468(6)	7774(6)	251(4)	88(3)
N(4')	1574(4)	5308(4)	-103(2)	60(2)

**Table 2.** Continued

	x	y	z	U(eq)
O(4')	2824(4)	5262(5)	-587(3)	125(3)
C(4')	2989(5)	7264(6)	-569(3)	90(3)
C(5')	528(5)	7241(5)	138(3)	67(2)
C(6')	94(6)	7925(6)	337(4)	98(3)
C(7')	2525(7)	7655(8)	798(5)	108(4)
C(8')	1657(5)	5988(5)	152(3)	63(2)
C(9')	1385(6)	4600(5)	181(3)	73(3)
C(10')	623(6)	4609(5)	471(3)	78(3)
C(11')	193(6)	3922(5)	245(3)	81(3)
C(12')	612(8)	3188(6)	405(4)	117(4)
C(13')	1359(8)	3182(5)	68(4)	114(4)
C(14')	1268(6)	3964(5)	-228(3)	74(2)
C(15')	1800(5)	4113(5)	-658(4)	82(3)
C(16')	384(5)	3989(4)	-320(3)	66(2)
C(17')	85(5)	4723(5)	-570(3)	72(2)
C(18')	85(6)	3325(5)	-640(3)	92(3)

---

**Table 3.** Bond lengths [ $\text{\AA}$ ] and angles [deg] for **130**

S-O(4)	1.419(6)	C(2')-C(3')	1.527(13)
S-O(3)	1.432(6)	N(3')-C(7')	1.132(13)
S-N(4)	1.663(6)	C(3')-C(7')	1.47(2)
S-C(15)	1.805(8)	N(4')-C(8')	1.368(10)
O(1)-C(5)	1.208(10)	N(4')-C(9')	1.477(10)
N(1)-C(5)	1.357(10)	C(5')-C(6')	1.500(13)
N(1)-N(2)	1.415(9)	C(9')-C(10')	1.530(12)
N(1)-C(1)	1.472(10)	C(9')-C(14')	1.562(12)
C(1)-C(2)	1.525(10)	C(10')-C(11')	1.527(12)
C(1)-C(8)	1.544(11)	C(11')-C(12')	1.527(14)
O(2)-C(8)	1.184(8)	C(11')-C(16')	1.543(11)
N(2)-C(3)	1.436(10)	C(12')-C(13')	1.57(2)
C(2)-C(4)	1.539(11)	C(13')-C(14')	1.576(12)
C(2)-C(3)	1.542(11)	C(14')-C(15')	1.490(12)
C(3)-C(7)	1.453(13)	C(14')-C(16')	1.553(12)
N(3)-C(7)	1.161(11)	C(16')-C(18')	1.523(11)
N(4)-C(8)	1.382(9)	C(16')-C(17')	1.526(11)
N(4)-C(9)	1.488(9)	O(4)-S-O(3)	116.0(4)
C(5)-C(6)	1.523(12)	O(4)-S-N(4)	109.4(3)
C(9)-C(14)	1.522(10)	O(3)-S-N(4)	109.9(4)
C(9)-C(10)	1.530(11)	O(4)-S-C(15)	112.7(4)
C(10)-C(11)	1.517(12)	O(3)-S-C(15)	111.6(4)
C(11)-C(12)	1.523(13)	N(4)-S-C(15)	95.1(3)
C(11)-C(16)	1.547(14)	C(5)-N(1)-N(2)	124.9(7)
C(12)-C(13)	1.547(13)	C(5)-N(1)-C(1)	121.8(6)
C(13)-C(14)	1.528(11)	N(2)-N(1)-C(1)	112.2(6)
C(14)-C(15)	1.484(11)	N(1)-C(1)-C(2)	103.4(6)
C(14)-C(16)	1.565(11)	N(1)-C(1)-C(8)	110.4(6)
C(16)-C(17)	1.517(11)	C(2)-C(1)-C(8)	110.1(6)
C(16)-C(18)	1.524(13)	N(1)-N(2)-C(3)	103.4(6)
S'-O(3')	1.403(6)	C(1)-C(2)-C(4)	112.6(7)
S'-O(4')	1.427(7)	C(1)-C(2)-C(3)	102.9(6)
S'-N(4')	1.665(7)	C(4)-C(2)-C(3)	110.2(7)
S'-C(15')	1.796(9)	N(2)-C(3)-C(7)	108.8(7)
N(1')-C(5')	1.351(10)	N(2)-C(3)-C(2)	105.7(6)
N(1')-N(2')	1.413(9)	C(7)-C(3)-C(2)	113.0(7)
N(1')-C(1')	1.465(10)	C(8)-N(4)-C(9)	118.1(6)
O(1')-C(5')	1.221(10)	C(8)-N(4)-S	125.7(5)
C(1')-C(8')	1.509(11)	C(9)-N(4)-S	112.5(5)
C(1')-C(2')	1.561(11)	O(1)-C(5)-N(1)	120.3(8)
O(2')-C(8')	1.229(9)	O(1)-C(5)-C(6)	123.6(9)
N(2')-C(3')	1.450(12)		
C(2')-C(4')	1.507(12)		

**Table 3.** Continued

N(1)-C(5)-C(6)	116.1(8)	N(1')-N(2')-C(3')	103.6(7)
N(3)-C(7)-C(3)	176.9(10)	C(4')-C(2')-C(3')	112.3(8)
O(2)-C(8)-N(4)	121.1(8)	C(4')-C(2')-C(1')	113.0(7)
O(2)-C(8)-C(1)	121.1(7)	C(3')-C(2')-C(1')	102.6(7)
N(4)-C(8)-C(1)	117.8(6)	N(2')-C(3')-C(7')	109.0(9)
N(4)-C(9)-C(14)	106.8(6)	N(2')-C(3')-C(2')	106.1(7)
N(4)-C(9)-C(10)	117.3(7)	C(7')-C(3')-C(2')	115.9(9)
C(14)-C(9)-C(10)	104.7(6)	C(8')-N(4')-C(9')	119.1(6)
C(11)-C(10)-C(9)	102.1(7)	C(8')-N(4')-S'	123.0(5)
C(10)-C(11)-C(12)	108.5(8)	C(9')-N(4')-S'	112.8(5)
C(10)-C(11)-C(16)	102.2(7)	O(1')-C(5')-N(1')	119.6(8)
C(12)-C(11)-C(16)	103.7(8)	O(1')-C(5')-C(6')	123.8(8)
C(11)-C(12)-C(13)	102.4(8)	N(1')-C(5')-C(6')	116.6(8)
C(14)-C(13)-C(12)	103.7(7)	N(3')-C(7')-C(3')	177(2)
C(15)-C(14)-C(9)	108.5(6)	O(2')-C(8')-N(4')	120.9(7)
C(15)-C(14)-C(13)	116.9(7)	O(2')-C(8')-C(1')	119.8(8)
C(9)-C(14)-C(13)	105.5(6)	N(4')-C(8')-C(1')	119.3(7)
C(15)-C(14)-C(16)	120.4(7)	N(4')-C(9')-C(10')	116.2(7)
C(9)-C(14)-C(16)	102.5(6)	N(4')-C(9')-C(14')	105.1(6)
C(13)-C(14)-C(16)	101.3(6)	C(10')-C(9')-C(14')	104.1(7)
C(14)-C(15)-S	106.9(5)	C(11')-C(10')-C(9')	102.5(7)
C(17)-C(16)-C(18)	107.4(7)	C(12')-C(11')-C(10')	108.0(9)
C(17)-C(16)-C(11)	114.3(8)	C(12')-C(11')-C(16')	103.4(8)
C(18)-C(16)-C(11)	115.3(8)	C(10')-C(11')-C(16')	102.6(7)
C(17)-C(16)-C(14)	116.0(7)	C(11')-C(12')-C(13')	103.8(8)
C(18)-C(16)-C(14)	111.6(8)	C(12')-C(13')-C(14')	101.3(8)
C(11)-C(16)-C(14)	92.0(6)	C(15')-C(14')-C(9')	109.2(7)
O(3')-S'-O(4')	116.6(5)	C(15')-C(14')-C(16')	119.1(7)
O(3')-S'-N(4')	109.9(3)	C(9')-C(14')-C(16')	102.6(7)
O(4')-S'-N(4')	108.9(4)	C(15')-C(14')-C(13')	118.0(8)
O(3')-S'-C(15')	111.8(4)	C(9')-C(14')-C(13')	104.3(7)
O(4')-S'-C(15')	111.7(5)	C(16')-C(14')-C(13')	101.6(8)
N(4')-S'-C(15')	95.9(4)	C(14')-C(15')-S'	106.7(6)
C(5')-N(1')-N(2')	125.0(7)	C(18')-C(16')-C(17')	105.7(7)
C(5')-N(1')-C(1')	122.5(7)	C(18')-C(16')-C(11')	114.4(7)
N(2')-N(1')-C(1')	112.5(7)	C(17')-C(16')-C(11')	114.5(7)
N(1')-C(1')-C(8')	111.4(7)	C(18')-C(16')-C(14')	113.8(7)
N(1')-C(1')-C(2')	103.1(7)	C(17')-C(16')-C(14')	115.3(7)
C(8')-C(1')-C(2')	113.4(7)	C(11')-C(16')-C(14')	93.2(7)

---

Symmetry transformations used to generate equivalent atoms:

**Table 4.** Anisotropic displacement parameters ( $\text{Å}^2 \times 10^3$ ) for **130**

The anisotropic displacement factor exponent takes the form:  
 $-2 \pi^2 [ h^2 a^{*2} U11 + \dots + 2 h k a^* b^* U12 ]$

	U11	U22	U33	U23	U13	U12
S	55(1)	54(1)	79(1)	-14(1)	-3(1)	6(1)
O(1)	63(4)	109(5)	109(5)	31(4)	13(4)	9(4)
N(1)	43(4)	81(5)	82(4)	19(4)	-1(4)	11(4)
C(1)	39(4)	60(5)	63(4)	6(4)	-12(4)	0(4)
O(2)	47(3)	73(4)	100(4)	-25(4)	3(3)	8(3)
N(2)	34(4)	87(5)	95(5)	17(4)	0(4)	10(3)
C(2)	43(5)	64(6)	83(5)	-5(5)	-3(4)	0(4)
C(3)	50(5)	73(6)	88(6)	-5(5)	15(5)	1(4)
O(3)	79(4)	99(5)	87(4)	-34(4)	-23(3)	3(4)
N(3)	77(6)	98(7)	120(6)	-18(5)	15(5)	19(5)
N(4)	41(4)	53(4)	67(3)	-22(3)	3(3)	5(3)
O(4)	76(4)	52(3)	109(4)	6(3)	-1(3)	-5(3)
C(4)	63(6)	74(6)	110(7)	15(5)	-18(5)	2(5)
C(5)	68(6)	71(6)	66(5)	6(5)	-12(5)	1(5)
C(6)	75(6)	71(6)	95(6)	10(5)	-29(5)	16(5)
C(7)	50(5)	78(7)	98(6)	-4(6)	22(5)	10(5)
C(8)	66(6)	41(5)	59(4)	-8(4)	13(4)	7(4)
C(9)	46(5)	63(5)	62(4)	-5(4)	-8(4)	6(4)
C(10)	63(6)	63(6)	109(7)	2(5)	4(5)	-7(4)
C(11)	59(6)	82(7)	109(6)	42(6)	-12(5)	-23(5)
C(12)	72(7)	108(9)	121(8)	13(7)	-11(6)	-28(6)
C(13)	50(5)	98(7)	86(6)	6(5)	-8(5)	5(5)
C(14)	42(4)	60(5)	61(4)	-5(4)	4(4)	7(4)
C(15)	48(5)	77(6)	87(5)	-21(5)	12(4)	18(4)
C(16)	40(5)	114(8)	76(5)	21(6)	4(5)	-7(5)
C(17)	70(6)	138(10)	81(6)	44(7)	9(5)	-3(6)
C(18)	60(7)	222(15)	102(7)	16(9)	21(6)	-10(8)
S'	60(2)	71(2)	88(2)	-1(1)	18(1)	5(1)
N(1')	64(5)	46(4)	83(4)	-9(4)	-2(4)	-5(4)
O(1')	68(4)	63(4)	114(4)	-22(4)	-8(3)	-6(3)
C(1')	61(5)	58(5)	66(5)	0(4)	-13(4)	-4(4)
O(2')	106(5)	60(4)	79(4)	3(3)	-9(4)	-5(3)
N(2')	82(6)	43(4)	110(6)	7(4)	-9(5)	-17(4)
C(2')	65(6)	76(6)	88(6)	17(5)	-21(5)	-11(5)

**Table 4.** continued



	U11	U22	U33	U23	U13	U12
O(3')	109(5)	70(4)	68(3)	8(3)	15(3)	5(3)
N(3')	149(10)	204(14)	96(7)	-13(8)	-27(7)	-35(8)
C(3')	85(8)	89(7)	90(7)	10(6)	-8(6)	-30(6)
N(4')	67(4)	49(4)	65(4)	3(3)	3(3)	3(3)
O(4')	54(4)	143(7)	177(7)	-23(6)	22(5)	-4(4)
C(4')	70(6)	105(8)	95(6)	22(6)	12(6)	-13(5)
C(5')	62(6)	56(6)	84(6)	-13(5)	-5(5)	3(5)
C(6')	78(7)	77(7)	140(9)	-27(7)	1(6)	-7(5)
C(7')	89(8)	140(11)	94(8)	-15(8)	-9(7)	-34(7)
C(8')	60(5)	71(6)	59(5)	5(5)	-3(4)	6(4)
C(9')	98(7)	49(5)	72(5)	18(5)	-6(5)	11(5)
C(10')	103(7)	58(6)	73(5)	0(5)	22(5)	-17(5)
C(11')	113(8)	58(6)	74(5)	12(5)	10(5)	-13(5)
C(12')	188(13)	68(7)	96(7)	22(6)	2(8)	-16(7)
C(13')	157(11)	54(6)	131(9)	19(6)	4(9)	25(7)
C(14')	94(7)	47(5)	81(5)	6(5)	1(6)	20(5)
C(15')	84(6)	62(6)	102(6)	-1(5)	27(6)	16(5)
C(16')	85(6)	43(5)	69(5)	7(4)	3(5)	-7(4)
C(17')	64(5)	69(6)	83(5)	-4(5)	-3(5)	-6(4)
C(18')	125(8)	60(6)	90(6)	-9(5)	6(6)	-15(6)

**Table 5.** Hydrogen coordinates ( $\times 10^4$ ) and isotropic displacement parameters ( $\text{Å}^2 \times 10^3$ ) for **130**

	x	y	z	U(eq)
H(1A)	7306(4)	6309(5)	1117(3)	81
H(2A)	9148(4)	5258(4)	933(3)	108
H(2B)	7460(4)	6247(5)	132(3)	96
H(3A)	8904(5)	5940(5)	177(3)	106
H(4A)	7714(5)	7413(5)	568(4)	123
H(4B)	8468(5)	7052(5)	792(4)	123
H(4C)	8411(5)	7221(5)	214(4)	123
H(6A)	8134(5)	3779(5)	1715(3)	121
H(6B)	8525(5)	3912(5)	1189(3)	121
H(6C)	8786(5)	4399(5)	1656(3)	121
H(9A)	5169(4)	5568(4)	368(3)	85
H(10A)	5536(5)	4371(5)	998(4)	118
H(10B)	5064(5)	4319(5)	496(4)	118
H(11A)	4271(5)	4089(6)	1265(4)	125
H(12A)	3224(6)	4714(6)	898(4)	150

**Table 5.** continued

	x	y	z	U(eq)
--	---	---	---	-------

---

H(12B)	3746(6)	4574(6)	426(4)	150
H(13A)	3430(5)	5988(6)	843(3)	117
H(13B)	3923(5)	5851(6)	359(3)	117
H(15A)	4610(4)	6980(5)	848(3)	106
H(15B)	4585(4)	6820(5)	1426(3)	106
H(17A)	4999(5)	4827(7)	2092(3)	144
H(17B)	5568(5)	5017(7)	1650(3)	144
H(17C)	5218(5)	5686(7)	1975(3)	144
H(18A)	3675(6)	5113(8)	2038(4)	193
H(18B)	3795(6)	5983(8)	1898(4)	193
H(18C)	3293(6)	5451(8)	1551(4)	193
H(1'A)	1689(4)	6633(5)	-491(3)	92
H(2'A)	1514(4)	8522(4)	117(3)	117
H(2'B)	2930(5)	6702(5)	102(3)	114
H(3'A)	2829(6)	8166(6)	155(4)	132
H(4'A)	3492(5)	7477(6)	-510(3)	135
H(4'B)	3035(5)	6807(6)	-771(3)	135
H(4'C)	2677(5)	7635(6)	-743(3)	135
H(6'A)	-435(6)	7783(6)	390(4)	148
H(6'B)	318(6)	8084(6)	650(4)	148
H(6'C)	119(6)	8342(6)	100(4)	148
H(9'A)	1800(6)	4462(5)	402(3)	110
H(10C)	352(6)	5082(5)	407(3)	117
H(10D)	699(6)	4552(5)	827(3)	117
H(11B)	-349(6)	3918(5)	319(3)	122
H(12C)	295(8)	2743(6)	347(4)	176
H(12D)	750(8)	3204(6)	755(4)	176
H(13C)	1350(8)	2753(5)	-159(4)	171
H(13D)	1822(8)	3164(5)	266(4)	171
H(15D)	1554(5)	3977(5)	-969(4)	124
H(17D)	-463(5)	4698(5)	-617(3)	108
H(17E)	209(5)	5147(5)	-353(3)	108
H(17F)	332(5)	4795(5)	-891(3)	108
H(18D)	-464(6)	3368(5)	-677(3)	138
H(18E)	323(6)	3340(5)	-966(3)	138
H(18F)	207(6)	2846(5)	-478(3)	138